Dissecting Pancreatic β-cell Stress Using Whole Transcriptome Sequencing

By

Jennifer Susan Stancill

Dissertation
Submitted to the Faculty of the
Graduate School of Vanderbilt University
in partial fulfillment of the requirements
for the degree of

DOCTOR OF PHILOSOPHY
in

Cell and Developmental Biology
May, 2017
Nashville, Tennessee

Approved:

Guoqiang Gu, Ph.D.
Christopher V. Wright, D. Phil.
David M. Miller, III, Ph.D.
David A. Jacobson, Ph.D.
Mark A. Magnuson, M.D.

To Mother, for teaching me to love science,

and to Daddy, for always believing in me, even when I didn't.

ACKNOWLEDGEMENTS

First, I have to thank my mentor, Mark Magnuson, for your invaluable guidance over the past five years. My project took many unexpected turns during that time, and you helped me survive them all. Even though we sometimes butted heads, you always tolerated my stubbornness, and I truly believe I am a better scientist because of your mentorship.

Next, I would like to thank the members of my thesis committee, Guoqiang Gu, Chris Wright, David Miller, and David Jacobson for providing feedback, constructive criticism, and much-appreciated guidance during the ups and downs of graduate school. Your advice has been instrumental in helping me complete this work and reach this point in my career. I could not have asked for a better committee. I'd also like to thank the department of Cell and Developmental Biology, the program in Developmental Biology, the Beta Cell Interest Group, and the Diabetes Research and Training Center for providing me with opportunities to present my work to colleagues, either through posters or oral presentations, over the years.

I would not have been able to complete this work without the help of past and present members of the Magnuson Lab. Hannah Worchel Clayton, you and I began this journey through graduate school together, and it was a blessing to have a friend to support me through each step along the way. We both survived and came out as stronger scientists because of it! I need to thank Chiyo Shiota, whose work on the *Abcc8*$^{-/-}$ mice laid the foundation for much of my thesis. Jody Peters and Pam Uttz, you both kept the lab running during my time there, and so much of what I was able to achieve was due to your administrative assistance. Thank you to Katherine Boyer, Lauren Stiehle, Jacob Coeur, Roxana Amirahmadi, and James O'Connor, the students I mentored during my graduate career, for contributing in various ways to the data presented in this thesis. I

want to thank Rama Gangula and Anna Osipovich for generating the *Ins2.Apple* mice. An additional thank you to Anna Osipovich for guiding me through experimental troubles and helping design many of my experiments. Karrie Dudek, thank you for helping to make my last couple of years in the lab a really enjoyable time. I know you will do great things in graduate school. Anna and Karrie, the lab is in your hands now! I am so excited to see what you are able to accomplish in the next few years.

Next, I want to thank J.P. Cartailler, of Creative Data Solutions, for performing all bioinformatics analyses using my RNA-sequencing data, including genome alignments, differential expression analyses, and WGCNA, and for creating figures to display that data. Thank you to members of the Jacobson Lab, Matthew Dickerson and Prasanna Dadi, without whom the membrane potential recordings and intracellular calcium measurements that were so integral to my project would not have been possible. I also want to thank the members of the β-cell research community at Vanderbilt, especially the Gannon, Stein, Wright, and Gu labs, who have provided advice on experiments and who have made working in this field a pleasure.

Additionally, I need to thank the various core facilities who helped me achieve this work. Thank you to the Vanderbilt Islet Procurement and Analysis Core for performing all of my islet isolations, Vanderbilt Technologies for Advanced Genomics (VANTAGE) for performing all cell sorting and RNA-sequencing, the Vanderbilt Cell Imaging Shared Resource for helping to acquire images, the Vanderbilt Tissue Pathology Shared Resource for processing and sectioning paraffin-embedded tissues, and the Vanderbilt Transgenic Mouse/ES Cell Shared Resource for reconstituting the *Abcc8*$^{-/-}$ mice.

I have been fortunate during graduate school to have a strong support group of friends, both within and outside of Vanderbilt. Thank you to Nicole Diggins, Amanda Duran, Gwynne Davis, Steve Schrider, and Peter Griffin for being some of my best friends in Nashville. Our times spent having movie or game nights, taking painting or art classes, decorating Christmas trees, carving pumpkins, and exploring middle Tennessee together are some of my most treasured memories of grad school. I know you will all accomplish amazing things in your lives, and I'm happy to have experienced at least part of it with you. Thank you to my fellow Zumba dancers, Rachel McCreery, Nicole Diggins, Gwynne Davis, Claire Marvinney, Laura Glass, Christina McGahan, and Cecilia Chung. Being able to work out with friends twice a week has been a great joy and has helped keep me sane. Thanks for keeping me dancing! Thank you to my fellow members of the Vanderbilt and Nashville Community Bands. Being able to have music in my life helped to keep me centered during graduate school. And thank you to my church family at Forest Hills United Methodist Church. Chris and Joanna Cummings, Mindi Godfrey, Caroline Scism, Katie Greene, Tara Fleisher, Hunter Pugh, and Jim Hughes, I have been truly blessed to know each of you. You made that church my home for six years, and I can never express enough gratitude.

Thank you to my parents for making me the person I am today. I could not have accomplished any of this without your support, emotional and financial, for my entire life. The two of you have always been my biggest supporters and have taught me to believe I can accomplish whatever I set my mind to. And finally, I want to thank my wonderful boyfriend, Dan. You have made my six years in Nashville the best years of my life so far. You always keep me laughing and remind me that life doesn't have to be so serious all the time. I know I would not have been able to come this far without your unconditional love and support. Thank you.

TABLE OF CONTENTS

LIST OF TABLES

LIST OF FIGURES

LIST OF ABBREVIATIONS

$[Ca^{2+}]_i$	Intracellular Ca^{2+} concentration
5-HT	Serotonin
7AAD	7-Aminoactinomycin D; used to label dead cells
Abcc8	ATP-binding cassette, sub-family C, member 8; gene encoding SUR1
ADP	Adenosine diphosphate
ALDH1A3	Aldehyde dehydrogenase family 1, subfamily A3
ASCL1	Achaete-scute family bHLH transcription factor 1
ATP	Adenosine triphosphate
CaM	Calmodulin, a Ca^{2+}-binding protein
cAMP	Cyclic adenosine monophosphate
CaMK	Ca^{2+}/Calmodulin-dependent kinase
cDNA	Complementary deoxyribonucleic acid; DNA synthesized from RNA
ChIP	Chromatin immunoprecipitation
CRE	cAMP response element
CREB	cAMP response element-binding protein
DAPI	4',6-diamidino-2-phenylindole; used as nuclear marker and to label dead cells
DAVID	Database for Annotation, Visualization, and Integrated Discovery
DNA	Deoxyribonucleic acid
ER	Endoplasmic reticulum
FACS	Fluorescence-activated cell sorting
FDR	False discovery rate
Gast	Gastrin
Gcg	Glucagon
GCK	Glucokinase
GCN	Gene correlation network
GFP	Green fluorescent protein
GLP-1	Glucagon-like peptide 1
GLP1R	Glucagon-like peptide 1 receptor

GLUT	Glucose transporter
GRN	Gene regulatory network
GWAS	Genome-wide association study
HFD	High-fat diet
hGH	Human growth hormone
Ins	Insulin
IPGTT	Intraperitoneal glucose tolerance test
IRS	Insulin receptor substrate
ITT	Insulin tolerance test
K_{ATP}-channel	ATP-sensitive potassium channel
KCl	Potassium chloride
Kcnj11	Potassium inwardly rectifying channel, subfamily J, member 11; gene encoding KIR6.2
KEGG	Kyoto Encyclopedia of Genes and Genomes
KIR6.2	Potassium inwardly rectifying channel, subfamily J, member 11; protein product of *Kcnj11*
LCA	Loxed cassette acceptor
LSL	Lox-STOP-Lox
mESC	Mouse embryonic stem cells
MIP	Mouse insulin promoter
MODY	Maturity-onset diabetes of the young
mTORC	Mechanistic target of rapamycin complex
NFAT	Nuclear factor of activated T-cells
P	Postnatal day
PCA	Principal component analysis
PCR	Polymerase chain reaction
PHHI	Persistent hyperinsulinemic hypoglycemia of infancy
PND	Persistent neonatal diabetes
PP	Pancreatic polypeptide
qRT-PCR	Quantitative reverse-transcription polymerase chain reaction
RFP	Red fluorescent protein

RIP	Rat insulin promoter
RMCE	Recombinase-mediated cassette exchange
RNA	Ribonucleic acid
RNA-seq	RNA sequencing
ROS	Reactive oxygen species
S100A4	S100 calcium binding protein A4
S100A6	S100 calcium binding protein A6
Sst	Somatostatin
STAT5	Signal transducer and activator of transcription 5
SUR1	Sulfonylurea receptor type 1; protein product of *Abcc8*
T1D	Type 1 diabetes
T2D	Type 2 diabetes
TUNEL	Terminal deoxynucleotidyl transferase dUTP (deoxyuridine triphosphate) nick end labeling; assay used to detect apoptosis
UPR	Unfolded protein response
VDCC	Voltage dependent calcium channel
WGCNA	Weighted gene correlation network analysis
YFP	Yellow fluorescent protein

CHAPTER I

INTRODUCTION

Pancreatic islet structure and function

The pancreas is a glandular organ of the digestive system made up of two major cell types: exocrine cells and endocrine cells (**Figure 1.1**). The exocrine compartment, which is responsible for synthesis and secretion of digestive enzymes, includes both acinar and ductal cells and makes up the vast majority of the pancreas. The Islets of Langerhans make up the endocrine compartment of the pancreas and contain five types of hormone-secreting endocrine cells: glucagon-secreting α-cells, insulin-secreting β-cells, somatostatin-secreting δ-cells, pancreatic polypeptide-secreting PP-cells, and ghrelin-secreting ε-cells. The main function of the pancreatic endocrine cells is to maintain blood glucose homeostasis through hormone secretion in response to specific stimuli. In humans, the endocrine cells make up approximately 4-5% of the total pancreas volume in the adult (1).

Insulin is released into the bloodstream in response to glucose uptake by the β-cells, the molecular mechanism of which is discussed in the following section. It is released in response to a rise in blood glucose concentration, and its primary function is to trigger glucose uptake in target tissues (**Figure 1.2**). Once in the bloodstream, insulin binds to insulin receptors expressed by target tissues, including hepatocytes of the liver, myocytes of skeletal muscle, adipocytes of fat tissue, cardiomyocytes of the heart, and neurons of the brain (2; 3). The effects of insulin in these tissues are mediated by signaling molecules called insulin receptor substrates 1-4 (IRS1-4) which are phosphorylated by the insulin receptor upon insulin binding.

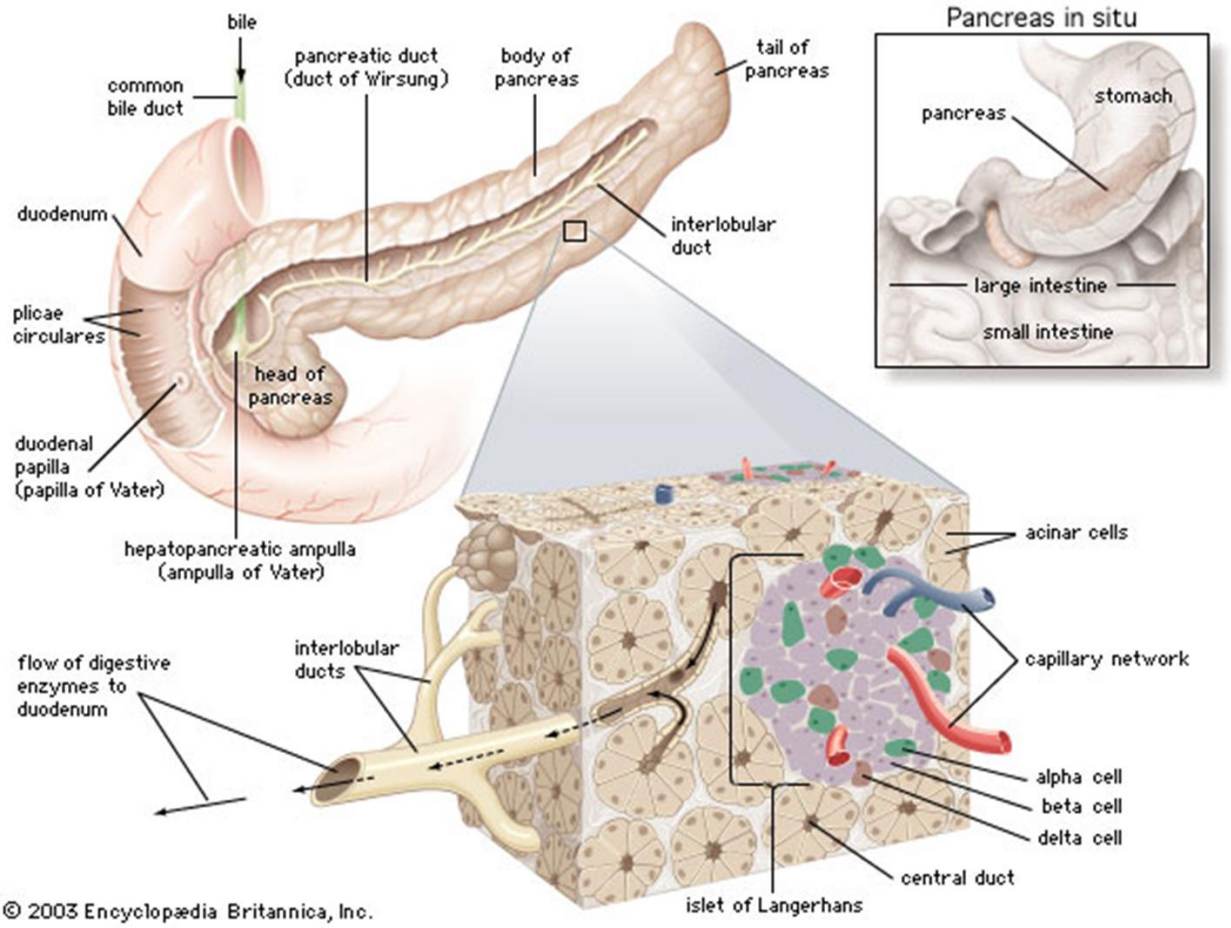

Figure 1.1. Anatomy of the pancreas. In humans, the pancreas is situated behind the stomach and lies transversely across the posterior wall of the abdomen. The head of the pancreas sits in the loop of the duodenum as it exits the stomach, and the tail of the pancreas is located near the spleen (not pictured). Most of the pancreas is made up of acinar cells which secrete enzymes to aid in food digestion. The Islets of Langerhans containing the endocrine cells of the pancreas, are dispersed throughout the acinar tissue and are highly vascularized. They are responsible for secreting endocrine hormones to regulate blood glucose homeostasis and consist of five endocrine cell types: α-, β-, and δ-cells (labeled above) and PP- and ε-cells (not labeled). © 2003 Encyclopedia Britannica, Inc. Reproduced in compliance with the online Terms of Use.

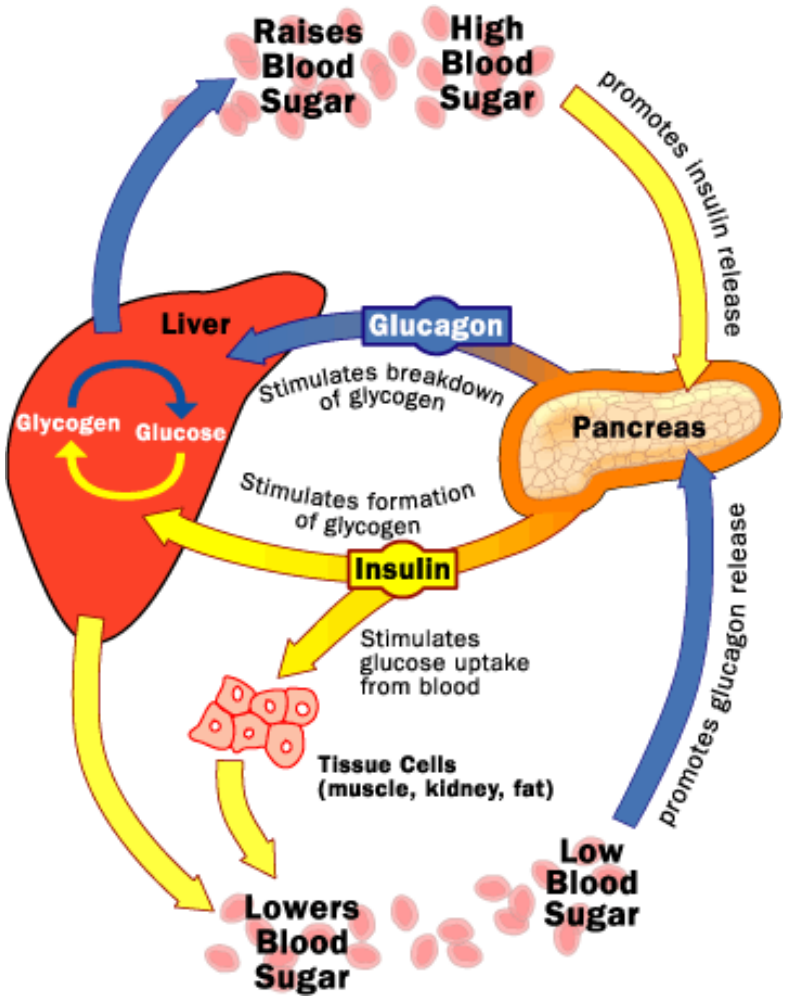

Figure 1.2. Insulin and glucagon action in the body. The two primary pancreatic hormones, insulin and glucagon, exert opposite effects on peripheral tissues to regulate blood glucose homeostasis. Insulin, released from the pancreatic β-cells under high blood glucose concentrations, stimulates glucose uptake, metabolism, and/or storage by glycogen formation in tissues such as the liver. Glucagon, on the other hand, is released from the pancreatic α-cells under low blood glucose concentrations and stimulates the breakdown of glycogen to glucose in the liver. Yellow arrows and text boxes represent the stimulus for and action of insulin. Blue arrows and text boxes represent the stimulus for and action of glucagon. © 2001 Craig Freudenrich, Ph.D., HowStuffWorks.com (4). Reproduced in compliance with the online Terms of Use.

This activation triggers a series of downstream phosphorylation events ultimately resulting in the translocation of glucose transporter 4 (GLUT4) to the membrane to facilitate the uptake of glucose from the bloodstream (5). In addition to acting on peripheral tissues in the body, insulin plays a feedback role in the β-cells themselves to promote β-cell proliferation and survival (6-8).

Glucagon, on the other hand, triggers the release of glucose into the bloodstream, opposing the action of insulin (**Figure 1.2**) (9). It is released from pancreatic α-cells in response to a fall in the blood glucose concentration. When glucagon reaches its primary target tissue, the liver, it binds to glucagon receptors, G-protein-coupled receptors, triggering the activation of G-proteins, synthesis of cyclic adenosine monophosphate (cAMP), and ultimately the breakdown of glycogen stores into glucose via phosphorolysis by glycogen phosphorylase (10).

The actions of the remaining pancreatic endocrine hormones are much less well-understood. Somatostatin, secreted from pancreatic δ-cells, is known to inhibit the secretion of both glucagon and insulin (11). Pancreatic polypeptide, secreted from PP-cells, is thought to be secreted in response to food intake, functioning as a satiety factor via signaling to hypothalamic nuclei (12; 13). It has an additional putative role in regulating gastrointestinal motility (14). Ghrelin-secreting ε-cells are prominent during both mouse and human pancreas development, but are rarely found in the adult. They are thought to represent a multipotent progenitor, or transient, population in the developing pancreas, with the ability to give rise to α-, PP-, and β-cells (15; 16). In the adult, ghrelin is primarily secreted by ghrelinergic cells in the gastrointestinal tract, and is thought to inhibit insulin secretion from the β-cells (17).

Islet architecture and cell composition differs between rodents and humans (**Figure 1.3**). In rodents, the β-cells are mostly confined to the core of the islet, while the α-, δ-, and PP-cells are

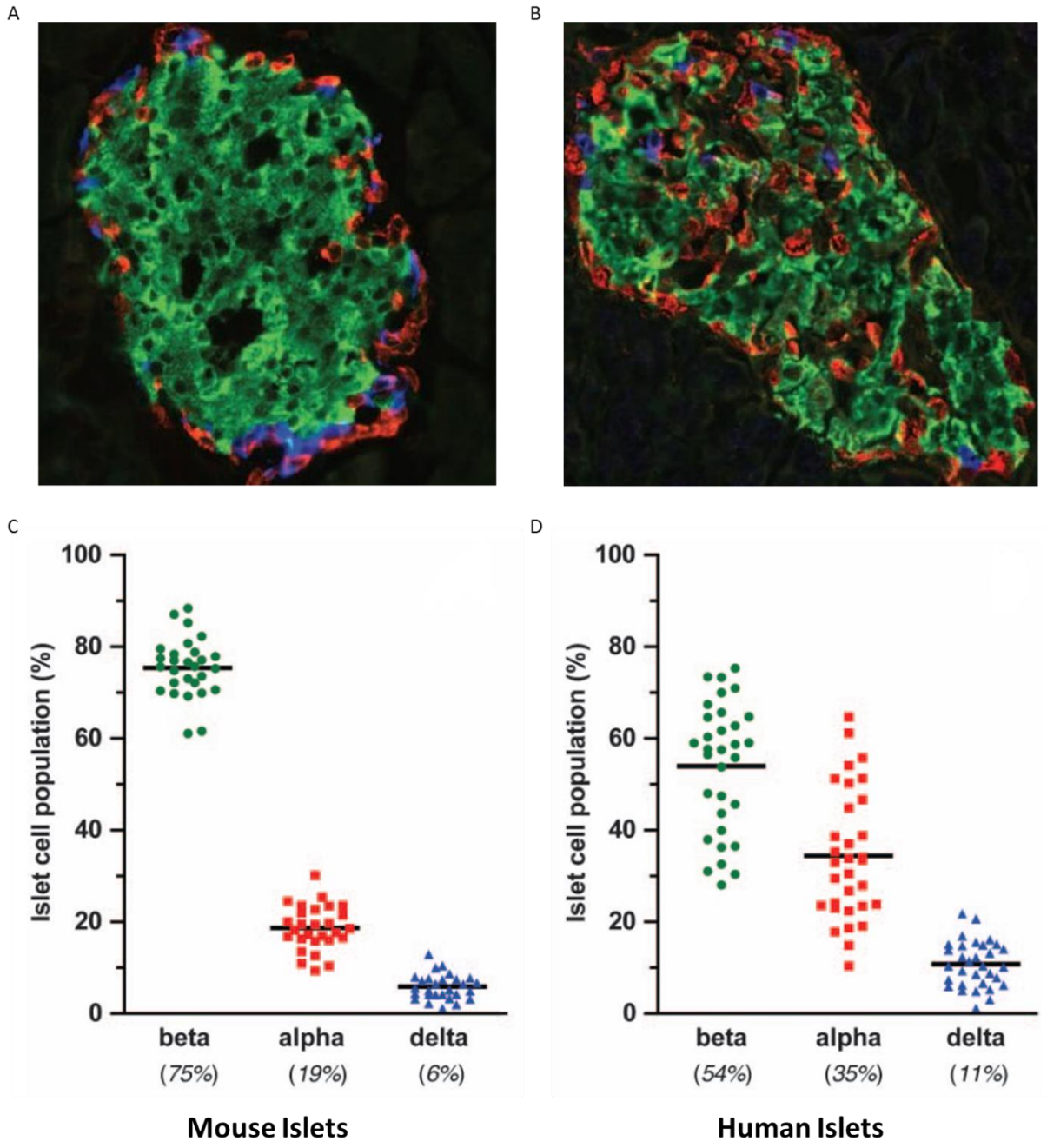

Figure 1.3. Islet morphology and composition in rodents and humans. (A-B) Immunolabeling of a mouse (A) and a human (B) islet sections for insulin (green), glucagon (red), and somatostatin (blue). **(C-D)** Endocrine cell composition of mouse islets (C) (n=28) and human islets (D) (n=32), as determined by analysis of optical sections through the entire islet. Horizontal bars represent the mean of each group. Image adapted from Brissova *et al.*, © 2005 SAGE Publications, (18) and reproduced in compliance with the copyright agreement of SAGE Publications.

restricted to the outer mantle. In humans, there is no discernible core, with the different endocrine cell types intermingled throughout the islet. Mature rodent islets are composed of about 75% β-cells, 19% α-cells, and 6% δ-cells, while mature human islets are composed of about 54% β-cells, 35% α-cells, and 11% δ-cells (18).

Mechanisms of glucose-stimulated insulin secretion

Studies beginning in the 1960s have provided a deep but still incomplete understanding of signal transduction within β-cells. A critical feature of the β-cell is its ability to link changes in metabolic flux, brought on by glucose metabolism, to changes in membrane excitability and subsequent alterations in intracellular Ca^{2+} concentration ($[Ca^{2+}]_i$) and signaling (19; 20). Excitable cells maintain a negative resting membrane potential, primarily mediated by the activity of the Na^+/K^+-ATPase, which pumps Na^+ ions out of and K^+ ions into the cell (21). This activity maintains a higher concentration of K^+ ions inside the cell than outside. During the resting state, ATP-sensitive potassium (K_{ATP}) channels are active, allowing potassium ions to diffuse down their concentration gradient out of the cell. In the triggering pathway of insulin secretion, glucose enters the β-cell through the GLUT2 transporter where it is metabolized in the mitochondria, causing an increase in the intracellular ATP:ADP ratio. This elevation in ATP closes K_{ATP}-channels, inhibiting potassium ion flow out of the cell and causing membrane depolarization and activation of voltage-dependent calcium channels (VDCCs). Opening of VDCCs allows for a transient elevation in $[Ca^{2+}]_i$, triggering insulin granule exocytosis (**Figure 1.4A**) (22). After action potential firing, several types of K-channels are activated to allow K^+ ions to flow out of the cell and mediate membrane re-polarization and returning the cell to the resting state. These channels include

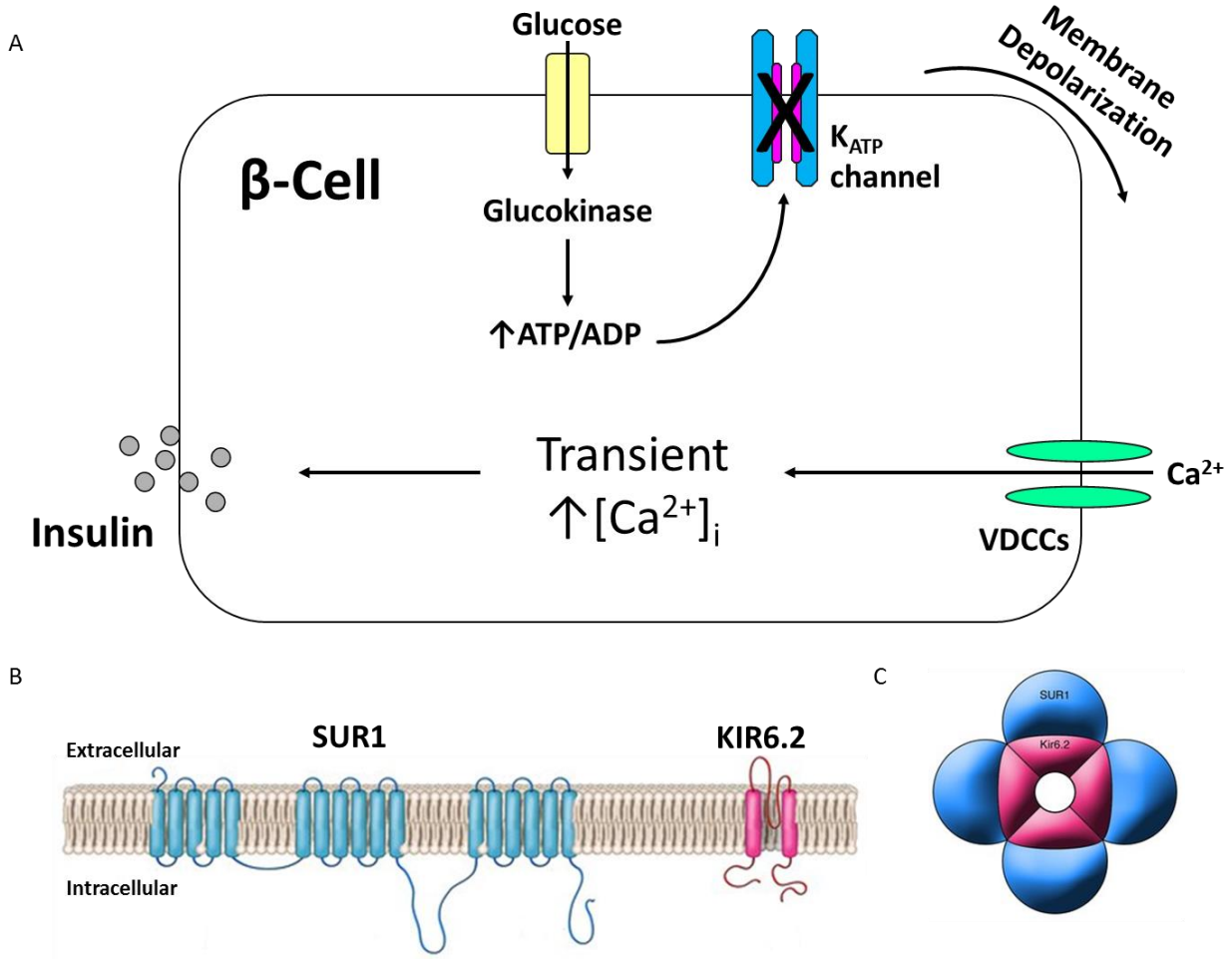

Figure 1.4. Glucose-stimulated insulin secretion in pancreatic β-cells. (A) Glucose enters the β-cell where it is metabolized, in a process initialized by glucokinase, to ultimately elevate the intracellular ATP:ADP ratio. The rise in ATP inhibits the K_{ATP}-channel, causing membrane depolarization and the opening of VDCCs (Voltage-dependent Ca^{2+}-channels). The resulting transient increase in $[Ca^{2+}]_i$ triggers insulin exocytosis. **(B)** Transmembrane topology of the two subunits of the K_{ATP} channel: SUR1 (shown in blue, encoded by *Abcc8*) and KIR6.2 (shown in magenta, encoded by *Kcnj11*). **(C)** Schematic of the heteroctameric structure of the K_{ATP}-channel. Four SUR1 subunits assemble to surround a core of four KIR6.2 subunits, forming the pore of the channel. Panels B and C were adapted from Ashcroft *et al.*, 2005 (22) and reproduced with permission (see Appendix A). © 2005 American Society for Clinical Investigation.

voltage-dependent potassium channels (VDKCs) as well as two-pore domain K+ (K2P) channels (23; 24).

This pathway highlights two well-established control points that regulate insulin secretion: glucokinase (GCK), which determines the rate of glucose phosphorylation (the rate-limiting step of glycolysis) and subsequent metabolism, and the K_{ATP}-channel, which serves to transduce changes in metabolism into electrochemical charge. Both of these control points have been established by experimentation in mouse models (25-28), and confirmed by the identification of genetic mutations in humans (29-33). Identification of specific gain- and loss-of-function mutations identified in humans has, in turn, helped to guide studies in mice, which have provided a very deep understanding of disease mechanisms. The K_{ATP}-channel is a hetero-octameric pore made up of four subunits each of the sulfonylurea receptor type 1 (SUR1) and the inward rectifying potassium channel 6.2 (KIR6.2), the protein products of *Abcc8* and *Kcnj11*, respectively (**Figure 1.4B, C**). Mouse gene knockout studies have shown that deletion of either gene results in a lack of functional K_{ATP} channels (25; 27; 34). The β-cells of these mice exhibit chronically elevated $[Ca^{2+}]_i$ due to persistent membrane depolarization. However, inactivation of either *Abcc8* or *Kcnj11* in mice does not result in hyperinsulinemia, as in humans with deactivating mutations in either gene (25; 27; 34; 35). These findings will be further examined in this thesis.

Pathogenesis of diabetes mellitus

Diabetes mellitus, affecting 29.1 million people in the United States alone (36), is a group of diseases characterized by high blood glucose, or hyperglycemia, brought on by failure of pancreatic β-cells to secrete enough insulin to meet the needs of the body. Type 1 diabetes (T1D),

which makes up about 5% of all diabetes cases (36), develops when β-cells are destroyed by an autoimmune mechanism. Type 2 diabetes (T2D), making up 90-95% of all cases (36), develops in a progressive manner due to the failure of β-cells to secrete enough insulin to match the demand brought on by age, inactivity, obesity, and genetic risk factors. Clinically, the lower-than-necessary insulin secretion first manifests itself as impaired glucose tolerance, and is referred to as pre-diabetes. However, as peripheral insulin resistance mounts, and the relative insulin deficiency worsens, fasting hyperglycemia may soon develop. When it does, hyperglycemia begins to impair β-cell function, starting a downhill spiral that can result in the dedifferentiation and/or death of these cells, and severe hyperglycemia, if not corrected (37-41). While the development of insulin resistance is a necessary prerequisite for this disease, only a fraction of insulin resistant people actually develop diabetes. Genome wide association studies have identified many loci that predispose a person to the development of T2D but we do not know how these genetic variations contribute to T2D disease risk or progression in most cases (42; 43).

Other types of diabetes, such as monogenic forms caused by mutations in single genes, constitute 1-5% of all cases of diabetes (36). For instance, mutations that impair the catalytic function or stability of GCK cause maturity onset diabetes of the young type 2 (MODY2) while heterozygous mutations that increase GCK activity cause persistent hyperinsulinemic hypoglycemia of infancy (PHHI) (32). Moreover, inactivating mutations in both alleles cause persistent neonatal diabetes (PND). Similarly, mutations in either *Abcc8* or *Kcnj11*, the two structural components of K_{ATP}-channels, also cause either PHHI or PND depending on whether they inhibit or stimulate channel activity, respectively (30; 31; 33).

Over the past decade there have been progressively larger waves of genome wide association studies (GWAS) in an attempt to identify the genetic basis for T2D. A recent study

examined 26.7 million variants for T2D association in 11,645 type 2 diabetics and 32,769 controls of European origin by inputting sequence-based genotypes from 13 prior studies (44). The collective effort of many groups has resulted in the identification of at least 85 different loci, most of which are common variants (minor allele frequency > 5%) that are robustly associated with T2D. However, it remains largely unknown how these GWAS-identified regions affect the function of adipose, muscle, and islets. Since the majority of the variants reside in non-coding regions of the genome, and thus are not easily linked to the function of a specific gene, biological experimentation is required to identify the causal gene and to uncover the mechanisms that link gene function with disease risk.

β-cell failure in diabetes

Genetic predisposition itself does not cause T2D. Rather, metabolic stress brought on by insulin resistance, β-cell Ca^{2+} dyshomeostasis, liptoxicity (38; 40; 45) and eventually glucotoxicity (37; 38; 40; 46), in combination with genetic predisposition, cause the disease. If left uncorrected, these stresses can lead to endoplasmic reticulum (ER) dysfunction, oxidative stress, and eventually DNA damage and cell death.

Two major factors contribute to the pathogenesis of T2D: insulin resistance and β-cell dysfunction or failure. Currently, both factors are thought to be important in the development of the disease, but β-cell failure is the final common pathway in the development of T2D (47). Insulin resistance occurs when tissues such as liver, adipose, and muscle no longer respond to the normal actions of insulin. The most common causes of insulin resistance are excess weight and physical inactivity, but other factors such as genetics, ethnicity, and old age can play a role. While insulin

resistance is thought to be necessary for the development of T2D, it cannot be the only factor, since many people with insulin resistance never develop T2D. Many experts in the field believe that β-cell failure, in the face of insulin resistance, is the key determinant in the development of T2D (38; 47-49).

Studies over the past decade strongly suggest that β-cell mass is relatively fixed, and that some individuals, depending on their genetic predisposition, are unable to even modestly increase their β-cell mass in response to mounting insulin resistance, causing their β-cells to become metabolically over-stimulated. At first, the over-stimulation may be transient, as evidenced by a modest postprandial hyperglycemia that soon returns to baseline. However, as glucose homeostasis fails due to insufficient insulin secretion, and hyperglycemia goes from transient to sustained, high blood glucose may soon begin to exert negative effects on the β-cell, and a downhill spiral, culminating in outright β-cell failure, may soon occur (41; 46; 50).

Several mechanisms have been proposed to contribute to loss of functional β-cell mass in T2D, including ER stress, oxidative stress, excitotoxicity, loss of islet integrity/organization, and loss of β-cell identity (**Figure 1.5**) (47). The cause of ER stress is thought to be increased insulin biosynthesis due to increased metabolic demand in the setting of insulin resistance, potentially overwhelming the ER folding capacity (51). Excessively high rates of insulin production place β-cells at risk for ER stress and activation of the unfolded protein response (UPR), which, if unresolved, causes β-cell death (51; 52).

Oxidative stress, a second contributor to β-cell failure, is caused by elevated levels of reactive oxygen species (ROS) due to elevated metabolic load. ROS are natural products of the mitochondrial electron transport chain activated during glucose metabolism. Under hyperglycemic

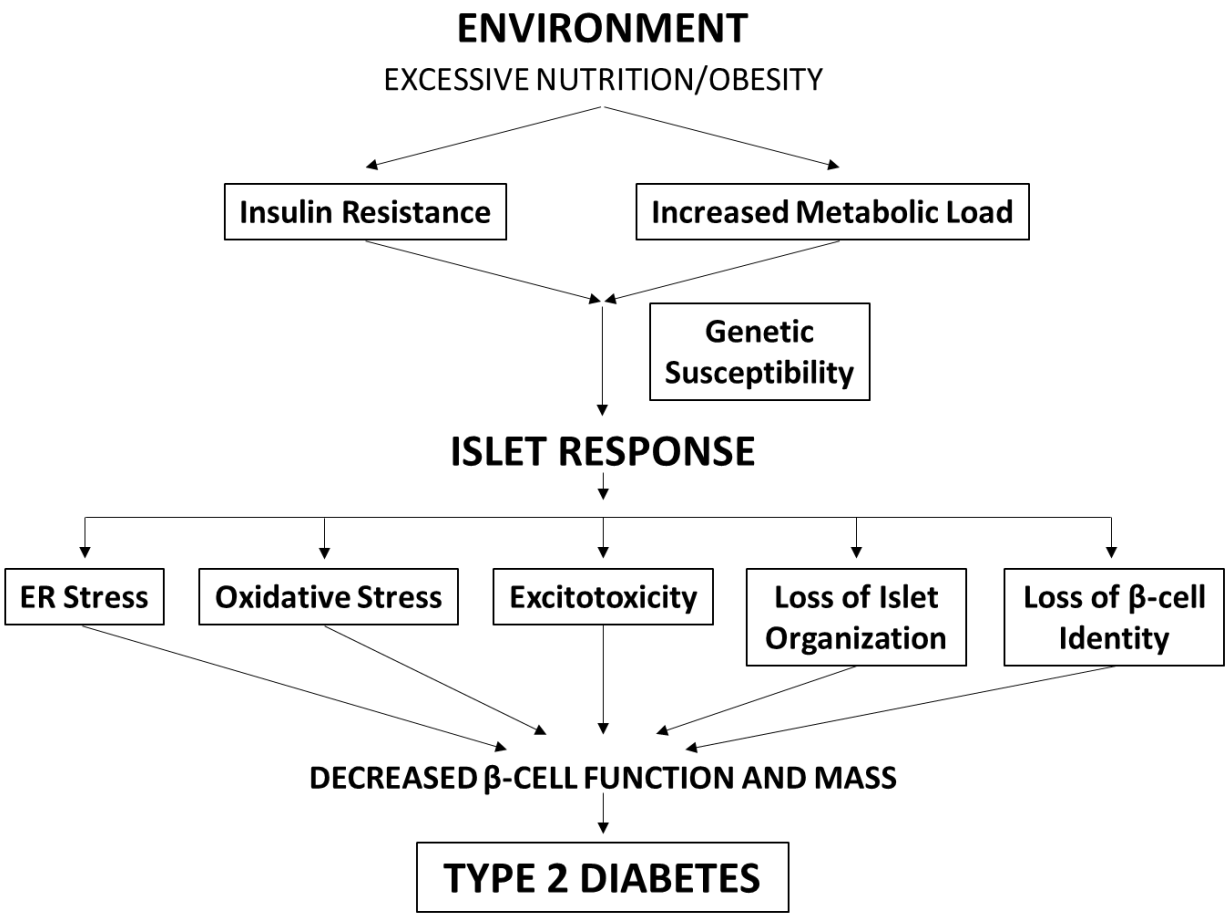

Figure 1.5. β-cell failure in Type 2 Diabetes. In the type 2 diabetic environment, characterized by insulin resistance and increased metabolic load, pancreatic β-cells are faced with many different types of stressors, some of which may be worsened by genetic susceptibility. β-cell stressors include ER stress, oxidative stress, excitotoxicity, loss of islet organization, and loss of β-cell identity, among others. One or any combination of these stressors contribute to decreased β-cell function and mass, ultimately leading to T2D.

conditions, however, β-cells are under elevated metabolic load, increasing the amount of glucose metabolism and ROS production. Additionally, because β-cells express unusually low levels of antioxidant enzymes, they are not able to effectively dispose of excess ROS, further exacerbating the oxidative stress (53). In accordance with this hypothesis, islets from T2D patients have increased markers of oxidative stress, and exhibit impairments in glucose-stimulated insulin secretion (54; 55).

Excitotoxicity, another potential cause of β-cell failure, is a phenomenon originally described in neurons that occurs when an excitable cell type, such as a neuron or a β-cell, experiences chronically elevated $[Ca^{2+}]_i$ due to excess stimulation. Excitotoxicity, caused by excessive stimulation by glucose, has been suggested to cause β-cell dysfunction and eventual death (46), but the molecular mechanisms and the relevance to T2D are not understood.

A fourth factor potentially contributing to β-cell failure is loss of islet organization. The arrangement of endocrine cells within the islet is critical for coordinated hormone secretion, which is maintained through autocrine and paracrine signaling (56). Although loss of islet structure has not been as well-studied as other sources of β-cell failure, hyperglycemia has recently been associated with disrupted islet morphology (57).

Historically, β-cell death was thought to be the main contributor to loss of functional β-cell mass in T2D. However, Talchai and colleagues identified an alternative mechanism called β-cell dedifferentiation, or loss of β-cell identity (41). In this process, elevated metabolic load causes some β-cells to lose expression of key functional markers and begin to express genes normally only expressed during developmental stages or in immature β-cells. Importantly, these dedifferentiated cells no longer function as β-cells should, effectively contributing to the loss of β-

cell mass seen in T2D. Interestingly, dedifferentiated β-cells sometimes transdifferentiate to other endocrine cell types and express other hormones, further contributing to dysregulated glucose homeostasis in T2D. More recent studies corroborate this idea, demonstrating that hyperglycemia alone is sufficient to cause a reversible loss of β-cell identity in mice (57; 58). However, studies of gene and protein expression in human islets have opposing conclusions about the role of β-cell dedifferentiation in the development of T2D, with some citing evidence that it occurs and others postulating that, though it may occur at a low rate, its role in T2D is likely to be minimal (59-62).

Controversy exists regarding the precise definition of β-cell dedifferentiation (63). Some employ a very strict criterion, stating that markers of progenitor cells must be expressed to define a cell as dedifferentiated. However, I prefer a broader definition and view a dedifferentiated β-cell as one in which aspects of differentiation have been lost, but not necessarily that progenitor markers have become expressed. In either case, it is important to determine how this process contributes to loss of functional β-cell mass in T2D, and whether or not it can be reversed.

Calcium signaling in β-cell health and function

As a major second messenger, $[Ca^{2+}]_i$ in β-cells is not only essential for insulin secretion, but it also regulates many cellular processes by modulating the activity of downstream signaling molecules, including Ca^{2+}-dependent enzymes and transcription factors (64; 65). One of the most highly-understood pathways is the calcineurin/nuclear factor of activated T-cells (NFAT) signaling pathway. Calcineurin, a Ca^{2+}-dependent serine/threonine phosphatase, is activated upon binding to both Ca^{2+} and to calmodulin, a Ca^{2+}-binding protein. Once activated, calcineurin de-phosphorylates cytoplasmic NFAT (NFATc), resulting in its translocation to the nucleus where it

interacts with the nuclear NFAT component (NFATn) to activate gene transcription (65). Since the observation that some patients treated with calcineurin inhibitors, such as cyclosporine A, develop post-transplantation diabetes (66), calcineurin has been hypothesized to play a role in islet function. Concordantly, calcineurin inhibition with tacrolimus causes an increase in β-cell death and an inhibition of β-cell proliferation (67). Importantly, all four NFATc proteins (NFATc1-4) are expressed in β-cells (68), providing further support that the calcineurin/NFAT signaling pathway may be active in β-cells.

In alignment with this hypothesis, Heit and colleagues found that knockout of the calcineurin subunit *Cnb1* specifically in β-cells results in severe diabetes due to a marked reduction in β-cell proliferation and glucose intolerance (68; 69). Calcineurin was found to act through NFATc1, which directly binds and regulates the transcription of critical genes controlling β-cell function, including *Ins1, Pdx1, Beta2, Glut2, Hnf4α, Gck, Hnf1α,* and *Hnf1β* as well as cell cycle regulators *Ccnd1* and *Cdk4* (68). In a study by Soleimanpour and colleagues, *Irs2*, another gene involved in β-cell replication and survival, was also found to be bound by NFATc1 in a calcineurin-dependent manner (67). Addition of conditionally active NFATc1 in *Cnb1*-deficient β-cells restores β-cell mass and prevents the onset of diabetes (68), revealing that the calcineurin/NFAT pathway is essential for maintaining pancreatic β-cell mass and function.

In addition to calcineurin, Ca^{2+} also regulates the activity of several Ca^{2+}/Calmodulin-dependent kinases (CaMKs), serine/threonine kinases that require the binding of Ca^{2+}/Calmodulin for enzymatic activity (65). In the β-cell, CaMKII, specifically, is known to play a role in promoting insulin release in response to glucose-stimulated Ca^{2+}-influx by phosphorylating downstream targets (70; 71). Dadi and colleagues recently generated a mouse model allowing for tetracycline-inducible inhibition of CaMKII activity specifically in β-cells (72). β-cells in these

mice exhibit reduced glucose-stimulated insulin secretion and glucose intolerance. Furthermore, they found that CaMKII functions as a Ca^{2+}-sensor, participating in a positive feedback mechanism to regulate cytoplasmic Ca^{2+} levels in the β-cell.

In addition to promoting insulin release, CaMKs have also been shown to control β-cell gene expression by modulating the activity of various transcription factors in response to Ca^{2+}/Calmodulin binding. Phosphorylation of the transcription factor cAMP response element-binding protein (CREB) at Serine 133 by CaMKs, triggers its activation and binding to target genes at the cAMP response element (CRE) sequence (73). Studies in the mouse have shown that the activity of CREB promotes β-cell survival through the induction of insulin receptor substrate 2 (IRS2) (74), a key regulator of β-cell mass (75; 76). More recently, studies in a β-cell line and in mouse islets revealed that CaMKIV phosphorylates CREB to activate IRS2 and prevents β-cell apoptosis (77; 78). Several other studies have also highlighted the importance of CREB coactivators, including transducer of regulated CREB protein 2 (TORC2) (79; 80) and cAMP-regulated transcriptional coactivator 2 (CRTC2) (81).

Calcium signaling in β-cell failure

Although activation of Ca^{2+}-dependent transcription is essential for β-cell development, function, and survival, the over-activation of similar pathways can also lead to β-cell failure and/or death. Transgenic mice over-expressing calmodulin specifically in β-cells develop severe diabetes due to markedly-reduced insulin content (82). Transgenic mice over-expressing constitutively-activated calcineurin develop hyperglycemia due to increased β-cell apoptosis and reduced β-cell proliferation (83). Additionally, over-activation of glucose metabolism by β-cell-specific

expression of mutant glucokinase in mice transiently causes increased β-cell proliferation, but chronically results in hyperglycemia due to increased β-cell apoptosis (46; 50). Chronic elevations in $[Ca^{2+}]_i$, alternately termed β-cell excitotoxicity, may be deleterious to β-cell function in a similar way that sustained neuronal excitation causes the dysfunction and death of neurons (84; 85). The idea that a sustained elevation of $[Ca^{2+}]_i$ has a deleterious effect on β-cells is consistent with the finding that inhibition of voltage-dependent calcium channels prevents β-cell death in the setting of insulin resistance (86).

Calcium signaling in loss of islet morphology

In addition to developing severe diabetes, transgenic mice engineered to over-express calmodulin specifically in β-cells also exhibit severely disrupted islet morphology, with a reduced number of β-cells, a greater number of α- and δ-cells, and a greater number of α- and δ-cells localized to the islet core (82). A similar phenotype has also been observed in animals deficient for the K_{ATP}-channel, whose β-cells exhibit chronically elevated $[Ca^{2+}]_i$ (25; 34; 35; 87), suggesting that overactivation of Ca^{2+}/Calmodulin-dependent signaling pathways causes a disruption in islet morphology, although a definitive cause for this phenotype has not been established.

Calcium signaling in loss of β-cell identity

It has long been known that pancreatic endocrine cell fate is plastic, with cells maintaining the ability to convert between lineages with relative ease. For example, forced expression of PAX4

or ARX promotes α- to β-cell or β- to α-cell conversion, respectively (88; 89), forced expression of PDX1 induces α- to β-cell reprogramming (90), and genetic loss of DNMT1 in β-cells can induce their conversion to an α-cell fate (91; 92). Additionally, extreme ablation of β-cells induces a genetically-encoded program in α-cells to promote their conversion to β-cells (93). However, these studies have been conducted under non-physiological conditions, and β-cell reprogramming had not, until recently, been observed in a disease context.

Talchai and colleagues were the first to observe loss of β-cell identity and subsequent conversion to other cell types in the context of metabolic stress (41). In this process, termed β-cell dedifferentiation, elevated metabolic load, induced by the combination of *Foxo1* loss and either multiparty or age, causes some β-cells to lose expression of key functional markers, including Insulin, *MafA*, and *Pdx1*, and begin to express *Ngn3*, a gene normally only expressed during developmental stages or in immature β-cells. These dedifferentiated cells no longer function normally, contributing to the loss of β-cell mass seen in T2D, and sometimes convert, or transdifferentiate, to other endocrine cell types and express other hormones, such a glucagon (41). Importantly, β-cell dedifferentiation was also observed in diabetic GIRKO (GLUT4-insulin receptor knock-out line 1) mice (41), suggesting that it may be part of the natural progression of the disease.

A more recent study from the same group identified a novel marker of dedifferentiated β-cells (94). ALDH1A3, also called RALDH3, is a retinaldehyde dehydrogenase that was found to be specifically enriched in β-cells of *Foxo* knockout mice and of *db/db* and GIRKO diabetic mouse models, as well as in islets of diabetic humans (60; 94). ALDH1A3^{+} cells are associated with weak MAFA expression and elevated L-myc and NGN3 expression. At present, the relationship between ALDH1A3 and β-cell dedifferentiation is not well-understood. ALDH1A3 may serve as only a

marker for β-cell dedifferentiation as it does not itself cause β-cell dysfunction, since acute gain of function of ALDH1A3 does not inhibit β-cell function (94).

Though chronically elevated β-cell $[Ca^{2+}]_i$ has been associated with β-cell failure, its role in loss of β-cell identity has only very recently been explored. Dahan and colleagues reported that the developmental endocrine hormone gastrin is induced in β-cells of *db/db* mice, Akita mice, and mice with diphtheria toxin-induced hyperglycemia, as well as in human type 2 diabetic β-cells (95). Interestingly, this increase in *Gast* expression was inhibited when Ca^{2+}-influx was blocked but was not increased when Ca^{2+}-influx was induced, suggesting that *Gast* expression in the context of hyperglycemia requires Ca^{2+}-influx, but that Ca^{2+}-influx is not sufficient. This Ca^{2+}-dependent increase in *Gast* expression requires the action of calcineurin, a Ca^{2+}-dependent phosphatase, since Tacrolimus, a calcineurin inhibitor, prevented hyperglycemia-induced *Gast* expression. The authors suggest that the process of Ca^{2+}-induced *Gast* expression represents a "reprogrammed" β-cell, since the β-cells become polyhormonal, expressing both insulin and gastrin, but not a true "dedifferentiated" β-cell, since they do not express developmental markers, such as NGN3.

Mouse models in diabetes research

The house mouse, *Mus musculus*, is a very common animal model in biomedical research for a variety of reasons. First, mice share over 90% of their genetic material with humans (96). Although this similarity is not as high as humans with non-human primates, mice exhibit a short generation time and can be easily genetically manipulated. Mice have been particularly useful for studying human pancreas development as well as diabetes disease progression. Furthermore, since

availability of human pancreas tissue samples is low and because the quality of such samples is variable, mice have provided a very robust experimental model.

The Mouse-ENCODE Consortium (97) has shown that there is substantial conservation between the mouse and human genome, and that many fundamental processes and pathways that control gene activity are conserved in both species. However, there are major differences between mice and humans, particularly with respect to islets and β-cells. For instance, the arrangement of endocrine cells in mice differs from that in humans (**Figure 1.3**), as does the expression of key transcription factors, such as MAFA and MAFB. In mice, both MAFA and MAFB are expressed during development, but MAFB becomes restricted to α-cells in the adult (98). In humans, both factors are expressed in adult β-cells (99). These differences have led some to assert that studies in mice are irrelevant to understanding of T2D in humans. While I consider that viewpoint to be extreme, and see value in robustly conducted studies in mice, I acknowledge the need to be able to translate and validate knowledge gained in mice to humans. The bulk of the current knowledge about β-cell development and function has been derived from mice, and studies from the Magnuson lab contributed greatly to the knowledge base enabling three coding variants arising from studies of T2D (GCKR, PPARG and ABCC8) to be considered as causal for their respective GWAS signals (44).

Since the discovery of the Cre/Lox system to genetically inactivate or over-express specific genes in a cell-type-specific way, a variety of pancreas-specific Cre-driving transgenic mouse models have been designed (100). Similarly, the ability to genetically tag specific cell types with fluorescent proteins using transgenic constructs has enabled the isolation of pure populations of cells using fluorescence-activated cell sorting (FACS, described in the following section).

Transgenes allowing for pancreatic progenitor cell-specific or β-cell-specific gene expression have been particularly useful in studying β-cell development and function.

FACS and transcriptome analysis of islet cell populations

Since the discovery of green fluorescent protein (GFP) and its utility as a reporter of gene expression, fluorescent proteins have been widely used in both transgenic and knock-in mouse models. Because of the utility of GFP, many other fluorescent proteins have been engineered to produce different colors to allow for simultaneous expression of more than one fluorescent reporter in the same mouse. These fluorescent proteins are used to report gene expression either by fluorescence microscopy or by FACS.

By incorporating cell type or population-specific fluorescent proteins into transgenic and knock-in mouse models, pure endocrine cell populations are easily obtained, and are often paired with high-throughput downstream applications, including RNA-sequencing, to understand global gene expression under various conditions. Studies of β-cell-specific gene expression in humans, however, have been limited by the fact that pure β-cell populations are not easily obtained, since genetically-encoded fluorescent reporters are not achievable in humans. As a consequence, whole-islet gene expression is often assayed, but these results are confounded by the fact that a heterogeneous cell population (containing not only β-cells, but also α- , δ-, and PP-cells as well as neurons and blood vessels) is used.

Markus Grompe's group first identified cell surface markers allowing for separation of pure human islet cell populations using FACS (101), and soon after began exploring the transcriptome from those sorted populations (102). Since then, FACS has been an invaluable

technique in increasing our understanding of the transcriptomes of human islet cell types (103-107). However, some argue that, since these studies examine the entire population of a specific cell type, they fail to address population heterogeneity. There is mounting evidence that subpopulations within major islet cell types exist and are defined by specific differences in gene expression and properties (108-110).

To overcome this issue, several groups have recently harnessed a new technology, called single-cell RNA-seq, to examine gene expression on the single-cell level (59; 62; 111; 112). This approach eliminates the need for fluorescent reporters or cell-type specific markers because cells are classified post-analysis based on gene expression of respective hormones. This technology also represents an important advance in the field, since researchers can begin to understand β-cell heterogeneity in both mice and humans, and to understand heterogeneity in normal and type 2 diabetic patients. However, there are limitations to the approach as well. Because of the huge number of cells sequenced in these studies and due to the miniscule amount of RNA obtained from individual cells, the data is limited by shallow sequencing depths (fewer than 1 million reads per sample), making it likely that important discoveries are missed. Therefore, until single-cell technologies allow for the depth of sequencing that can be attained using cell populations, a combination of both approaches is needed to achieve a complete understanding of islet cell gene expression.

In the following chapters, I describe our collection of seventeen RNA-seq datasets from FACS-purified mouse β-cells with the goal of better understanding the mechanism by which β-cells fail in response to different types of stress. First, we used mice lacking *Abcc8*, a key component of the β-cell K_{ATP}-channel, to analyze the effects of a sustained elevation in the intracellular Ca^{2+} concentration ($[Ca^{2+}]_i$) on β-cell identity and gene expression. We found that

chronically elevated β-cell $[Ca^{2+}]_i$ results in the dysregulation of over 4,200 genes, as well as modest loss of β-cell identity, characterized by decreased expression of key functional genes, increased expression of genes associated with β-cell dedifferentiation, increased β-cell transdifferentiation to PP-expressing cells, and decreased β-cell function. These studies prompted us to propose a model by which chronically elevated β-cell $[Ca^{2+}]_i$ acts through a putative Ca^{2+}-regulated transcription factor, ASCL1, to disrupt a network of genes, contributing to β-cell failure.

In addition to exploring the effects of chronically elevated $[Ca^{2+}]_i$ on β-cell gene expression, we analyzed β-cells from mice ectopically expressing human growth hormone (hGH), mice made insulin resistant by feeding a high-fat diet (HFD), and mice of different sexes. We found that both ectopic hGH and HFD have beneficial effects (induction of β-cell proliferation genes) as well as deleterious effects (increased expression of ER stress genes) on β-cell function. Ultimately, the collection of 17 RNA-sequencing datasets allowed us to perform weighted gene correlation network analysis (WGCNA) to generate modules of similarly-expressed genes. Several of these initial modules have meaningful correlations to specific β-cell stresses. Overall, these studies highlight the power of using whole transcriptome datasets from highly-pure cell populations and have allowed us to elucidate how stress alters the β-cell gene regulatory network.

CHAPTER II

MATERIALS AND METHODS

Mouse models and husbandry

All animal experimentation was approved by the Vanderbilt Institutional Animal Care and Use Committee. Mice were fed a standard chow diet (PicoLab, 5L0D) unless otherwise specified, maintained on a 12-hour light/dark cycle, and were specific-pathogen-free. For glucose homeostasis characterization, male mice were given either a 10% fat (by kilocalories) control diet (Research Diets, Inc., D12450B) or a 60% fat diet (HFD, Research Diets, Inc., D12492). For RNA-sequencing, mice were fed either a chow diet or a 60% fat diet for 30 days beginning at postnatal day (p)30.

Mice bearing the *Sur1*^{neo} allele (*Abcc8*$^{tm1.1Mgn}$, MGI: 2388392) were maintained in a congenic C57BL/6 background and genotyped as previously described (25). *MIP-GFP* mice (*Tg(Ins1-EGFP/GH1)*^{14Hara}, MGI:3583654) were maintained in a congenic CD-1 line and genotyped as previously described (113). *RIP-Cre* mice (*Tg.Ins2-cre*^{25Mgn}, MGI: 2176227) were maintained in a congenic C57BL/6 background and were genotyped using primers 5'-CTCTGGCCATCTGCTGATCC-3' and 5'-CGCCGCATAACCAGTGAAAC-3'. *Gt(ROSA)26Sor*$^{tm1(EYFP)Cos}$ mice were purchased from The Jackson Laboratory and were genotyped as previously described (114). For RNA-sequencing, the C57BL/6 line bearing the *Sur1*^{neo} allele was interbred with the CD-1 line containing the MIP-GFP transgene. Offspring of these matings were then interbred resulting in mice that were a random mix of both CD-1 and C57BL/6 strains.

Generation of *Ins2*$^{Apple.LCA}$ mice

To facilitate the generation of new transgenic mouse lines with pancreatic β-cell specific gene expression we used recombinase-mediated cassette exchange (RMCE) utilizing *Cre* recombinase and two heterotypic *Lox* sites (115). This is a two-step procedure that generally requires the generation of mouse embryonic stem cells (mESCs) containing a loxed cassette acceptor (LCA) allele followed by RMCE to introduce the desired gene sequences into this site. To simplify this strategy, we designed a targeting vector for the *Ins2* locus that expresses an H2B-Apple fusion protein and functions as an LCA allele. The targeting vector was made based on pSP72.Ins2.GFP.LNL (116), which was a gift from Lori Sussel (Barbara Davis Center, University of Colorado). This plasmid, which contains 5' and 3' homology arms of 7078 and 3570 bps, respectively, was modified to contain a Lox66 site, the H2B-Apple sequence, an FRT-flanked PU-ΔTK (puromycin resistance-Δ-thymidine kinase) selection cassette, and a Lox2272 site. Inclusion of the Lox66, Lox2272, and PU-ΔTK features enables dual function as an LCA **(Figure 2.1A)**. After electroporation, 162 puromycin-resistant mESC clones were obtained and were screened by Southern blot hybridization using region-specific 5' and 3' probes. Six correctly targeted clones were identified, one of which (1C4) was injected into mouse blastocysts to generate chimeric mice **(Figure 2.1B)**. After germline transmission, the *Ins2*$^{LCA.Apple}$ mice were genotyped using the following primers: Ins2F1 (5'-GAGGTGTTGACGTCCAATGAG-3') and Ins2R1 (5'-GAACTCACCTTGTGGGTCCTC-3'), which produce a wild type band of 562 bp; Ins2F and AppleR1 (5'-CATGTTATTCTCCTCGCCCTTG-3'), which produce an *Ins2*$^{LCA.Apple}$ allele specific band of 876 bp; and Cherry 2F (5'-CAGTTCATGTACGGCTCC-3') and InsSeqR1 (5'-CAGTGGCAGAACTCACCTTG-3'), which produce an *Ins2*$^{LCA.Apple}$ allele specific band of 684 bp after PU-ΔTK is deleted by Flpe **(Figure 2.1C)**.

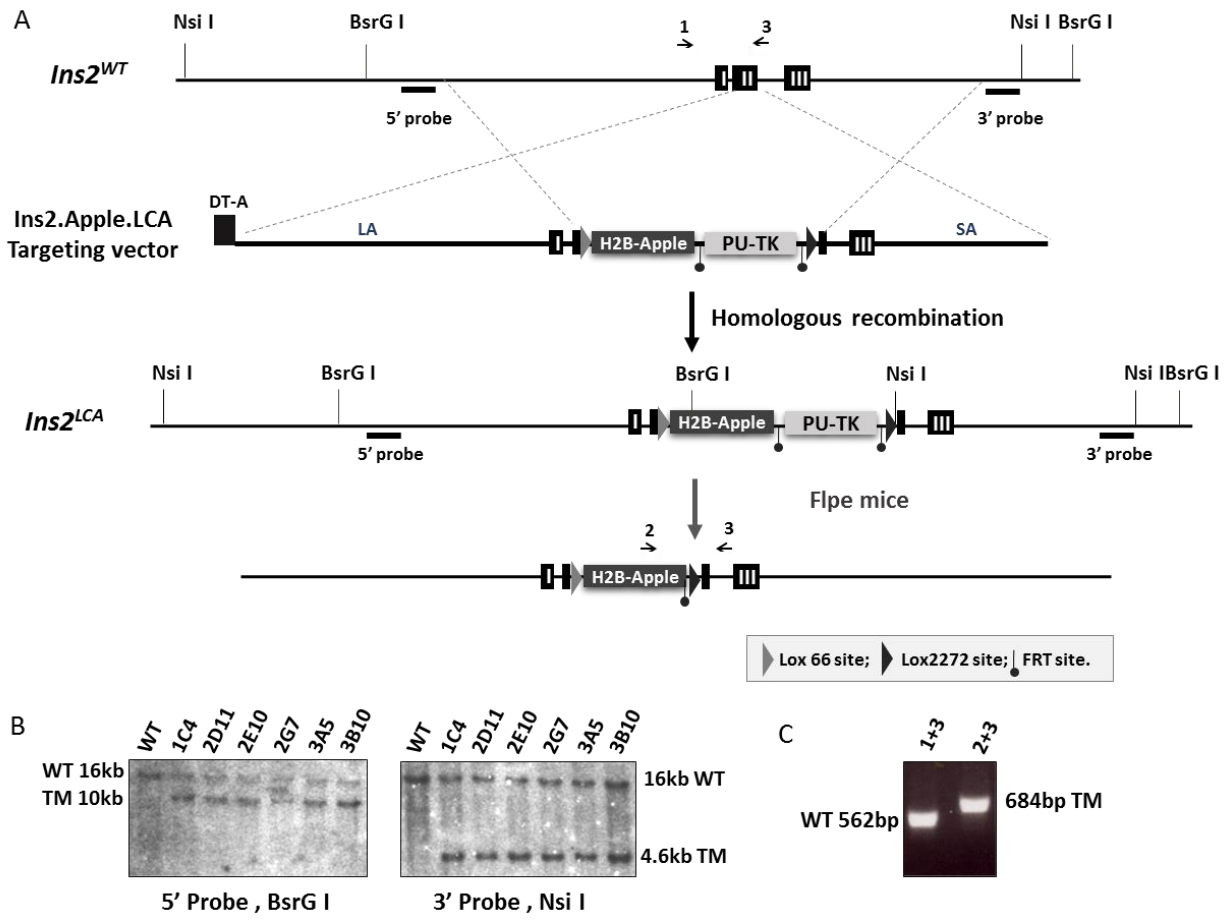
A
Nsi I
BsrG I
1
3
Nsi I BsrG I
Ins2WT
5' probe
3' probe
Ins2.Apple.LCA
Targeting vector
DT-A
LA
H2B-Apple
PU-TK
SA
Homologous recombination
Nsi I
BsrG I
BsrG I
Nsi I
Nsi IBsrG I
Ins2LCA
5' probe
3' probe
Flpe mice
2
3
H2B-Apple
Lox 66 site;
Lox2272 site;
FRT site.
B
WT
1C4
2D11
2E10
2G7
3A5
3B10
WT 16kb
TM 10kb
16kb WT
4.6kb TM
5' Probe , BsrG I
3' Probe , Nsi I
C
1+3
2+3
WT 562bp
684bp TM
D
Insulin
Apple

Figure 2.1. Generation of *Ins2*$^{Apple.LCA}$ mice. (A) Schematic of the Ins2.Apple.LCA targeting vector, which contains a Lox66 site, the H2B-Apple sequence, an FRT-flanked PU-ΔTK selection marker, and a Lox2272 site. *Ins2*^{WT} represents the wildtype *Ins2* allele. The *Ins2*^{LCA} allele was created by homologous recombination in mouse ES cells. To generate the final allele, mice expressing the *Ins2*$^{Apple.LCA}$ allele were crossed with mice expressing Flpe, to excise the PU-ΔTK cassette. Primer binding sites are represented by arrows above the schemes. **(B)** Southern blot analyses using either BsrGI-digested ES cell clone DNA and the 5' probe or NsiI-digested ES cell clone DNA and the 3' probe. Clone 1C4 was injected into mouse blastocysts to generate live mice. **(C)** PCR analysis used to distinguish between the wildtype and targeted *Ins2* alleles. **(D)** Representative images from frozen pancreatic sections from *Ins2*$^{Apple.LCA}$ mice stained for Insulin and RFP. Panels B-D show primary data generated by Rama Gangula and Anna Osipovich.

Generation of *Ins2*$^{Apple.hGH}$ mice

The variant *Ins2*$^{LCA.Apple.hGH}$ allele was made by inserting human growth hormone (hGH) genomic sequences downstream of H2B-Apple using RMCE. First, an exchange vector (pIns2.H2B-Apple.hGH) was made based on the pMCS.71/2272.hygro vector (117). This plasmid contains a Lox71 site, H2B-Apple, a 3 kb fragment of the hGH gene, a Lox2272 site, and an FRT-flanked pgk-Hygro positive selection cassette **(Figure 2.2A)**. Clone 1C4 *Ins2*$^{LCA.Apple}$ mESCs were then co-electroporated with the exchange plasmid and pBS185, a *Cre*-expression plasmid, as previously described (117). Of 90 hygro-resistant clones, nine survived ganciclovir selection, all of which were determined by PCR to be correctly exchanged. Clone 1C4/1A1 (68% normal karyotype) was injected into mouse blastocysts to achieve germ-line transmission. To genotype the *Ins2*$^{LCA.Apple.hGH}$ mice, the following primers were used: Ins2F1 and AppleR1, which produce a band of 713 bp, and Hygro.3R (5'-ACCGATGGCTGTGTAGAAGTACT-3') and Ins2R1, which produce a band of 739 bp **(Figure 2.2B)**. The pgk-Hygro selection cassette was removed by interbreeding with mice containing a Flpe-expressing transgene (118), then backcrossed into a C57BL/6 background. All mice used for experiments were at least 94% congenic for C57BL/6.

Glucose tolerance testing

Following a 16-hour fast, male mice were given an intraperitoneal injection of D-glucose (2 mg per g body weight). Blood glucose concentrations were taken at 0, 15, 30, 60, and 120 minutes post glucose bolus and were measured using a BD Logic glucometer.

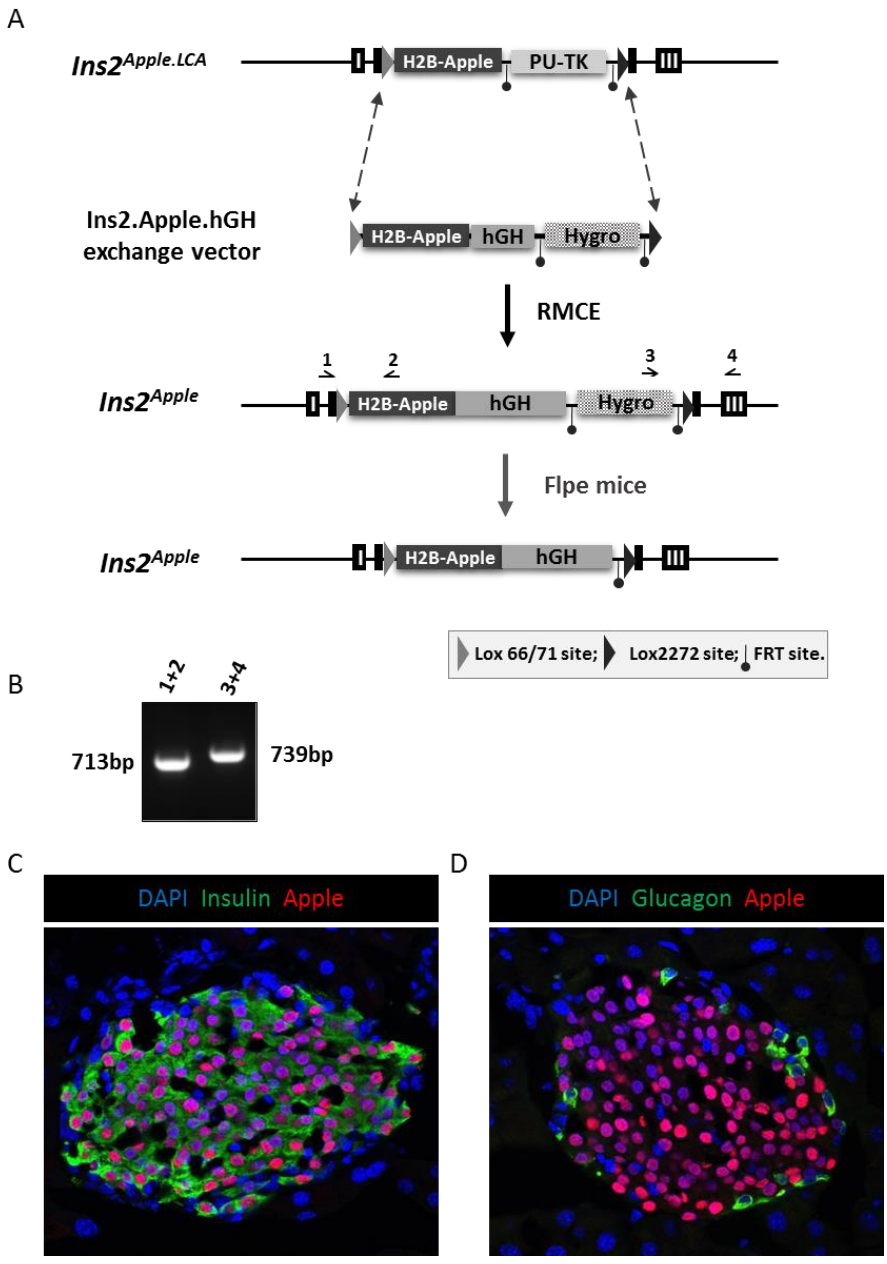

Figure 2.2. Generation of *Ins2*$^{Apple.hGH}$ mice. (A) Schematic of the Ins2.Apple.hGH exchange vector, which contains a Lox71 site, the H2B-Apple sequence, a 3kb fragment of hGH, an FRT-flanked pgk-Hygro selection marker, and a Lox2272 site. The *Ins2*^{Apple} allele was generated by RMCE in mouse ES cells expressing the *Ins2*$^{Apple.LCA}$ allele. To generate the final allele, mice expressing the *Ins2*^{Apple} allele were crossed with mice expressing Flpe to excise the pgk-Hygro cassette. Primer binding sites are represented by arrows above the schemes. **(B)** PCR analysis used to identify mice expressing the targeted allele and mice in which pgk-Hygro has been excised **(C)** Frozen pancreatic sections from adult *Ins2*$^{Apple.hGH}$ mice stained for DAPI, Insulin, and Apple. **(D)** Frozen pancreatic sections from adult *Ins2*$^{Apple.hGH}$ mice stained for DAPI, Glucagon, and Apple. Panel B shows primary data generated by Rama Gangula.

Insulin tolerance testing

Following a 6-hour fast, male mice were given an intraperitoneal injection of human insulin (0.75 mU/g body weight). Blood glucose concentrations were taken at 0, 15, 30, and 60 minutes post insulin bolus and were measured using a BD Logic glucometer.

Verapamil administration

Adult *Abcc8*$^{+/+}$*; MIP-GFP* and *Abcc8*$^{-/-}$*; MIP-GFP* mice were given either Splenda (2%) or a combination of Verapamil (1mg/mL, Sigma, V4629) and Splenda in their drinking water for three weeks. Splenda was used to mask any taste of Verapamil.

Immunofluorescence microscopy

Whole pancreata were fixed for 4 hours in 4% paraformaldehyde, incubated overnight at 4°C in 30% sucrose, embedded in OCT compound (Tissue Tek), frozen on dry ice, and sectioned at a depth of 8 microns. For TUNEL assay, whole pancreata were fixed overnight in 10% formalin, embedded in paraffin, and sectioned at a depth of 5 microns. Immunofluorescence staining was performed as previously described (119). Antibodies used are listed in **Table 2.1**. After antibody staining, slides were mounted with Prolong Gold with DAPI (Invitrogen). Images were acquired using either a Zeiss Axioplan-II upright microscope or an Olympus FV-1000 inverted confocal microscope, were pseudo-colored using ImageJ (NIH), and are representative of the phenotype observed in at least three different animals per group per time point.

Table 2.1: Primary antibodies used

Antibody	Species	Company	Dilution
ALDH1A3	Rabbit	Novus Biologicals	1:500
GFP (YFP)	Chicken	Invitrogen	1:2000
Glucagon	Rabbit	Linco	1:1000
Insulin	Guinea pig	Invitrogen	1:1000
Insulin	Rabbit	Cell Signaling	1:100
Pancreatic polypeptide	Guinea pig	Linco	1:1000
RFP (Apple)	Rabbit	Rockland	1:1000
S100A6	Sheep	R&D Systems	1:100
Serotonin (5-HT)	Rabbit	ImmunoStar	1:1000
Somatostatin	Rabbit	ICN Biomedicals	1:1000

Morphometric analysis

In general, morphometric analysis was performed by manual cell counting of 10-15 representative islets per animal using immunofluorescent images in ImageJ. To determine percentages of each endocrine cell type, the total number of cells expressing a specific hormone and the total number of cells within the islet were counted. To determine the percentages of each endocrine cell type inside the islet core, the total number of cells expressing the specific hormone that were greater than two cell diameters inside the islet were determined. To assess β-cell death, an In Situ Cell Death Detection Kit (TUNEL, Roche, 11684795910) was used on paraffin-

embedded pancreatic sections from *Abcc8*$^{-/-}$ and *Abcc8*$^{+/+}$ mice at 12 weeks of age. Insulin co-staining was performed to label pancreatic β-cells. For each *Abcc8*$^{-/-}$*; R26*$^{LSL.YFP}$*; RIP-Cre* and *Abcc8*$^{+/+}$*; R26*$^{LSL.YFP}$*; RIP-Cre* animal, the total number of cells co-expressing YFP and a specific hormone were determined.

Islet isolation

Pancreata were digested by injection of 0.6 mg/mL Collagenase P (Roche) into the pancreatic bile duct. Partially dissociated tissue was fractionated using a Histopaque-1077 (Sigma) gradient followed by hand-picking of islets. For FACS and RNA-sequencing, islets from 3-7 mice were pooled for each sample. For qRT-PCR, islets from a single mouse were used per sample.

Resting membrane potential and Ca^{2+} imaging

Islets were isolated from the pancreata of 7- to 10-week-old *Abcc8*$^{+/+}$; *MIP-GFP* and *Abcc8*$^{-/-}$; *MIP-GFP* mice and cultured in poly-d-lysine (Sigma) coated 35-mm glass-bottom dishes (Cellvis) in RPMI 1640 supplemented with 15 % FBS, 100 IU/ml penicillin, and 100 mg/ml streptomycin at 37 °C, 5% CO_2 for 42 hrs. A perforated patch-clamp technique was employed to record plasma-membrane potentials from single β-cells using an Axopatch 200B amplifier with pCLAMP10 software. Cells were washed twice with Krebs-Ringer–HEPES buffer (KRHB) with (in mmol/L) 119.0 NaCl, 2.0 $CaCl_2$, 4.7 KCl, 25.0 HEPES, 1.2 $MgSO_4$, and 1.2 KH_2PO_4 (adjusted to pH 7.35 with NaOH) with 11.0 mM glucose. Patch electrodes (3-5 MΩ) were filled with an intracellular buffer (IC) with (in mmol/L) 150.0 KCl, 3.0 $MgCl_2$, 0.03 amphotericin B, and 10.0

HEPES (adjusted to pH 7.25 with KOH). Membrane potential was held at -80 mV, and islets were perifused with KRHB with 11 mM glucose while a seal was being formed between the recording pipette and the cell membrane. Once a seal was formed (≥ 1 GΩ) β-cell membrane potential was monitored at 11 mM glucose for 10 min then perifusion was switched to KRHB with 2 mM glucose for 30 min. For intracellular calcium imaging, islets were isolated from pancreata of 9- to 11-week-old *Abcc8*$^{+/+}$and *Abcc8*$^{-/-}$ mice, and imaging of cytoplasmic calcium was performed as previously described (120).

Islet culture

Purified islets were incubated overnight at 37°C in RPMI-1640 (Gibco 11879-020) growth medium supplemented with 10% heat-inactivated FBS (Gibco, 16140-071), 1% penicillin-streptomycin (Pen/Strep, Gibco, 15140-122), and 11 mM D-glucose (Research Products International Corp, G32040). The next morning, islets were incubated in DMEM (Gibco, 11966-025) supplemented with 5.6 mM glucose, 10% FBS, and 1% Pen/Strep for two hours at 37°C. Islets were then incubated in either experimental or control medium, and incubated for 24 hours at 37°C. Experimental media were made from DMEM (5.6 mM D-glucose, 10% FBS, and 1% Pen/Step) and contained 100 μM tolbutamide (Sigma, T0891) or 20 mM KCl (Sigma, P5405), with or without 50 μM verapamil (Sigma, V4629).

Cell isolation

Purified islets were dispersed in an Accumax (Sigma) and 1U/mL DNase (Invitrogen, AM2222) solution at 37°C. Flow Cytometry Buffer (FCB, R&D systems, FC001) supplemented with DNase and 0.5M EDTA was added to the cell suspension, and cells were filtered using a 35-μm cell strainer. Cell pellets were resuspended in FCB supplemented with DNase and EDTA. Either 7AAD (ThermoFisher, A1310, final concentration 1 μg/mL, for *MIP-GFP* islets) or DAPI (ThermoFisher, D21490, final concentration 5 μg/mL, for *Ins2.Apple* islets) was added to the sorting media for exclusion of dead cells. Live cells expressing the fluorescent reporter were collected with a 100-μm nozzle using the FACS Aria II (BD Biosciences) instrument. Cells were collected in the Maxwell 16 LEV simplyRNA Tissue Kit (Promega, TM351) Homogenization Solution supplemented with 1-thioglycerol.

RNA purification and quality control

RNA was isolated from either FACS-purified β-cells or whole islets using the Maxwell 16 LEV simplyRNA Tissue Kit (Promega, TM351). After purification, RNasin (40 U/uL, Promega) was added to the RNA samples before storage at -80°C. RNA samples were analyzed using the Agilent 2100 Bioanalyzer, and only samples with an RNA integrity number greater than 7 were used for sequencing or qRT-PCR.

Library assembly and sequencing

RNA samples from FACS-purified β-cells were amplified using the SMART-Seq v4 Ultra Low Input RNA Kit for Sequencing (Clontech) using 8 cycles of PCR. cDNA libraries were constructed using the Low Input Library Prep Kit (Clontech). RNA sequencing of *Abcc8*$^{+/+}$*; MIP-GFP* and *Abcc8*$^{-/-}$*; MIP-GFP* samples was performed on the Illumina NextSeq500 instrument using paired-end, 75 nucleotide reads. RNA-seq data are available in the ArrayExpress database (www.ebi.ac.uk/arrayexpress) under the accession number E-MTAB-4726. RNA sequencing of *Ins2*$^{Apple/+}$ samples was performed on the Illumina HiSeq3000 instrument using paired-end, 75 nucleotide reads.

Bioinformatics analysis

Raw sequencing reads were processed utilizing TrimGalore 0.4.0 (which relies on CutAdapt 1.9.dev2) to remove adapter sequences and pairs that were either shorter than 20 bp or that had Phred scores less than 20. The Spliced Transcripts Alignment to a Reference (STAR) application (121) was used to perform sequence alignments to the mm10 (GRCm38) mouse genome reference and GENCODE comprehensive gene annotations (Release M8). STAR's two-pass mapping approach was used to increase the detection of reads mapping to novel junctions identified during the first mapping pass. Overall, approximately 88-91% of the raw sequencing reads were uniquely mapped to genomic sites. Finally, HTSeq was used for counting reads mapped to genomic features (122), and DESeq2 was employed for differential gene expression analysis (123), using the Advanced Computing Center for Research and Education (ACCRE) at Vanderbilt University.

Pathway analysis and upstream regulator prediction

The DAVID Bioinformatics Resource 6.8 Beta was used for functional annotation clustering and to identify KEGG pathways enriched in different conditions using differentially-expressed genes generated from RNA-seq data. iRegulon (124) was used to predict gene regulatory networks. Default search parameters were used (20kb centered around the transcription start site, 7 species conservation). Enrichment score threshold was 3.0.

Quantitative reverse transcription polymerase chain reaction (qRT-PCR)

The High Capacity cDNA Reverse Transcription Kit (Life Technologies) was used to convert whole islet RNA to cDNA. qRT-PCR was performed on the Applied Biosystems 7900HT instrument using the 2X SyBR Green PCR Master Mix (Life Technologies). Samples were analyzed in triplicate, and were normalized to Hprt expression. Primer sequences are listed in **Table 2.2**.

Table 2.2: qRT-PCR primer sequences

Gene	Forward Primer	Reverse Primer
Aldh1a3	5’-GGGTCACACTGGAGCTAGGA	5’-CTGGCCTCTTCTTGGCGAA
Ascl1	5’-GACTTTGGAAGCAGGATGGCA	5’-CACCCCTGTTTGCTGAGAAC
Hprt	5’-TACGAGGAGTCCTGTTGATGTTGC	5’-GGGACGCAGCAACTGACATTTCTA
S100a4	5’-AGCACTTCCTCTCTCTTGGTC	5’-TCATCTGTCCTTTTCCCCAGG
S100a6	5’-CACATTCCATCCCCTCGACC	5’-GTGGAAGATGGCCACGAGAA

Weighted gene correlation network analysis (WGCNA)

WGCNA is a method used to determine highly-correlated gene modules relating clusters of genes to each other and to pre-determined sample traits. Briefly, WGCNA determines a connection weight between pairs of genes and identifies gene modules by applying a soft threshold power to correlations between pairs of genes within a network. Starting with seventeen RNA-Seq datasets from FACS-purified β-cells, we utilized WGCNA (version 1.51) (125) to remove expressed genomic features that had excessive missing values using an iterative function called "goodSampleGenes." We proceeded with network construction and module detection, by first choosing a soft-thresholding power β against which co-expression similarity is used to calculate adjacency (126). Several candidate β values were tested, the resultant network topologies inspected, and a β value of 0.8 identified as the lowest power for which the scale-free topology fit index is optimal. The actual network was constructed using the following parameters, including the soft thresholding power of 0.8, a relatively large minimum module size of 50, a medium sensitivity for cluster splitting, and a block size larger than the number of genomic features to avoid the splitting of data. Computation was performed on Vanderbilt's ACCRE computing cluster, with 96GB of RAM resourced to ensure matrix calculations for the entire gene set could be executed:

```
blockwiseModules(datExpr, maxBlockSize = 25000, power = 8, deepSplit = 2,
                        TOMType = "unsigned", minModuleSize = 50,
                        reassignThreshold = 0, mergeCutHeight = 0.25,
                        numericLabels = TRUE, pamRespectsDendro = FALSE,
                        saveTOMs = TRUE,
                        saveTOMFileBase = "wgcnaTOM",
                        verbose = 3)
```

This WGCNA script implements all of the steps of module detection. Specifically, it automatically constructs a correlation (co-expression) network, creates a cluster tree, defines modules as branches, and merges close modules. We determined module-trait relationships by correlating gene-module membership against gene-trait significance, and then determined the overall correlation of all genes with modules to the individual traits. Relationships with p-value < 0.05 were considered significant. Correlation networks were exported for modules of interest and visualized in Cytoscape 3.

Statistical analysis

Statistical significance was determined using two-tailed Student's t-test. Data is represented as mean ± s.e.m. A threshold of $p < 0.05$ was used to declare significance.

CHAPTER III

CHRONIC β-CELL DEPOLARIZATION IMPAIRS β-CELL IDENTITY BY DISRUPTING A NETWORK OF CA^{2+}-REGULATED GENES

Introduction

In Type 2 Diabetes (T2D), pancreatic β-cells fail to respond appropriately to metabolic stresses brought on by age, obesity, and genetic risk factors. The mechanisms by which chronic metabolic stress, including insulin resistance, glucotoxicity, and lipotoxicity (39; 40; 46) impair β-cell function are not understood. While metabolic stress is usually considered to be exogenous to the β-cell, chronic stimulation leads to changes within the β-cell, impairing function. One such factor is chronic elevation in $[Ca^{2+}]_i$, sometimes called excitotoxicity (85), which may be triggered by sustained β-cell depolarization due to chronic stimulation.

Ca^{2+} is a ubiquitous second messenger that is central to regulating cellular dynamics of many cell types, including β-cells. Genetic and pharmacological perturbations that either stimulate or impair Ca^{2+}-signaling have dramatic effects on β-cell function. For instance, the disruption of calcineurin, a Ca^{2+}-dependent phosphatase, or either CaMKII or CamKIV, two Ca^{2+}-dependent kinases, profoundly impairs β-cell function, likely by modulating the activity of Ca^{2+}-responsive transcription factors such as NFAT, CREB, and TORC2 (67; 68; 72; 79; 81). Conversely, the constitutive activation of calcineurin or calmodulin, a Ca^{2+}-binding protein, also causes marked β-cell dysfunction (46; 82; 83).

Acutely, glucose metabolism induces ATP-sensitive potassium (K_{ATP}) channel closure, membrane depolarization, opening of voltage-gated Ca^{2+}-channels, a rise in $[Ca^{2+}]_i$, and insulin secretion. However, sustained elevation in $[Ca^{2+}]_i$ has multiple effects on β-cell function that can either be adaptive or maladaptive. β-cell proliferation induced by glucose metabolism (50) is an example of an adaptive response to sustained elevations in $[Ca^{2+}]_i$. However, chronically elevated $[Ca^{2+}]_i$ can also induce maladaptive responses, since prevention of Ca^{2+}-influx in the setting of insulin resistance prevents β-cell death (86). In either case, mice lacking K_{ATP}-channels exhibit disrupted islet morphology, characterized by α-cells being located in the islet core (87; 127). The cause is not understood, but could reflect either loss of cell identity or impairments in cell adhesion.

In this chapter, I will show that β-cells in *Abcc8*$^{-/-}$ mice exhibit chronic membrane depolarization that results in a sustained elevation in $[Ca^{2+}]_i$. The persistent increase in $[Ca^{2+}]_i$, in turn, alters the expression of over 4,200 genes, some of which are involved in cell adhesion, Ca^{2+}-binding and Ca^{2+}-signaling, and maintenance of β-cell identity. We found that *Abcc8*$^{-/-}$ mice exhibit β-cell to PP-cell trans-differentiation and have increased expression of *Aldh1a3,* a gene recently suggested as a marker of de-differentiating β-cells. Additionally, we show that *S100a6* and *S100a4,* two EF-hand Ca^{2+}-binding proteins, are acutely regulated in β-cells by membrane depolarization agents, suggesting that they may be markers for β-cell excitotoxicity. Finally, we performed a computational analysis to predict components of the gene regulatory network that may govern the observed gene expression changes and found that one of the predicted regulators, *Ascl1*, is directly regulated by Ca^{2+} influx in β-cells.

Results

Abcc8$^{-/-}$ β-cells exhibit persistent membrane depolarization and elevated $[Ca^{2+}]_i$

Previous studies have shown chronically elevated $[Ca^{2+}]_i$ and continuous action potential firing in β-cells of mice lacking K_{ATP}-channels (25; 27; 34). To definitively establish *Abcc8*$^{-/-}$ mice as a model for chronically elevated β-cell $[Ca^{2+}]_i$, we measured membrane potential at high (11mM) and low (2mM) glucose concentrations (**Figure 3.1A, B**). While *Abcc8*$^{-/-}$ β-cells exhibit action potentials in high glucose, they fail to undergo membrane potential polarization in low glucose (**Figure 3.1B**). Quantification of the changes in *Abcc8*$^{-/-}$ β-cell membrane potentials confirms that *Abcc8*$^{-/-}$ β-cells show no difference in membrane potential between high and low glucose, contrary to *Abcc8*$^{+/+}$ β-cells (**Figure 3.1C, D**). Importantly, continual depolarization of *Abcc8*$^{-/-}$ β-cells causes a chronic elevation in $[Ca^{2+}]_i$, as shown by Ca^{2+}-imaging at both low and high glucose (**Figure 3.2A**). Quantification of area under the curve shows that *Abcc8*$^{-/-}$ β-cells have significantly higher $[Ca^{2+}]_i$ than *Abcc8*$^{+/+}$ β-cells at each time interval measured (**Figure 3.2B**). Interestingly, despite having chronically elevated β-cell $[Ca^{2+}]_i$, *Abcc8*$^{-/-}$ mice have long been known to have surprisingly small disturbances in their plasma glucose concentrations (25). First, as previously reported (128) they exhibit outright hypoglycemia in the fasted state (**Figure 3.4A**). Second, we have also observed that they exhibit a trend toward mild hyperglycemia in the fed state (**Figure 3.4B**).

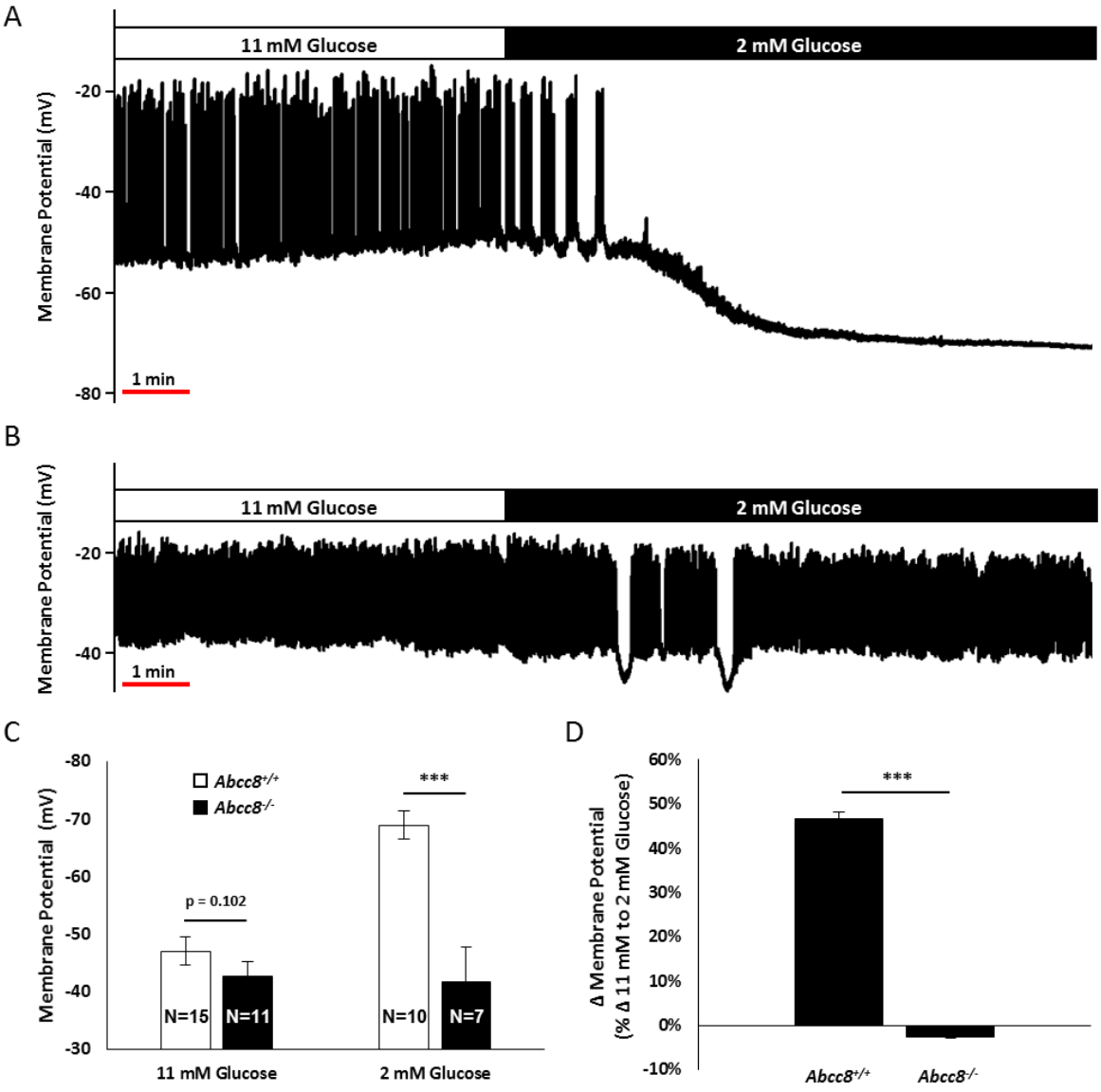

Figure 3.1. *Abcc8*$^{-/-}$ β-cells exhibit persistent membrane depolarization. A perforated patch recording technique was employed to monitor the membrane potential of *Abcc8*$^{+/+}$ and *Abcc8*$^{-/-}$ β-cells in whole islets. **(A)** *Abcc8*$^{+/+}$ β-cells display normal activity at 11mM glucose and become hyperpolarized in response to 2mM glucose (representative recording). **(B)** *Abcc8*$^{-/-}$ β-cells display activity similar to *Abcc8*$^{+/+}$ β-cells at 11mM glucose (with a trend toward a depolarized plateau potential); however, their activity remains statistically unchanged in response to 2mM glucose (representative recording). **(C)** Quantification of the potentials of *Abcc8*$^{+/+}$ and *Abcc8*$^{-/-}$ β-cells at 11mM and 2mM glucose. *Abcc8*$^{+/+}$ β-cells become significantly more polarized in response to 2mM glucose while there is no difference between *Abcc8*$^{-/-}$ β-cells at 11mM and 2mM glucose. **(D)** Quantification of the percent change in membrane potential between 11mM and 2mM glucose for *Abcc8*$^{+/+}$ and *Abcc8*$^{-/-}$ β-cells. The membrane potential of *Abcc8*$^{+/+}$ β-cells changes significantly more than *Abcc8*$^{-/-}$ β-cells. ***p<0.001. This data was generated by Matthew Dickerson and David Jacobson.

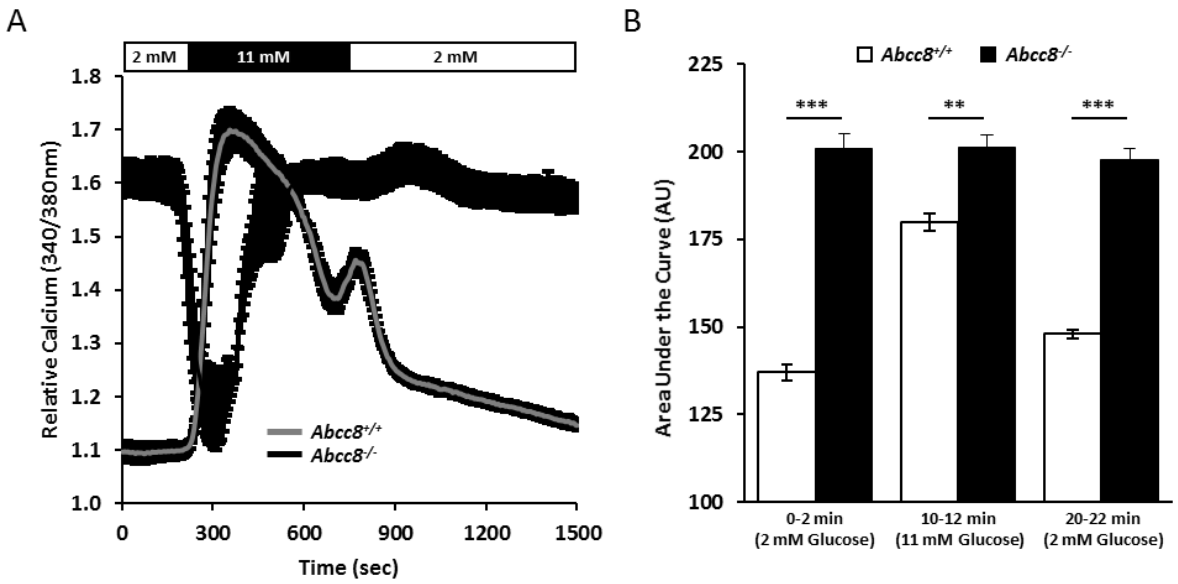

Figure 3.2. ***Abcc8*$^{-/-}$ β-cells exhibit elevated [Ca^{2+}]$_i$. (A)** Intracellular Ca^{2+} was monitored in *Abcc8*$^{+/+}$ and *Abcc8*$^{-/-}$ islets with Fura-2 AM. Islets were equilibrated in 2mM glucose, stimulated with 11mM glucose, and returned to 2mM glucose as indicated by the bars above the traces (overall averages are shown). **(B)** Intracellular Ca^{2+} area under the curve (AUC) was quantified at intervals representing low glucose conditions (0-2 min), glucose-stimulation (10-12 min), and a return to low glucose (20-22 min). Data are an average of $n \geq 21$ islets from three animals. **$p<0.01$, ***$p<0.001$. This data was generated by Matthew Dickerson and David Jacobson.

β-cell identity becomes compromised in *Abcc8*$^{-/-}$ mice

During prolonged metabolic stress, β-cells can lose expression of functional markers and convert to other endocrine cell types (41). However, β-cell de-differentiation has not been studied in the context of chronically elevated $[Ca^{2+}]_i$. Thus, we performed β-cell lineage tracing using *Abcc8*$^{-/-}$*; RIP-Cre*; *Rosa26*$^{LSL.YFP/+}$ mice. While there was no evidence for either β- to α-cell or β- to δ-cell trans-differentiation (**Figure 3.3D, E**), we observed an increase in YFP/PP co-expression (**Figure 3.3C**). Most YFP/PP co-expressing cells are poly-hormonal, expressing both PP and insulin (**Figure 3.3A**), but a few cells (0.24% of the YFP$^+$ cells, 10% of the YFP/PP double$^+$ cells, **Figure 3.3F**) have ceased insulin expression (**Figure 3.3B**). Administration of a Ca^{2+}-channel blocker to *Abcc8*$^{-/-}$ mice resulted in a decrease in Insulin/PP co-expressing cells, but the difference was not significant (**Figure 3.3G**). The loss of β-cell identity correlates with impaired glucose tolerance not attributable to β-cell death (**Figure 3.4A, C**). Complete dedifferentiation, retention of YFP expression but loss of hormone expression, was only observed at a very low rate that was similar among wildtype and knock-out animals (0.19% and 0.21%, respectively, **Figure 3.3H**).

RNA expression profiling of *Abcc8*$^{-/-}$ and *Abcc8*$^{+/+}$ β-cells

To determine how chronically elevated β-cell $[Ca^{2+}]_i$ affects gene expression, we performed RNA-sequencing using FACS-purified β-cells from *Abcc8*$^{-/-}$*; MIP-GFP* mice at 8-9 weeks of age. Since the inclusion of an hGH mini-gene in the *MIP*-GFP allele causes both hGH expression and activation of STAT5 signaling (129), we used *MIP-GFP*-expressing mice as controls. Principal component and gene clustering analyses (**Figure 3.5B, C**), performed on RNA-Seq data from FACS-purified cells (**Figure 3.5A**), indicates that most of the top 500 differentially-

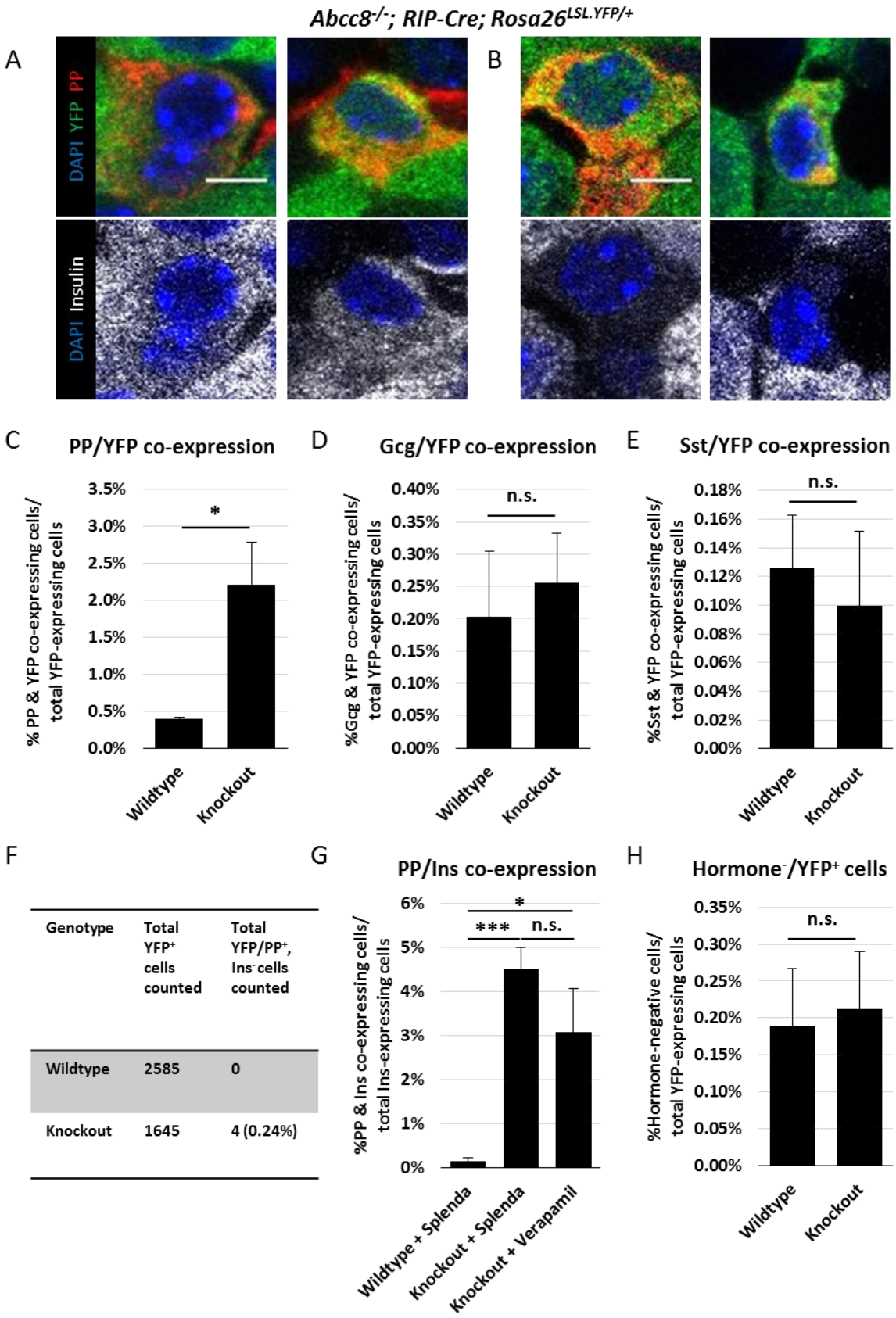
Abcc8-/-; RIP-Cre; Rosa26LSL.YFP/+
A
DAPI YFP PP
DAPI Insulin
B
C
PP/YFP co-expression
% PP & YFP co-expressing cells/ total YFP-expressing cells
3.5%
3.0%
2.5%
2.0%
1.5%
1.0%
0.5%
0.0%
*
Wildtype
Knockout
D
Gcg/YFP co-expression
%Gcg & YFP co-expressing cells/ total YFP-expressing cells
0.40%
0.35%
0.30%
0.25%
0.20%
0.15%
0.10%
0.05%
0.00%
n.s.
Wildtype
Knockout
E
Sst/YFP co-expression
%Sst & YFP co-expressing cells/ total YFP-expressing cells
0.18%
0.16%
0.14%
0.12%
0.10%
0.08%
0.06%
0.04%
0.02%
0.00%
n.s.
Wildtype
Knockout
F
Genotype
Total YFP+ cells counted
Total YFP/PP+, Ins- cells counted
Wildtype
2585
0
Knockout
1645
4 (0.24%)
G
PP/Ins co-expression
%PP & Ins co-expressing cells/ total Ins-expressing cells
6%
5%
4%
3%
2%
1%
0%
*
***
n.s.
Wildtype + Splenda
Knockout + Splenda
Knockout + Verapamil
H
Hormone-/YFP+ cells
%Hormone-negative cells/ total YFP-expressing cells
0.35%
0.30%
0.25%
0.20%
0.15%
0.10%
0.05%
0.00%
n.s.
Wildtype
Knockout

Figure 3.3. Loss of strict β-cell identity in *Abcc8*$^{-/-}$ mice. We performed β-cell lineage tracing using *Abcc8*$^{-/-}$*; RIP-Cre; R26*$^{LSL.YFP/+}$ animals and assessed β-cell dedifferentiation at 12 weeks of age. **(A)** Representative examples of polyhormonal cells co-expressing YFP, PP, and insulin. **(B)** Representative examples of YFP-labeled cells that are expressing PP but not expressing insulin. **(C)** Quantification of PP/YFP double^{+} cells shows an increase in their occurrence in *Abcc8*$^{-/-}$*; RIP-Cre; R26*$^{LSL.YFP/+}$ mice compared to *Abcc8*$^{+/+}$*; RIP-Cre; R26*$^{LSL.YFP/+}$ mice at 12 weeks of age. **(D, E)** Quantification of YFP/Glucagon double^{+} cells (D) or YFP/Somatostatin double^{+} cells (E) shows no difference in the prevalence of these cells in wild type and knockout mice, suggesting that *Abcc8*$^{-/-}$ β-cells do not transdifferentiate to α- or δ-cells. **(F)** Summary of the total number of YFP and PP double-positive, but insulin-negative, cells observed in *Abcc8*$^{+/+}$*; RIP-Cre; R26*$^{LSL.YFP}$ and *Abcc8*$^{-/-}$*; RIP-Cre; R26*$^{LSL.YFP}$ animals at 12 weeks of age. **(G)** Quantification of PP/Insulin double^{+} cells in frozen pancreatic sections shows a trend towards a decrease in polyhormonal cells in 8-9-week-old *Abcc8*$^{-/-}$ mice after 3 weeks of verapamil administration ($p=0.26$). However, the difference is not statistically significant. **(H)** Quantification of the number of YFP-positive, hormone-negative cells observed in *Abcc8*$^{+/+}$*; RIP-Cre; R26*$^{LSL.YFP}$ and *Abcc8*$^{-/-}$*; RIP-Cre; R26*$^{LSL.YFP}$ animals at 12 weeks of age. N=3-4 animals, 10-15 islets counted per animal. Scale bar = 5μm. *$p < 0.05$, ***$p < 0.001$, n.s. = Not Significant.

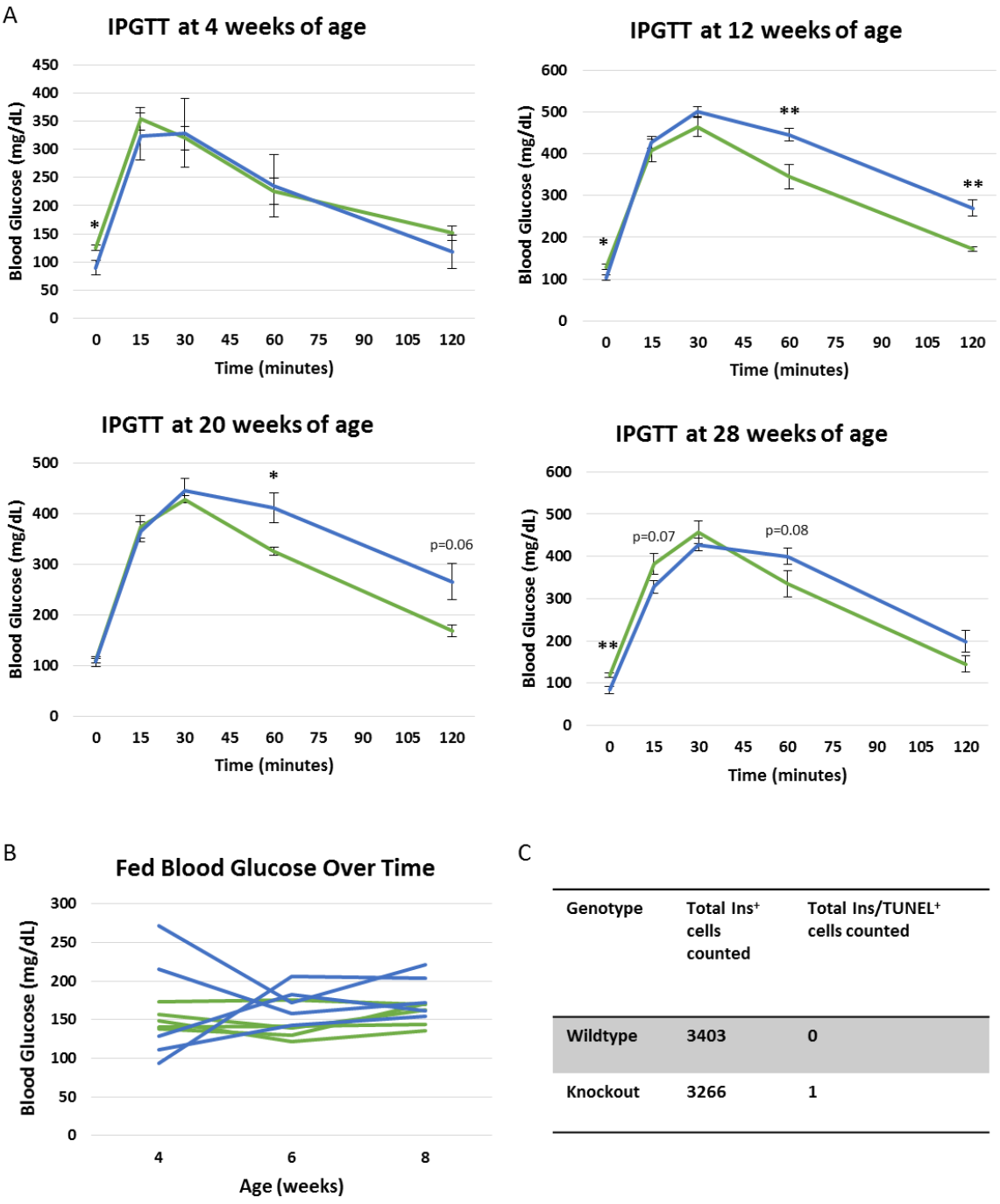

C

Genotype	Total Ins$^+$ cells counted	Total Ins/TUNEL$^+$ cells counted
Wildtype	3403	0
Knockout	3266	1

Figure 3.4 Mild glucose intolerance in *Abcc8*$^{-/-}$ mice. (A) Glucose tolerance tests using male *Abcc8*$^{+/+}$ or *Abcc8*$^{-/-}$ C57BL/6 mice at 4, 12, 20, and 28 weeks of age. Green lines represent *Abcc8*$^{+/+}$ mice. Blue lines represent *Abcc8*$^{-/-}$ mice. Error bars represent standard error. *p<0.05, **p<0.01. n=4-10 mice. **(B)** Fed blood glucose concentration in a cohort of *Abcc8*$^{+/+}$ and *Abcc8*$^{-/-}$ mice between from 4 to 8 weeks of age showing no difference between the groups. n=5 animals per genotype. Green lines represent *Abcc8*$^{+/+}$ mice. Blue lines represent *Abcc8*$^{-/-}$ mice. **(C)** Rate of β-cell death as assessed by TUNEL assay at 12 weeks of age in *Abcc8*$^{+/+}$ and *Abcc8*$^{-/-}$mice.

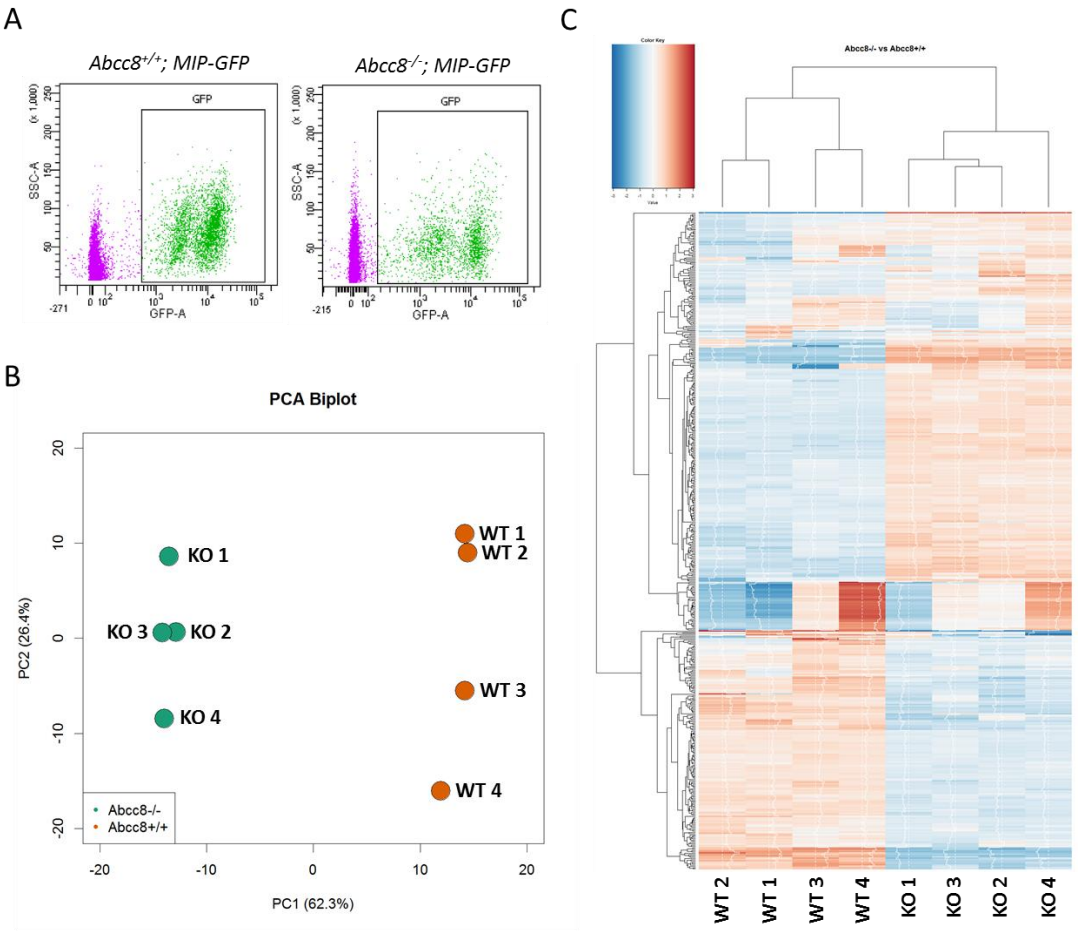

Figure 3.5. Principal Component Analysis and Gene Clustering Analysis. (A) FACS profiles of sorted populations from *Abcc8*$^{+/+}$*; MIP-GFP* and *Abcc8*$^{-/-}$*; MIP-GFP* mice indicating that β-cells from both genotypes can be purified similarly. **(B)** Principal component analysis shows that the eight samples used for RNA-sequencing cluster by genotype, with some variation in the second principal component. **(C)** Heat map depicting gene clustering analysis using the top 500 differentially-expressed genes. "WT" = *Abcc8*$^{+/+}$. "KO" = *Abcc8*$^{-/-}$. J.P. Cartailler of Creative Data Solutions generated panels B and C.

expressed genes cluster as expected. Differential expression analysis (**Figure 3.6B**) reveals 4,208 differentially-expressed genes (2,152 downregulated and 2,056 upregulated) in *Abcc8*$^{-/-}$ β-cells (adjusted p-value < 0.05). Approximately 90% are protein-coding, 3% are non-coding RNAs, 2% are pseudogenes, and 3% are other types of processed transcripts (**Figure 3.6A**).

Abcc8$^{-/-}$ β-cells exhibit changes in expression of genes involved in β-cell maturation, Ca^{2+}-signaling, and cell adhesion

To correlate gene expression with the functional abnormalities of *Abcc8*$^{-/-}$ islets, we examined genes known to be highly enriched in mature β-cells and observed that *Ins1*, *Slc2a2*, *Neurod1*, *Gck*, *Glp1r*, *Npy*, several synaptotagmins, *Tph1*, *Tph2*, and *Egfr* are all down-regulated (**Figure 3.6C**). Conversely, *Ppy* is upregulated in *Abcc8*$^{-/-}$ β-cells, consistent with our observation of poly-hormonal cells.

Since *Abcc8*$^{-/-}$ β-cells have chronically elevated $[Ca^{2+}]_i$, we examined genes involved in Ca^{2+}-binding or signaling. The genes affected included *Myo7a*, a Ca^{2+}/Calmodulin-binding myosin motor protein, *Pcp4*, a calmodulin-binding protein known to protect neurons from Ca^{2+}-induced toxicity (130), and *Cacng3*, a subunit of a voltage-dependent Ca^{2+}-channel. In addition, *Nfatc1*, *Mef2c*, and *Mef2d*, three calcium-regulated transcription factors; *Camk1d*, *Camkk1*, and *Camkk2*, three kinases involved in calcium-signaling; and *S100a1*, *S100a3*, *S100a4*, *S100a6*, and *S100a13*, five EF-hand calcium-binding proteins, are up-regulated (**Figure 3.6C**).

We and others have previously observed that mice lacking K_{ATP}-channels have severely disrupted islet morphology (25; 34; 87). To better understand the progressive deterioration in islet morphology, we quantified the changes occurring over time in the number and location within

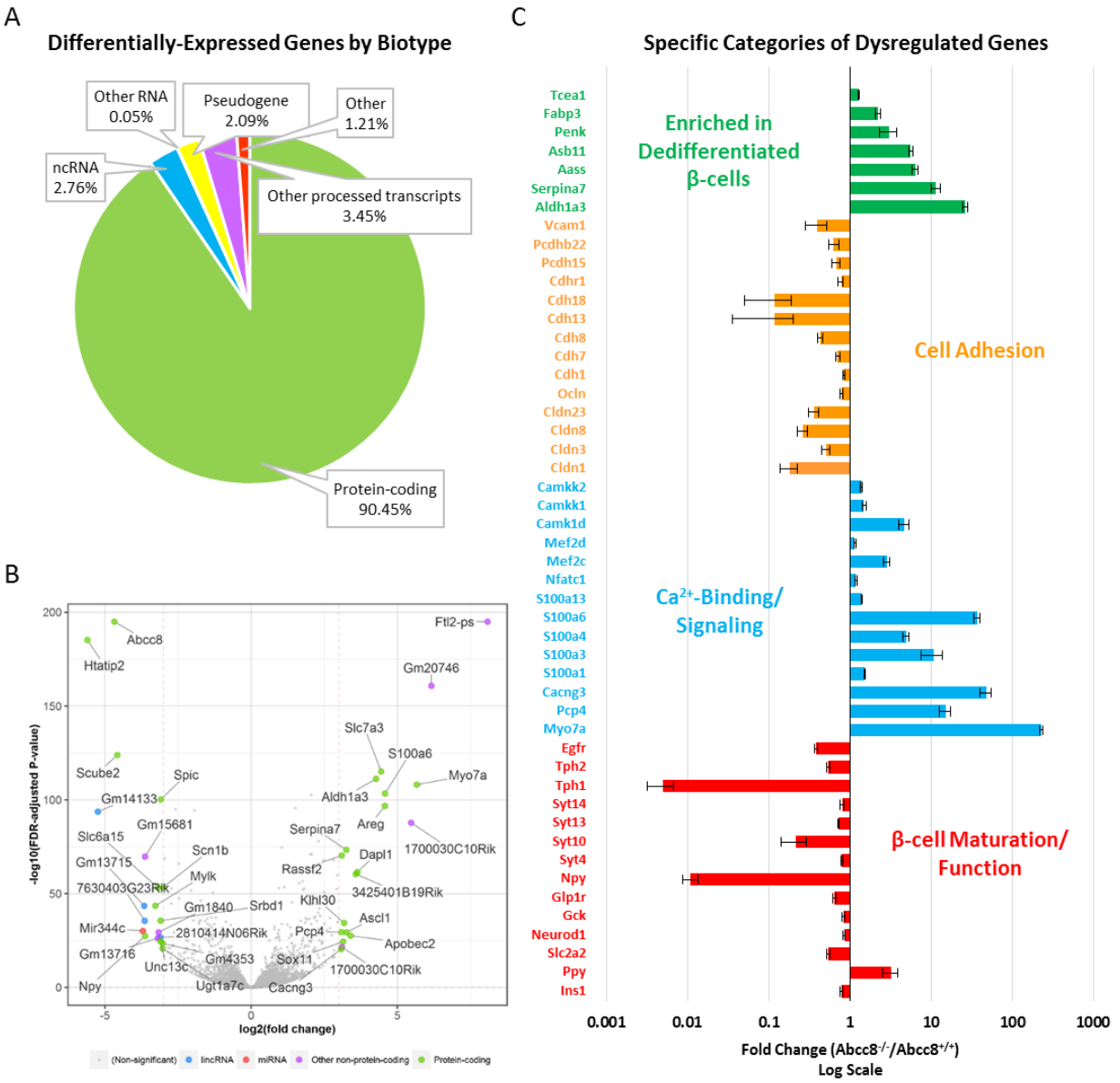

Figure 3.6. RNA-sequencing of *Abcc8*$^{-/-}$ β-cells. With the assistance of J.P. Cartailler, we performed RNA-sequencing of FACS-purified β-cells from *Abcc8*$^{-/-}$*; MIP-GFP* and *Abcc8*$^{+/+}$*; MIP-GFP* animals. **(A)** Pie chart showing the percentage of differentially-regulated genes that fall into biotype categories of protein-coding, non-coding RNA, other RNA, pseudogene, other processed transcripts, and other types of transcripts. **(B)** Volcano plot showing the most differentially-expressed genes in *Abcc8*$^{-/-}$*; MIP-GFP* β-cells based on the -$\log_{10}$ (FDR-adjusted P-value) and the $\log_2$ (fold change). Genes with a $\log_2$ (fold change) greater than 3 are labeled and grouped into categories based on biotype characterization. **(C)** Selected differentially-expressed genes grouped in categories of interest in *Abcc8*$^{-/-}$*; MIP-GFP* β-cells. All genes shown were manually selected and have FDR-adjusted p-values < 0.05.

islets of α-, β-, δ-, and PP-cells in *Abcc8*$^{-/-}$ mice (**Figure 3.7**). We observed both a decrease in the percentage of β-cells per islet (**Figure 3.8A**), and an increase in the percentage of α-, δ-, and PP-cells per islet (**Figure 3.8B-D**) in *Abcc8*$^{-/-}$ mice compared to *Abcc8*$^{+/+}$ controls, though the total number of cells per islet did not differ (**Figure 3.8H**). The striking difference in visual appearance of the *Abcc8*$^{-/-}$ islets led us to quantify the location of cells within islets, finding that *Abcc8*$^{-/-}$ mice have an age-dependent increase in α-, PP-, and δ-cells (**Figure 3.8E-G**) located in the islet core.

To correlate gene expression with this disrupted islet architecture, we examined expression of cell adhesion molecules, hypothesizing that a reduction in such genes could result in loss of islet structure. Consistently, we observed reduction in multiple cell adhesion molecules, including *Cldn1, Cldn3, Cldn8, Cldn23,* and *Ocln,* genes involved in tight junctions; *Cdh1, Cdh7, Cdh8, Cdh13,* and *Cdh18,* encoding cadherins; *Cdhr1*, a cadherin-related protein; *Pcdhb15* and *Pcdhb22*, encoding protocadherins; and *Vcam1*, a vascular cell adhesion molecule (**Figure 3.6C**).

Aldh1a3, a retinaldehyde dehydrogenase recently suggested to be a marker for β-cell dedifferentiation (94), is 27-fold upregulated in *Abcc8*$^{-/-}$ β-cells by RNA-seq (**Figure 3.6C).** In addition, six other genes (*Serpina7*, *Aass*, *Asb11*, *Penk*, *Fabp3*, and *Tcea1*) enriched in dedifferentiated β-cells (94) are upregulated in *Abcc8*$^{-/-}$ β-cells **(Figure 3.6C)**. Co-immunostaining with insulin indicates that while ALDH1A3 is expressed in only 0.4% of *Abcc8*$^{+/+}$ β-cells, it is expressed in 29.1% of *Abcc8*$^{-/-}$ β-cells **(Figure 3.9A, D)**, However, this fraction was reduced to 11.4% in *Abcc8*$^{-/-}$ mice administered the Ca^{2+}-channel blocker verapamil **(Figure 3.9A, B)**, further suggesting that a chronic increase in $[Ca^{2+}]_i$ impairs the maintenance of cell identity.

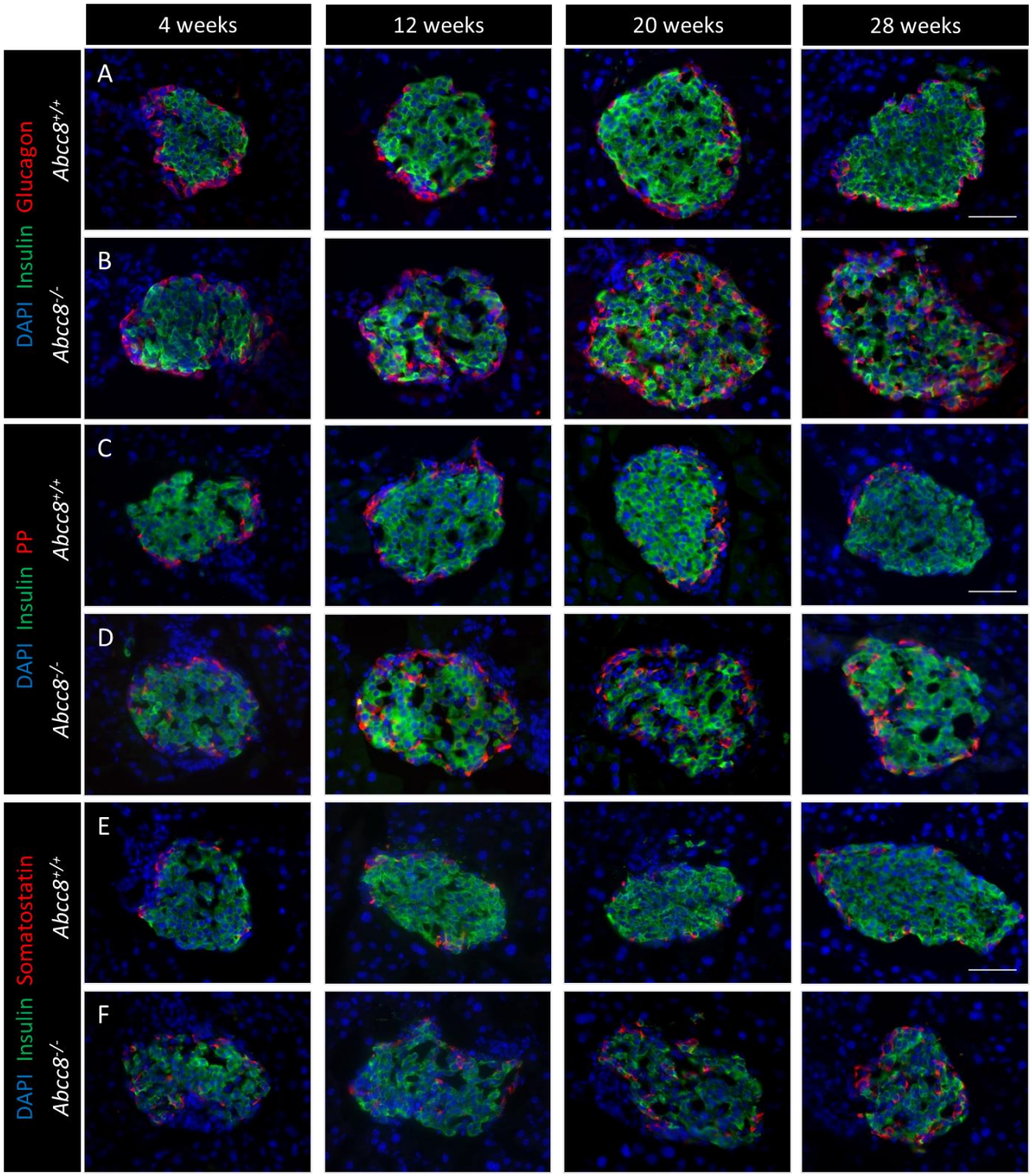

Figure 3.7 *Abcc8*$^{-/-}$ islets have disrupted islet morphology that worsens over time. Immunostaining of frozen pancreatic sections at 4, 12, 20, and 28 weeks of age with antibodies against insulin, glucagon, pancreatic polypeptide, and somatostatin shows that **(A, B)** α-cells, **(C, D)** PP-cells, and **(E, F)** δ-cells become localized to the islet core in *Abcc8*$^{-/-}$ islets but are restricted to the periphery in *Abcc8*$^{+/+}$ islets. Scale bar = 50μm.

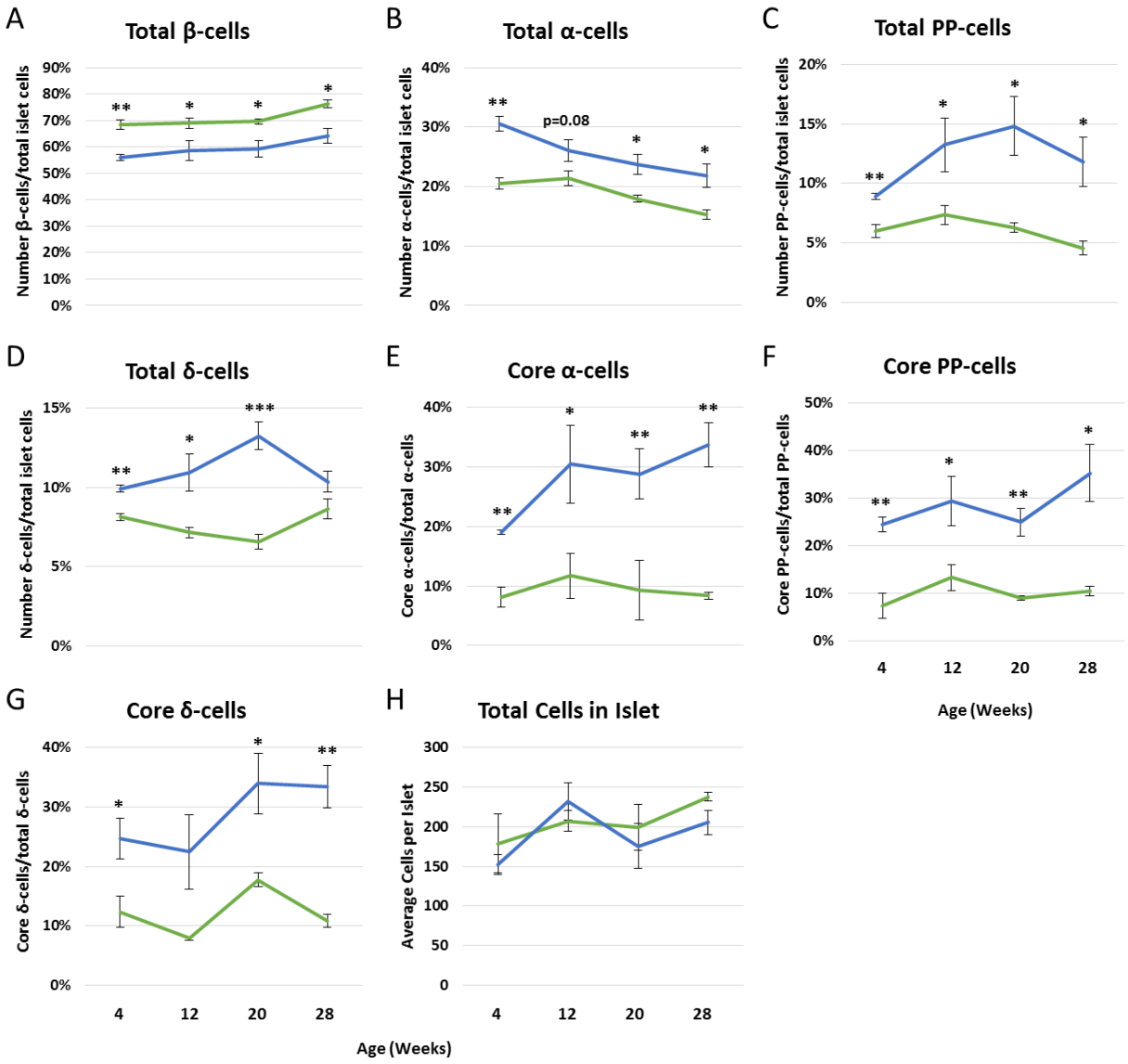

Figure 3.8 Quantification of islet morphology changes. Cell counting at 4, 12, 20, and 28 weeks of age shows that *Abcc8*$^{-/-}$ islets have **(A)** a smaller percentage of β-cells and a greater percentage of **(B)** α-cells, **(C)** PP-cells, and **(D)** δ-cells in the islet. *Abcc8*$^{-/-}$ islets also have an increasing percentage of core **(E)** α-cells, **(F)** PP-cells, and **(G)** δ-cells beginning by 4 weeks of age. **(H)** The average number of cells per islet does not differ between Abcc8$^{+/+}$ and Abcc8$^{-/-}$ islets. Green lines represent *Abcc8*$^{+/+}$ islets. Blue lines represent *Abcc8*$^{-/-}$ islets. N=3-4 animals per genotype, 10-15 islet sections counted per animal. Error bars represent standard error. *p<0.05, **p<0.01, ***p<0.001.

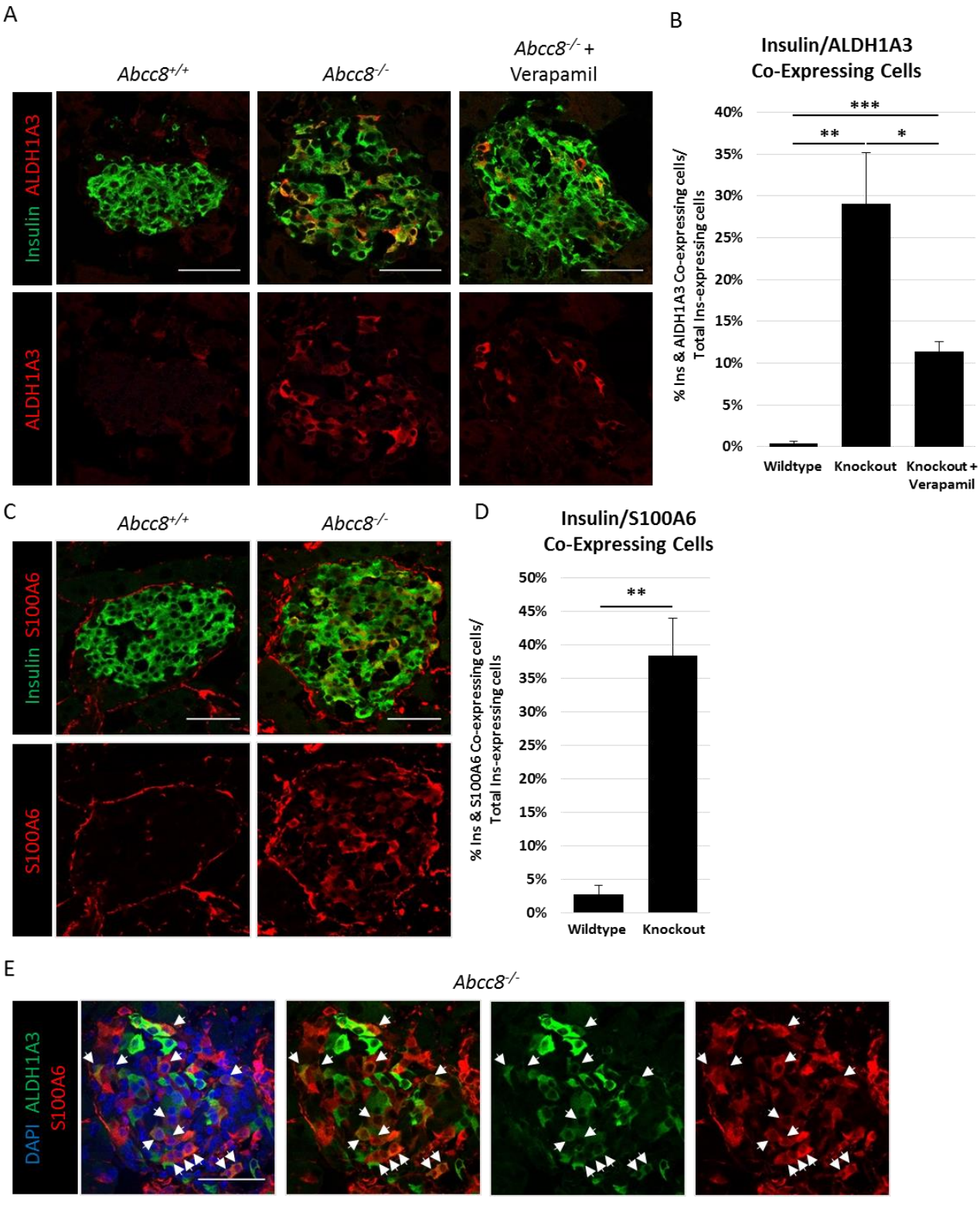
A
Abcc8+/+
Abcc8-/-
Abcc8-/- + Verapamil
Insulin ALDH1A3
ALDH1A3
B
Insulin/ALDH1A3 Co-Expressing Cells
% Ins & AlDH1A3 Co-expressing cells/ Total Ins-expressing cells
40%
35%
30%
25%
20%
15%
10%
5%
0%
***
**
*
Wildtype
Knockout
Knockout + Verapamil
C
Abcc8+/+
Abcc8-/-
Insulin S100A6
S100A6
D
Insulin/S100A6 Co-Expressing Cells
% Ins & S100A6 Co-expressing cells/ Total Ins-expressing cells
50%
45%
40%
35%
30%
25%
20%
15%
10%
5%
0%
**
Wildtype
Knockout
E
Abcc8-/-
DAPI ALDH1A3 S100A6

Figure 3.9. Heterogeneous expression of S100A6 and ALDH1A3. (A) Co-immunostaining of ALDH1A3, a potent marker of dedifferentiated β-cells, and insulin in pancreatic sections from *Abcc8*$^{+/+}$, *Abcc8*$^{-/-}$, and *Abcc8*$^{-/-}$ mice given Verapamil. **(B)** Quantification of (A) showing the percentage of Insulin and ALDH1A3 co-expressing cells in each group. Verapamil treatment partially rescues the percentage of ALDH1A3-expressing β-cells in *Abcc8*$^{-/-}$ mice. **(C)** Co-immunostaining of S100A6 and insulin in *Abcc8*$^{+/+}$ and *Abcc8*$^{-/-}$ pancreatic sections. **(D)** Quantification of (C) showing the percentage of Insulin-expressing cells that co-express S100A6 in *Abcc8*$^{+/+}$ and *Abcc8*$^{-/-}$ mice. **(E)** Co-immunostaining of ALDH1A3 and S100A6 shows that there is not strict co-localization of these two factors, again emphasizing the heterogeneous nature of β-cell failure. Arrows indicate cells that co-express ALDH1A3 and S100A6. Scale bar = 50μm. N=3 animals, 8-12 islet sections counted per animal. *$p<0.05$, **$p<0.01$, ***$p<0.001$.

S100a6 and *S100a4* are markers of excitotoxicity in β-cells

To identify genes that could serve as markers of β-cell excitotoxicity, we further analyzed *S100a6* and *S100a4*. Both genes are appealing targets due to their functions as EF-hand Ca^{2+}-binding proteins, the association of *S100a6* with insulin secretion (131), and the increased expression of members of the *S100* gene family in islets from humans with hyperglycemia (132). Moreover, they are among the most highly-upregulated genes in *Abcc8*$^{-/-}$ β-cells, with *S100a6* and *S100a4* increasing 37- and 5-fold, respectively. While S100A6 is only expressed in 2.8% of *Abcc8*$^{+/+}$ β-cells, it is expressed in 38.4% of *Abcc8*$^{-/-}$ β-cells **(Figure 3.9C, D)**. Additionally, qRT-PCR using whole islet RNA confirms the upregulation of *S100a6* and *S1004* in *Abcc8*$^{-/-}$ islets **(Figure 3.10A)**.

To determine if the observed changes in *S100a6* and *S100a4* expression in *Abcc8*$^{-/-}$ β-cells are due to chronically elevated $[Ca^{2+}]_i$, and not to unknown compensatory effects, we treated wildtype islets with either KCl or tolbutamide and found that membrane depolarization is associated with an increase in both *S100a6* and *S100a4* expression **(Figure 3.10B-E)**, mirroring the expression pattern in *Abcc8*$^{-/-}$ β-cells. Importantly, these changes are reversed when islets are treated with both a depolarizing agent and the Ca^{2+}-channel inhibitor verapamil **(Figure 3.10B-E)**. Moreover, the expression of *S100a6* and *S100a4* is decreased when Ca^{2+} influx is pharmacologically inhibited in *Abcc8*$^{-/-}$ mice **(Figure 3.10F, G)**. These results suggest that *S100a6* and *S100a4* expression in *Abcc8*$^{-/-}$ β-cells is tightly correlated with $[Ca^{2+}]_i$. Finally, co-immunostaining with S100A6 and ALDH1A3 indicates that several, but not all, cells co-express these two proteins **(Figure 3.9E)**. Quantification reveals that 15.4 ± 2.1% of insulin-expressing cells in *Abcc8*$^{-/-}$ mice express both S100A6 and ALDH1A3.

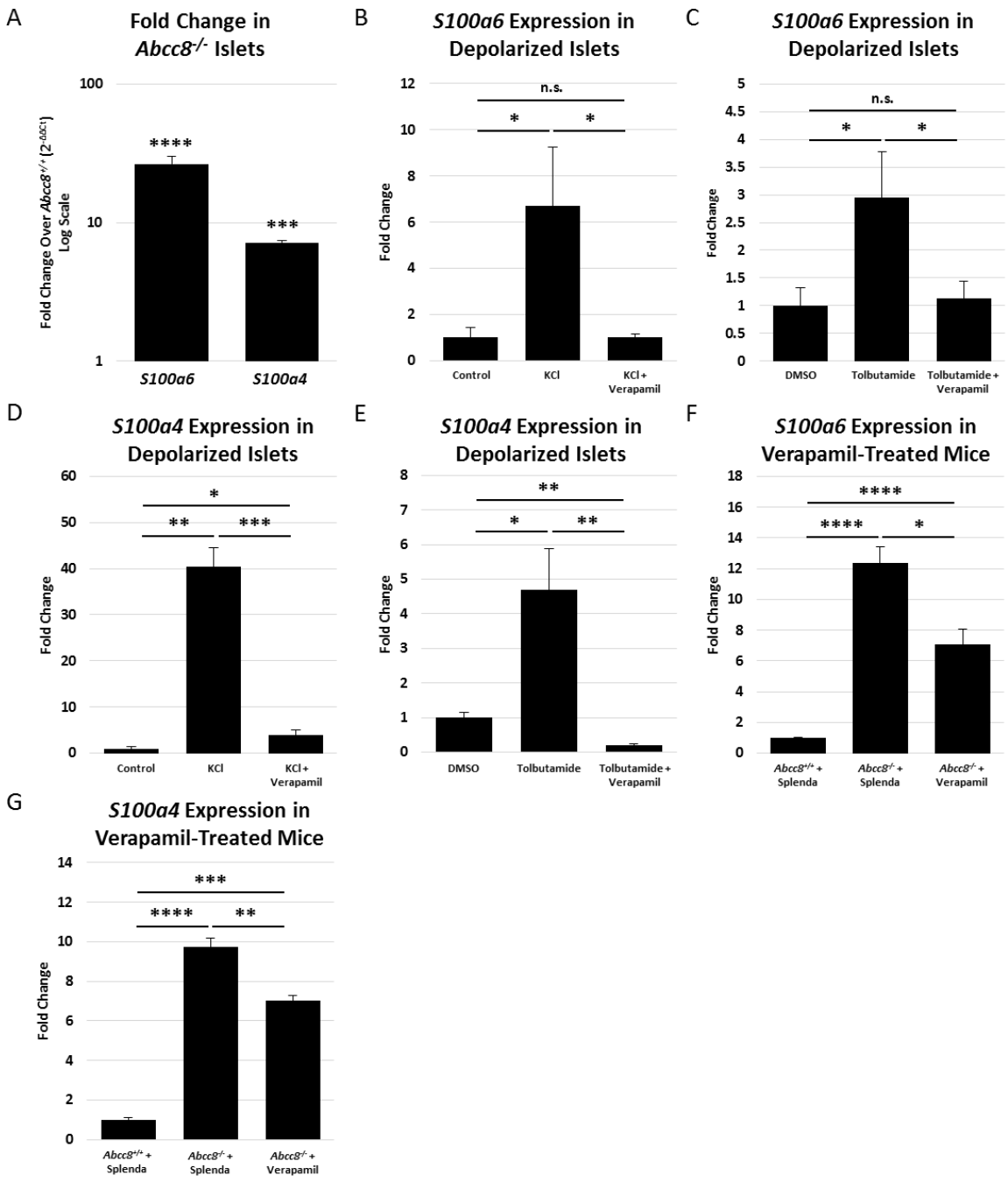

Figure 3.10. *S100a6* and *S100a4* serve as markers of excitotoxicity in β-cells. (A) qRT-PCR using whole islet RNA confirms upregulation of *S100a6* and *S100a4* in *Abcc8*$^{-/-}$ islets compared to *Abcc8*$^{+/+}$ islets. **(B-E)** qRT-PCR using whole islet RNA from wild type islets treated with either 100μM tolbutamide or 20mM KCl with or without 50μM verapamil for 24 hours. *S100a6* (B, C) and *S100a4* (D, E) are significantly upregulated in response to membrane depolarization, but this effect is negated when Ca^{2+} influx is blocked. **(F, G)** qRT-PCR using whole islet RNA from animals administered verapamil (1mg/mL) in the drinking water for 3 weeks indicates that both *S100a6* and *S100a4* expression is significantly downregulated when Ca^{2+} influx is inhibited. n.s. = not significant, *p<0.05, **p<0.01, ***p<0.001, ****p<0.0001.

Prediction of upstream regulators

To determine if there are similarities in the regulation of differentially-expressed genes in *Abcc8*$^{-/-}$ β-cells $[Ca^{2+}]_i$, we utilized iRegulon, which searches for common DNA binding motifs in co-expressed genes (124), to identify potential upstream regulators. Analysis of the top 500 upregulated genes reveals that binding sites for ASCL1, CEBPG, and RARG are common, and many genes, including *Aldh1a3*, are predicted to be regulated by all three **(Figure 3.11, 3.13A)**. Interestingly, all three predicted regulators are upregulated in *Abcc8*$^{-/-}$ β-cells **(Figure 3.13C)**. Conversely, analysis of the top 500 downregulated genes predicts binding sites for TEAD1, HNF1A, and ZFP647 (**Figure 3.12, 3.13B**). The expression of these regulators is unchanged in *Abcc8*$^{-/-}$ β-cells **(Figure 3.13C)**.

Ascl1 is regulated by $[Ca^{2+}]_i$ in β-cells

Since *Ascl1* is 22-fold upregulated in *Abcc8*$^{-/-}$; *MIP-GFP* β-cells **(Figure 3.6B)** and 24-fold upregulated in *Abcc8*$^{-/-}$ islets **(Figure 3.13D)**, and has been shown by ChIP to bind near 51% of the predicted targets (133-135), we studied its responsiveness to changes in $[Ca^{2+}]_i$ in isolated islets. Consistent with *Ascl1* being regulated by $[Ca^{2+}]_i$, its expression increases in response to membrane depolarization, an effect that is reversed when Ca^{2+} influx is inhibited by verapamil, both in isolated islets **(Figure 3.13E)** and in mice **(Figure 3.13F)**. These results support the idea that ASCL1 could play a central role in regulating gene expression in β-cells with chronically elevated $[Ca^{2+}]_i$.

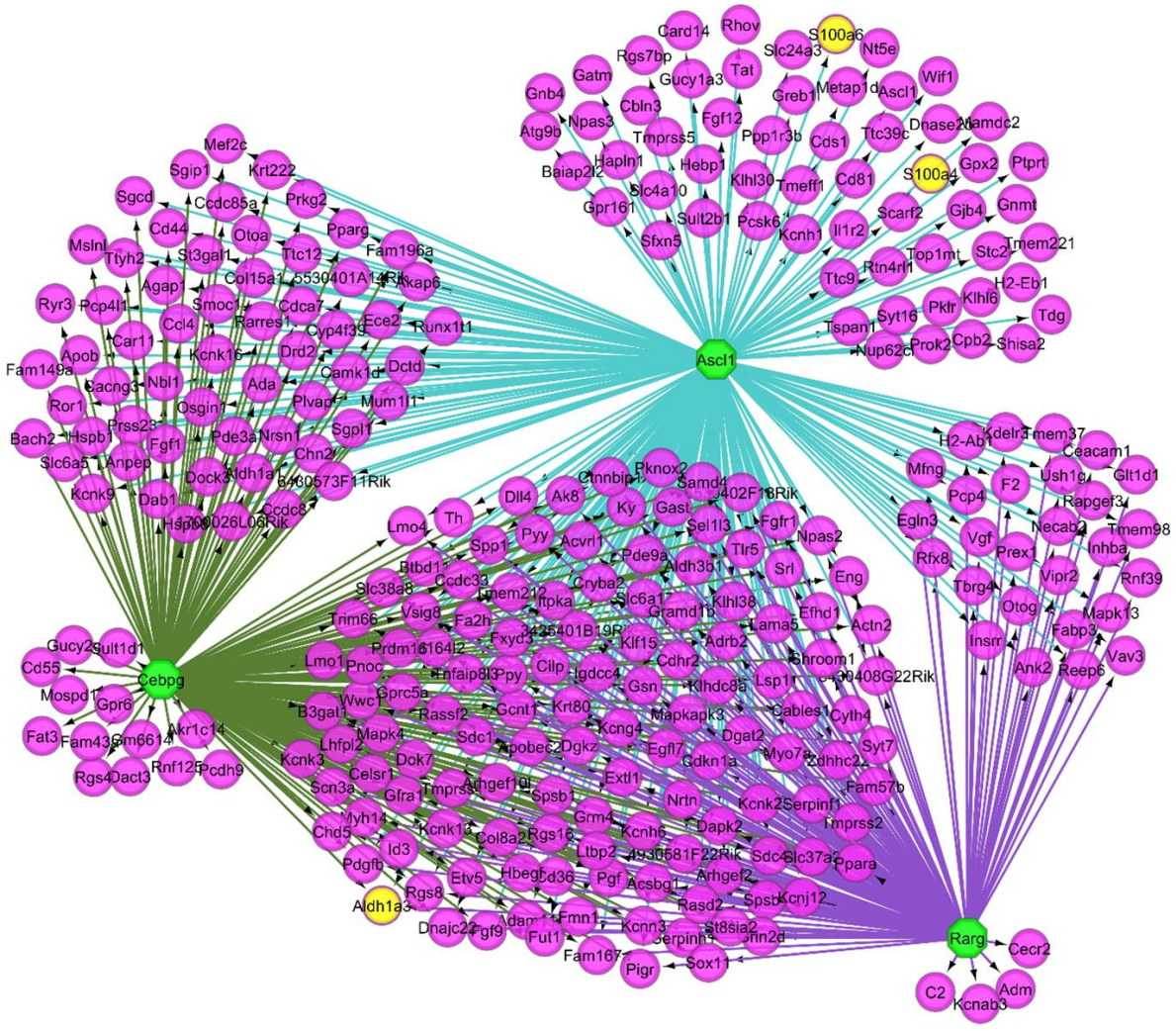

Figure 3.11. iRegulon-predicted network of regulators of the top 500 upregulated genes in *Abcc8*$^{-/-}$ β-cells. Map depicting the top 3 predicted regulators (green octagons) and their predicted target genes (magenta circles). A majority of the genes are predicted to be co-regulated by two or more regulators. Genes of interest (*S100a6*, *S100a4*, and *Aldh1a3*) are highlighted yellow.

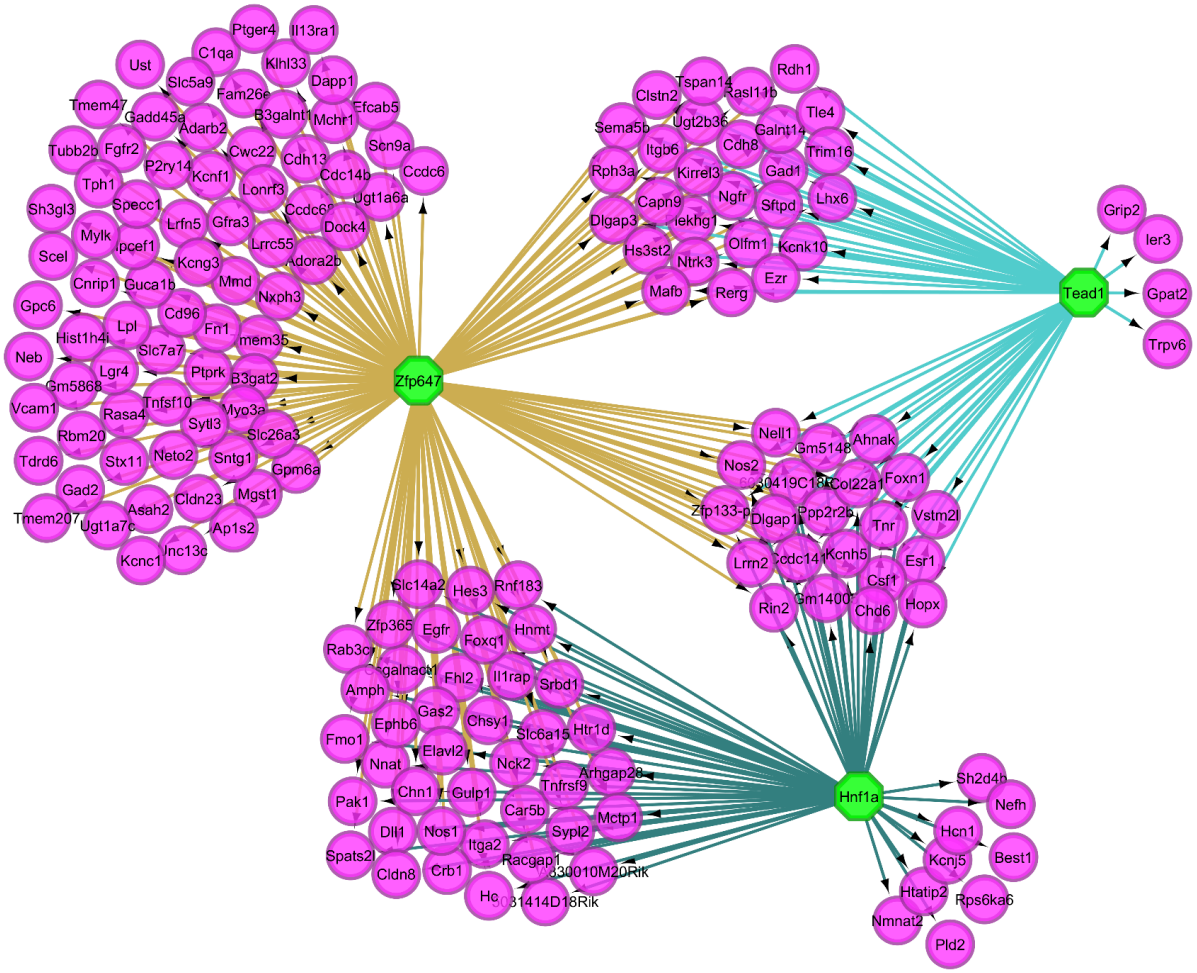

Figure 3.12. iRegulon-predicted network of regulators of the top 500 downregulated genes in *Abcc8*$^{-/-}$ β-cells. Map depicting the top 3 predicted regulators (green octagons) and their predicted target genes (magenta circles).

A

Regulator	Enrichment Score	No. Predicted Targets
ASCL1	3.704	271
CEBPG	3.143	199
RARG	3.062	155

B

Regulator	Enrichment Score	No. Predicted Targets
TEAD1	3.848	52
HNF1A	3.313	70
ZFP647	3.277	163

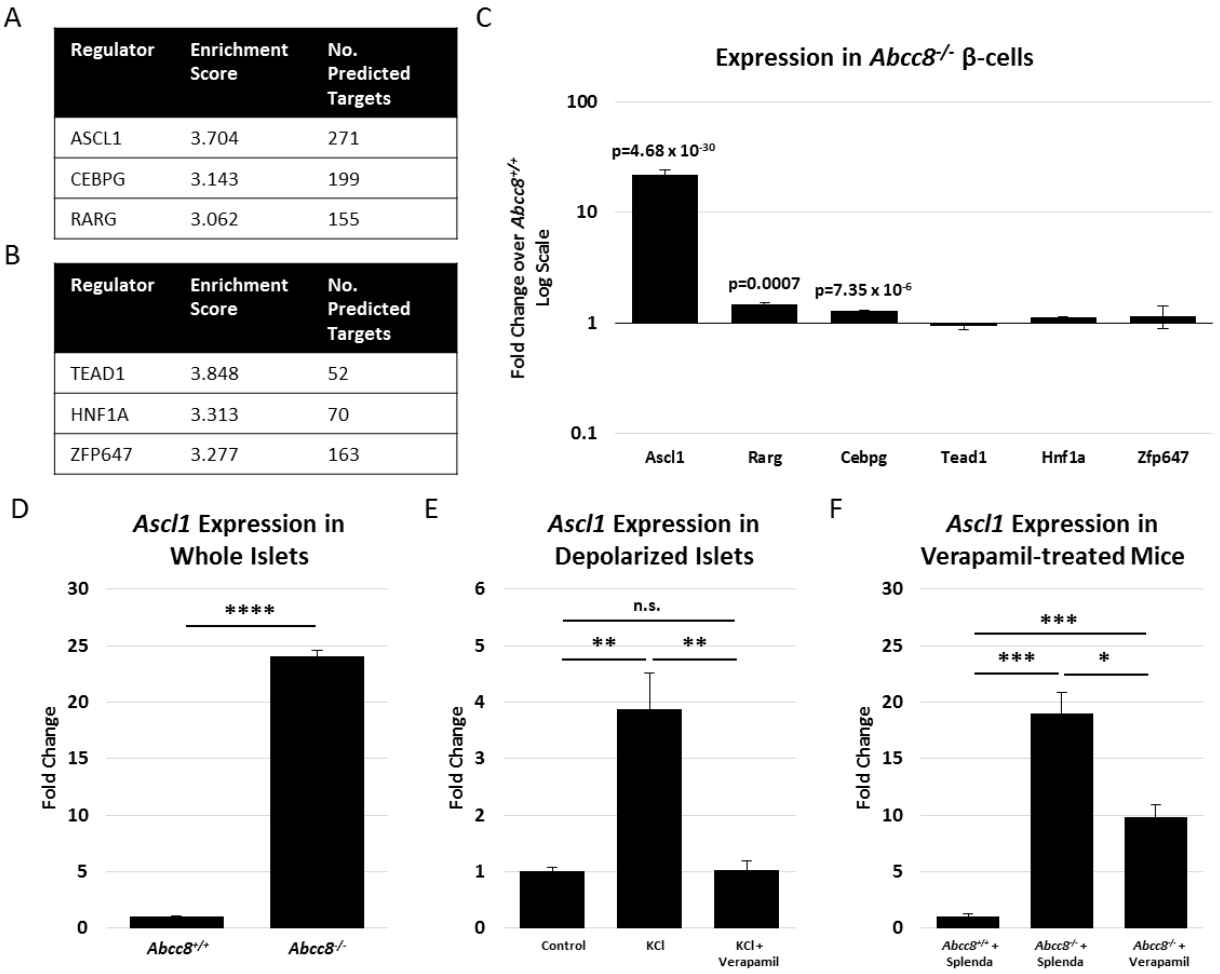

Figure 3.13. Upstream regulator prediction using iRegulon. Using the top 500 up- and down-regulated genes in *Abcc8*$^{-/-}$ β-cells, we utilized iRegulon to predict common upstream regulators based on enriched DNA binding motifs. **(A, B)** Tables summarizing the top 3 predicted regulators of upregulated (A) and downregulated (B) genes, their enrichment scores, and the number of predicted targets. **(C)** Expression of the predicted regulators in *Abcc8*$^{-/-}$ β-cells, as determined by RNA-seq. **(D)** qRT-PCR using whole islet RNA confirms upregulation of *Ascl1* in *Abcc8*$^{-/-}$ islets compared to *Abcc8*$^{+/+}$ islets. **(E)** qRT-PCR for *Ascl1* using whole islet RNA from wildtype islets treated with 20mM KCl with or without 50μM verapamil for 24 hours. (**F**) qRT-PCR using whole islet RNA from animals administered verapamil. n.s. = not significant, *p<0.05, **p<0.01, ***p<0.001, ****p<0.0001.

Discussion

Chronically elevated $[Ca^{2+}]_{i,}$ within pancreatic β-cells perturbs the expression of over 4,200 genes, compromising cell identity, causing β- to PP-cell trans-differentiation, and impairing islet morphology. Such an increase in $[Ca^{2+}]_{i,}$ may also occur when insulin secretion is inadequate to overcome insulin resistance during the early stages of β-cell failure, or when a sulfonylurea is used as therapy. While some of the changes may be adaptive, such as the increase in *Pcp4*, a calmodulin-binding protein that protects neurons from Ca^{2+}-induced excitotoxicity (130), many of the observed changes, such as the reduction in cell adhesion molecules and the increase in genes associated with β-cell failure, are likely to be maladaptive.

$[Ca^{2+}]_i$ in *Abcc8*$^{-/-}$ β-cells

While we observed persistent membrane depolarization and a sustained elevation of the $[Ca^{2+}]_i$, others have observed oscillations in intracellular calcium in β-cells from K_{ATP}-channel knockout mice (136; 137). This is likely attributable to our experimental conditions, which involved only a very brief stimulation with glucose and averaging of the calcium traces, which did not allow for $[Ca^{2+}]_i$ oscillations to be identified (**Figure 3.2A**). We did, however, observe a transient drop in $[Ca^{2+}]_i$ in *Abcc8*$^{-/-}$ islets following glucose stimulation (**Figure 3.2A**) that was not seen in *Abcc8*$^{+/+}$ islets. This drop is due to brief membrane hyperpolarization caused by transient activation of the sodium potassium ATPase (136), and has also been observed previously in islets treated with K_{ATP}-channel inhibitors (138) as well as in other K_{ATP}-channel-deficient mice (136). Thus, our findings are in agreement with other studies (136) that have also observed persistent

membrane depolarization and continuous action potential firing leading to elevated $[Ca^{2+}]_i$ in β-cells from K_{ATP}-channel knockout mice.

A chronic increase in $[Ca^{2+}]_i$ impairs β-cell identity

Recent studies have suggested that β-cell dedifferentiation contributes to the development of T2D (41; 94). We found that the expression of genes involved in maintaining β-cell identity and function were adversely affected in *Abcc8*$^{-/-}$ mice, including *Ins1*, *Slc2a2*, *Neurod1*, *Gck*, and *Syt10*. However, some of the transcription factors previously associated with β-cell dedifferentiation (41), including *Mafa*, *Pdx1*, *Nkx6.1*, *FoxO1*, *Ngn3*, *Oct4*, and *Nanog*, are unchanged in *Abcc8*$^{-/-}$ β-cells. This difference may explain the modest loss of β-cell identity observed in *Abcc8*$^{-/-}$ mice, with only 2.21% of β-cells undergoing trans-differentiation to either INS/PP poly-hormonal or PP mono-hormonal cells. Importantly, we observed that, while it did not reverse the INS/PP poly-hormonal cells, treatment with a Ca^{2+}-channel blocker resulted in a decrease in the percentage of *Abcc8*$^{-/-}$ β-cells expressing the dedifferentiation marker ALDH1A3, further supporting our claim that a chronic increase in $[Ca^{2+}]_i$ contributes to loss of β-cell identity. It is important to distinguish our results, reflecting the loss of K_{ATP}-channels, from studies using K_{ATP}-channel gain-of-function mutants (57; 58). The current study examines the effects of elevated $[Ca^{2+}]_i$ in a euglycemic setting, while the latter reflects decreased $[Ca^{2+}]_i$ in a hyperglycemic setting.

Based on our finding of compromised β-cell identity in *Abcc8*$^{-/-}$ mice, we suggest that chronically elevated $[Ca^{2+}]_i$, or excitotoxicity, if left uncorrected, may contribute to β-cell failure in T2D. However, it can also be argued that the loss of β-cell identity is an adaptive mechanism

that helps prevent the development of hyperinsulinemia in response to chronically elevated $[Ca^{2+}]_i$. These findings also have important implications for the use of sulfonylureas, including tolbutamide and glibenclamide, as therapies for T2D. Sulfonylureas have been widely prescribed for patients with T2D for decades, but our results suggest that, by inhibiting K_{ATP}-channels to cause chronically-elevated $[Ca^{2+}]_i$ and to increase insulin secretion, they might also cause maladaptive effects, resulting in loss of β-cell function and identity and potentially exacerbating the disease. Indeed, the observation that patients prescribed sulfonylureas often experience a loss in efficacy of the drug after about six years, requiring the addition of exogenous insulin to maintain glycemic control (139), suggests that β-cell function deteriorates with this use of these drugs.

A network of $[Ca^{2+}]_i$-regulated genes

Many of the dysregulated genes in *Abcc8*$^{-/-}$ β-cells, such as *S100a6, Myo7a, Pcp4, Cacng3, Mef2c*, and *Camk1d*, are involved in Ca^{2+} binding and signaling. The *S100* gene family, for instance, modulates the activity of other proteins upon Ca^{2+} binding (140). Moreover, S100A6, specifically, promotes Ca^{2+}-stimulated insulin release (131). *Camk1d*, *Camkk1*, and *Camkk2*, three protein kinases, *Myo7a*, a myosin motor protein, and *Mef2d* and *Mef2c*, are involved in Ca^{2+}/calmodulin-dependent signaling, or are regulated by $[Ca^{2+}]_i$ (65; 141). While we only cite selected examples, our results are consistent with a network of Ca^{2+}-modulated genes being required in β-cells for the maintenance not only of internal Ca^{2+}-homeostasis but also the regulation of key biological responses. However, despite strong evidence that the chronic increase in $[Ca^{2+}]_i$ perturbs many genes involved in Ca^{2+}-signaling, it remains possible that some of the gene

expression changes that occur in *Abcc8*$^{-/-}$ β-cells are due to paracrine and/or neuronal signaling, since *Abcc8* is expressed in other islet cell types and neurons.

We focused on two $[Ca^{2+}]_i$-regulated genes, *S100a6* and *S100a4*, since they are highly up-regulated in *Abcc8*$^{-/-}$ β-cells and are acutely regulated by treatment with depolarizing agents and a Ca^{2+}-channel blocker. The upregulation of these and other members of the *S100* gene family of Ca^{2+}-binding proteins may reflect a buffering mechanism existing in the β-cell to sequester excess Ca^{2+} ions and prevent over-activation of downstream signaling pathways. Interestingly, administration of a Ca^{2+}-channel blocker to *Abcc8*$^{-/-}$ mice did not fully rescue the expression levels of *S100a6* or *S100a4* **(Figure 3.10F, G)** or of *Ascl1* **(Figure 3.13F)**. The failure of Verapamil to fully restore basal expression levels of these genes, or to significantly reverse the percentage of Ins/PP polyhormonal cells **(Figure 3.3G),** is likely due to limitations in the experimental design. For instance, it is possible that the animals were not given an adequate dose of Verapamil to completely rescue the effect. It is also possible that the duration of Verapamil administration was not sufficient. Therefore, we can conclude that expression of *S100a6* and *S100a4* is regulated by Ca^{2+}-influx in the β-cell and that these genes are promising as markers for β-cell excitotoxicity.

In support of this, members of the *S100* gene family, including *S100A3, S100A6, S100A10, S100A11,* and *S100A16,* have been associated, in human islets, with hyperglycemia (132), and *S100A6*, specifically, was shown to be positively correlated with increased body mass index in β-cells from type 2 diabetic donors (112). Recently, several groups have performed single-cell RNA-sequencing of human pancreatic cells types from both normal and type 2 diabetic donors (59; 111; 112). Although one of these studies revealed slightly increased expression of *S100A6* in β-cells from type 2 diabetic donors compared to normal donors (RPKM of 282 vs. 224, respectively) (111), no study reported a statistically significant difference in expression of *S100A6, S100A4*, or

ASCL1. However, because single cells were sequenced in these studies, and since expression data from multiple single cells was not pooled to increase depth, the data is limited by shallow sequencing depths (fewer than 1 million reads per sample), making it likely that important correlations were missed. Indeed, only a small number of genes were reported to be differentially expressed in β-cells from normal compared to type 2 diabetic donors (48 in one study (111), and 76 in another (112)). Therefore, a more directed effort needs to be made in order to establish if these genes are correlated with type 2 diabetes in human β-cells.

Effects of a sustained increase in $[Ca^{2+}]_i$ on islet morphology

Perturbations in Ca^{2+}-signaling provide a compelling explanation for the disrupted islet morphology observed in K_{ATP}-channel knockout mice. Among the down-regulated genes are many that encode cell adhesion molecules, such as *Ocln*, *Tln1*, and *Cdh1*. An attractive hypothesis is that deterioration of β-cell to β-cell adhesion over time allows other endocrine cells types to infiltrate to the core of the islet. In accordance with this, $[Ca^{2+}]_i$ is known to be required for maintenance of tight junctions and adherens junctions, and focal adhesion disassembly occurs in response to elevated $[Ca^{2+}]_i$ (142). However, this hypothesis fails to explain the change in overall number of each of the islet cell types. The observed decrease in β-cell number may be accounted for by elevated apoptosis, as has been observed by some (34; 35), but was not observed in our studies. Another possibility, which I favor, is that disruption of Ca^{2+}-influx during development, as in the case in constitutive loss of K_{ATP}-channels, causes a disruption in endocrine lineage allocation.

Identification of putative upstream regulators

Bioinformatics analysis of genes that are either up- or down-regulated by $[Ca^{2+}]_i$ suggests commonalities in the upstream transcriptional control regions. Our analysis suggests that genes that are upregulated by $[Ca^{2+}]_i$ contain binding sites for ASCL1, CEBPG, and RARG. ASCL1, also known as MASH1, plays a role in neuronal commitment and differentiation (143). Retinoic acid receptors, including RARG, play a role in both endocrine cell development and maintenance of proper insulin secretion and β-cell mass (144). Finally, CEBPB, a closely related protein to CEBPG, represses the insulin promoter under conditions of chronically-elevated glucose, and its accumulation in β-cells increases vulnerability to ER stress (145; 146). Although our computational analysis is purely predictive, it is partially validated by the fact that 51% of the ASCL1 target genes and 60% of the RARG binding sites were previously established by ChIP (133-135; 147). Importantly, *S100a4* is among the ASCL1 targets that have been experimentally validated (133-135), and our in-depth analysis of *Ascl1* strongly supports the idea that it is regulated by Ca^{2+}-influx, strengthening our putative model.

Conversely, analysis of genes that are down-regulated by $[Ca^{2+}]_i$ predicts binding sites for TEAD1, HNF1A, and ZFP647. Although *Tead1* gene expression is unaffected in *Abcc8*$^{-/-}$ β-cells, the activity of TEAD1, a member of the Hippo pathway that interacts with YAP/TAZ to promote proliferation, is directly inhibited by Ca^{2+} (148). Furthermore, since a gene knock-out of *Hnf1a* results in β-cell failure and diabetes (149), a predicted decrease in its activity could explain the decrease in genes involved in β-cell function in *Abcc8*$^{-/-}$ β-cells.

Excitotoxicity in β-cell failure

Despite altering the expression of 4,208 genes, chronic β-cell depolarization does not, itself, cause overt T2D, at least within the timeframe studied here, although mild glucose intolerance was observed. This suggests that a combination of stresses may be required for β-cell failure (46). Moreover, our finding that S100A6 and ALDH1A3 do not strictly co-localize in *Abcc8*$^{-/-}$ β-cells is consistent with β-cell failure occurring in a stochastic manner, and suggests that some cells may fail before others. Regardless, our findings provide insights into the adaptive and maladaptive responses that occur when β-cells are chronically depolarized. These responses may require the individual or combined activity of ASCL1, RARG, and CEBPG, in the case of genes up-regulated by $[Ca^{2+}]_i$, or TEAD1, HNF1A, and ZFP647, in the case of genes down-regulated by $[Ca^{2+}]_i$. While further studies are necessary to validate this model, our studies clearly show that a chronic increase in $[Ca^{2+}]_i$ results in dysregulation of many genes and modest loss of β-cell identity (**Figure 3.14**). Although β-cells may have mechanisms that limit the maladaptive effects of an increase in $[Ca^{2+}]_i$, our findings suggest that β-cell excitotoxicity, in combination with other metabolic stresses, may contribute to β-cell dedifferentiation and failure.

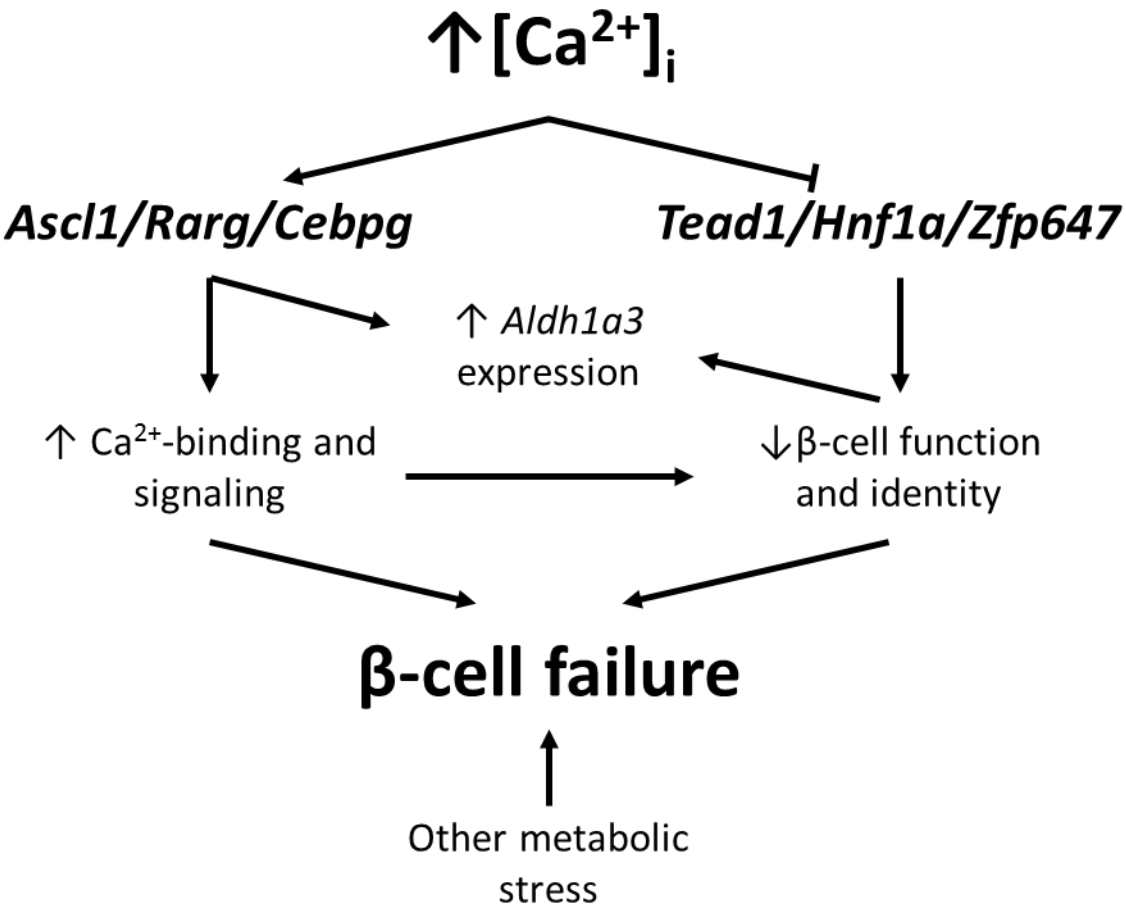

Figure 3.14. Model showing the effects of chronically elevated $[Ca^{2+}]_i$ in the β-cell. Our results suggest that there is a putative gene regulatory network mediating the effects of chronically elevated $[Ca^{2+}]_i$ in the β-cell. Elevated $[Ca^{2+}]_i$ activates predicted regulators ASCL1, RARG, and CEBPG, causing an elevation in Ca^{2+}-binding and signaling. Our results also suggest that the combined actions of ASCL1, RARG, and CEBPG activate *Aldh1a3* expression. Elevated $[Ca^{2+}]_i$ may negatively regulate the activity of TEAD1, HNF1A, and ZFP647, leading to loss of β-cell function and stable β-cell identity. Loss of β-cell function and identity further contributes to the upregulation of *Aldh1a3*. Finally, the combination of elevated Ca^{2+}-binding and signaling, decreased β-cell function and identity, and other metabolic stresses leads to β-cell failure.

CHAPTER IV

THE EFFECTS OF HUMAN GROWTH HORMONE ON β-CELL FUNCTION AND GENE EXPRESSION

Introduction

The ability to genetically tag specific cell types with fluorescent proteins using transgenic constructs has enabled the isolation of pure cell populations using fluorescence-activated cell sorting (FACS). Transgenes allowing for pancreatic progenitor cell-specific or β-cell-specific gene expression have been particularly useful in studying β-cell development and function. However, the utility of some such lines has been limited by low or variegated expression in the cell type of interest, presumably due to chromatin inaccessibility. In an attempt to overcome issues of low transgene expression, studies in the late 1980s and early 1990s discovered that inclusion of intronic sequences and polyadenylation signals increases transgene expression *in vivo* by enhancing chromatin accessibility (150; 151). Since these initial studies, inclusion of the entire human growth hormone (hGH) coding sequence, including introns, has been widely used to enhance expression of transgenes driving cell-type-specific constructs.

Recently, the Magnuson lab and others have reported that the hGH minigene present in many pancreas-specific drivers, originally thought not to produce a functional protein, causes ectopic expression of hGH in pancreatic tissues (129; 152; 153). The hGH protein has marked effects on the physiology of these animals, with elevated STAT5 signaling, causing increased expression of islet serotonin, β-cell proliferation, and subsequent β-cell mass (**Figure 4.1**) (129; 152; 153). By a mechanism that is apparently independent of STAT5 signaling, ectopic hGH can

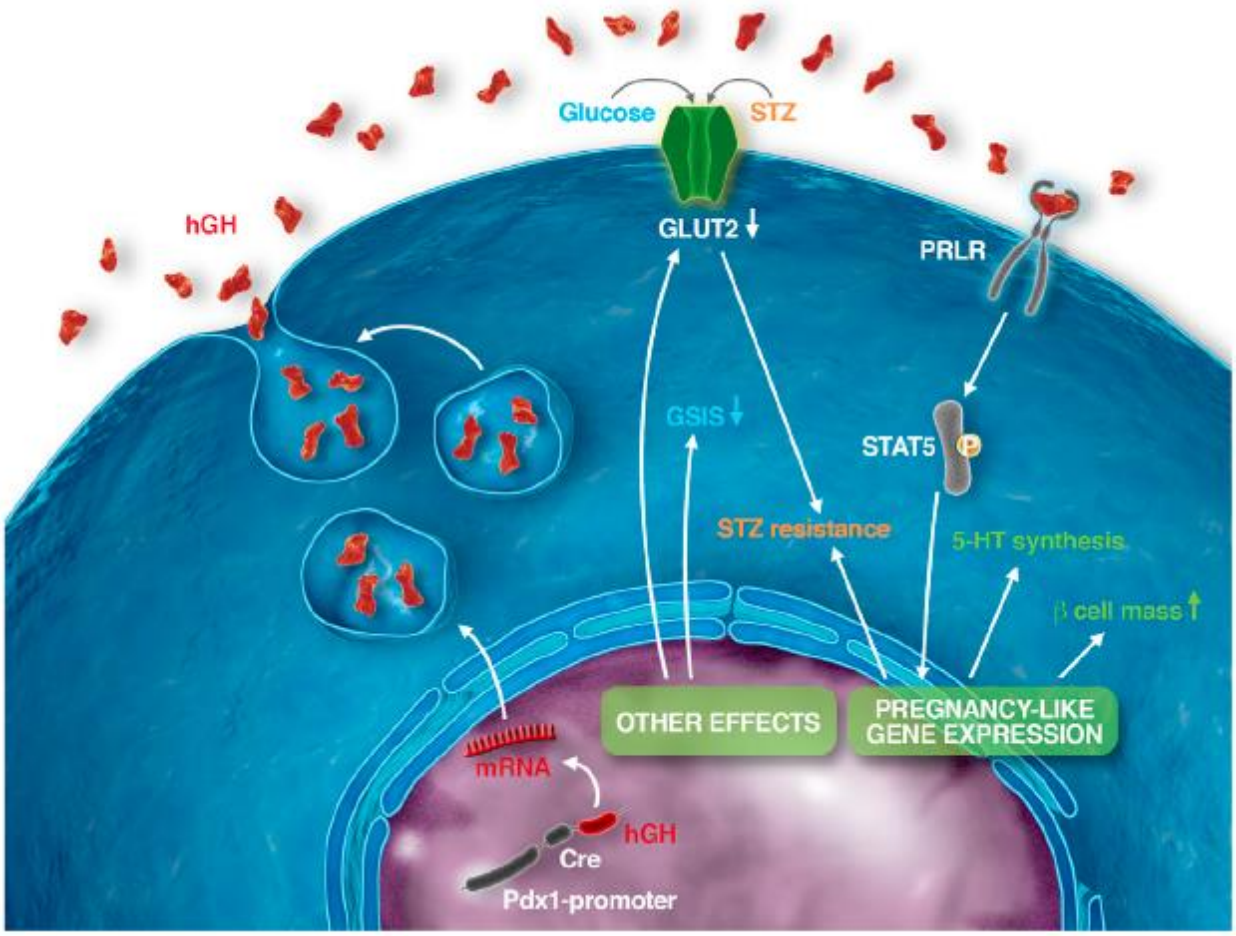

Figure 4.1. Effects of ectopic hGH expression on β-cell mass and function. Pancreas-specific transgenic mouse lines containing an hGH minigene (*Pdx1-Cre* shown in this example) can drive the ectopic expression of hGH in β-cells. hGH binds prolactin receptors (PRLR) on the surface of β-cells, triggering STAT5 phosphorylation and induction of pregnancy-like gene expression. Activation of pregnancy-like genes results in serotonin (5-HT) synthesis and increased β-cell proliferation. In addition to activating STAT5 signaling, hGH expression causes other effects, such as reduction in glucose-stimulated insulin secretion (GSIS) and decreased GLUT2 expression. The combination of elevated β-cell mass and decreased GLUT2 expression causes resistance to streptozotocin (STZ)-induced diabetes. Reprinted from Brouwers *et al.* (129) © 2014, with permission from Elsevier (see Appendix B).

also result in decreased β-cell expression of GLUT2 as well as impaired glucose tolerance (129).

One transgene made by this strategy that is widely used to identify and isolate pure β-cell populations is the *MIP-GFP* mouse (113), containing the mouse insulin promoter driving the expression of green fluorescent protein (GFP). With these new findings in mind, it is imperative to determine the expression status of hGH protein in mouse models made in this way and to ensure that proper controls are used to avoid misinterpretation of results.

In this chapter, I will describe the generation of a novel *Ins2.Apple* allele, which contains the hGH minigene, that allows for nuclear-labeling specifically of β-cells with exquisite separation of the Apple-expressing population by FACS. Furthermore, RNA-sequencing of both $Ins2^{Apple/+}$ and *MIP-GFP* β-cells reveals severe defects in the latter population that are drastically reduced or absent in the former. Together, our results suggest that, while the hGH minigene is present in our *Ins2.Apple* allele, the effects of it are diminished, making it an improved alternative to the *MIP-GFP* allele for investigators wishing to genetically label mouse β-cells.

Results

Generation of Ins2.Apple.LCA mice

In order to generate mice expressing a fluorescent reporter in the *Ins2* locus, we first generated a targeting vector containing the H2B-Apple fusion protein (a nuclear red fluorescent protein) sequence followed by an FRT-flanked PU-ΔTK positive selection cassette, both flanked by homology arms to the second exon of the mouse *Ins2* locus (**Figure 2.1A**). To increase the future utility of this allele, we inserted two LoxP sites, one upstream of the H2B-Apple sequence and one downstream of the PU-ΔTK cassette, to facilitate future gene targeting into the *Ins2* locus using Recombinase-Mediated Cassette Exchange (RMCE). This vector was inserted into the mouse *Ins2* Locus by homologous recombination in mESCs to generate an Ins2.Apple.LCA allele. The final allele was generated after Flpe-mediated excision of the PU-ΔTK cassette. Southern blot analysis confirmed the presence of both wildtype and targeted bands of the expected size in six mouse embryonic stem cell (mESC) clones (**Figure 2.1B**). Clone 1C4 was used to generate live mice. PCR genotyping produces a 562-bp band for the wildtype allele and a 684-bp band for the targeted mutation (**Figure 2.1C**).

Ins2.Apple.LCA mice have variegated expression of H2B-Apple

To test the functionality of our newly-generated Ins2.Apple.LCA allele, we performed immunofluorescence staining on pancreatic sections for Insulin and Apple to find that the allele is highly variegated in Insulin-expressing β-cells (**Figure 2.1D**). The cause of this variegation is not known, but likely is due to epigenetic modifications to the genomic area resulting in silencing of

the allele in a population of the cells. To remedy this variegation, we generated a second Ins2.Apple allele containing a human growth hormone (hGH) minigene, a sequence known to improve transgene expression by increasing DNA accessibility (150; 151). To achieve this, we made an Ins2.Apple.hGH exchange vector containing the H2B-Apple sequence, followed by an hGH minigene and an FRT-flanked Hygro positive selection cassette (**Figure 2.2A**). This exchange vector was incorporated into the Ins2.Apple.LCA allele via RMCE. Flpe-mediated excision of the Hygro cassette generated the *Ins2*^{Apple} mice used for subsequent experiments.

Ins2$^{Apple/+}$ mice have specific expression of H2B-Apple in β-cells

To determine if the inclusion of the hGH minigene improves the expression of H2B Apple, we performed immunofluorescence staining of frozen pancreatic sections to find that 77.56 ± 0.3% of insulin-expressing β-cells also express Apple (**Figure 2.2C**), indicating that a small amount of variegation still exists. Additionally, Apple expression is specific to β-cells, as no expression is seen in glucagon-producing α-cells (**Figure 2.2D**). The *Ins2*^{Apple} allele also has great utility as a fluorescent reporter to be used for fluorescence-activated cell sorting (FACS), since it allows for better separation of the β-cell population than the *MIP-GFP* allele (**Figure 4.3A**).

Ins2$^{Apple/+}$ mice do not have ectopic hGH expression

Recently, we and others have reported that the hGH minigene present in many transgenes causes ectopic expression of hGH in pancreatic tissues (129; 152; 153), resulting in marked abnormalities in β-cells, including elevated STAT5 signaling and impaired glucose tolerance. To determine if the *Ins2*$^{Apple/+}$ mice have any of these abnormalities, we performed

immunofluorescence staining for serotonin, a product of the pregnancy-like gene expression signature induced by STAT5 signaling in mice with ectopic hGH expression (129). We found that *Ins2*^{Apple} β-cells do not overexpress serotonin (**Figure 4.2A**), suggesting that, although the hGH minigene is present in the Ins2.Apple.hGH allele, it may not make a functional protein.

RNA expression profiling of *MIP-GFP* and *Ins2*$^{Apple/+}$ β-cells

To determine if ectopic hGH alters gene expression, we performed RNA-sequencing using four replicates of FACS-purified *MIP-GFP* β-cells (discussed in Chapter III) compared to six replicates of FACS-purified *Ins2*$^{Apple/+}$ β-cells at p60. The four *MIP-GFP* β-cell samples were mixed-gender while the six *Ins2*$^{Apple/+}$ β-cell samples were segregated by sex, with three from males and three from females. To avoid biases introduced by sex differences, the six gender-separated *Ins2*$^{Apple/+}$ β-cell samples were analyzed as six replicates. After isolation of both populations and performing RNA-seq, principal component analysis (PCA) and gene clustering analysis were performed. These analyses indicated the samples (**Figure 4.3B**) and the top 500 differentially-expressed genes (**Figure 4.3C**) cluster largely by genotype. Differential expression analysis of the ten samples revealed 9,128 genes (4,718 upregulated, 4,410 downregulated) that were significantly dysregulated (based on FDR-adjusted p-value < 0.05) in *MIP-GFP* β-cells compared to *Ins2*$^{Apple/+}$ β-cells, 87% of which were protein-coding, 3% were non-coding RNA, 4% were pseudogenes, and 6% were other types of transcripts (**Figure 4.4A**). Fold change between the two groups was as high as about 6,500-fold, and p-values for six of the transcripts were too small to estimate, indicating the extent to which gene expression differs between the two models.

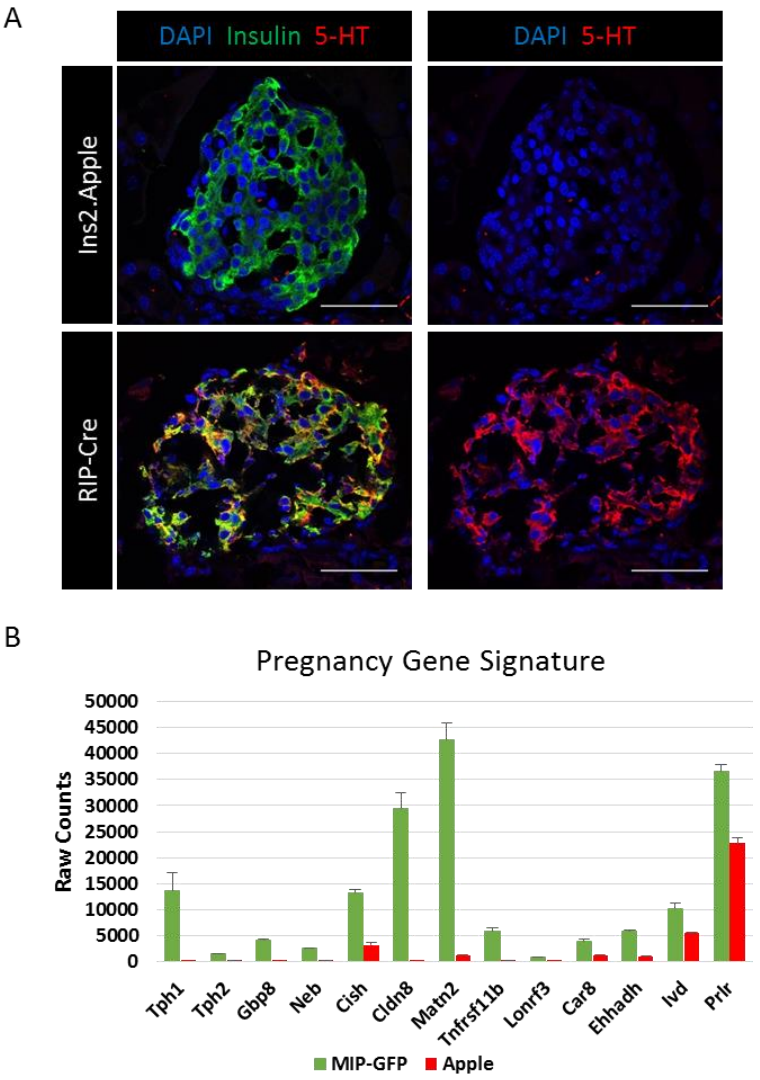

Figure 4.2. *Ins2*$^{Apple/+}$ mice do not have ectopic hGH expression. (A) Co-immunostaining of pancreatic sections from *Ins2*$^{Apple/+}$ and *RIP-Cre*, a transgene in which hGH is expressed, mice for insulin and serotonin (5-HT). Scale bar = 50μm. **(B)** Expression of pregnancy-related genes in FACS-purified β-cells from *Ins2*$^{Apple/+}$ and *MIP-GFP* mice, as determined by RNA-seq. Genes were hand-picked and have $p < 0.05$.

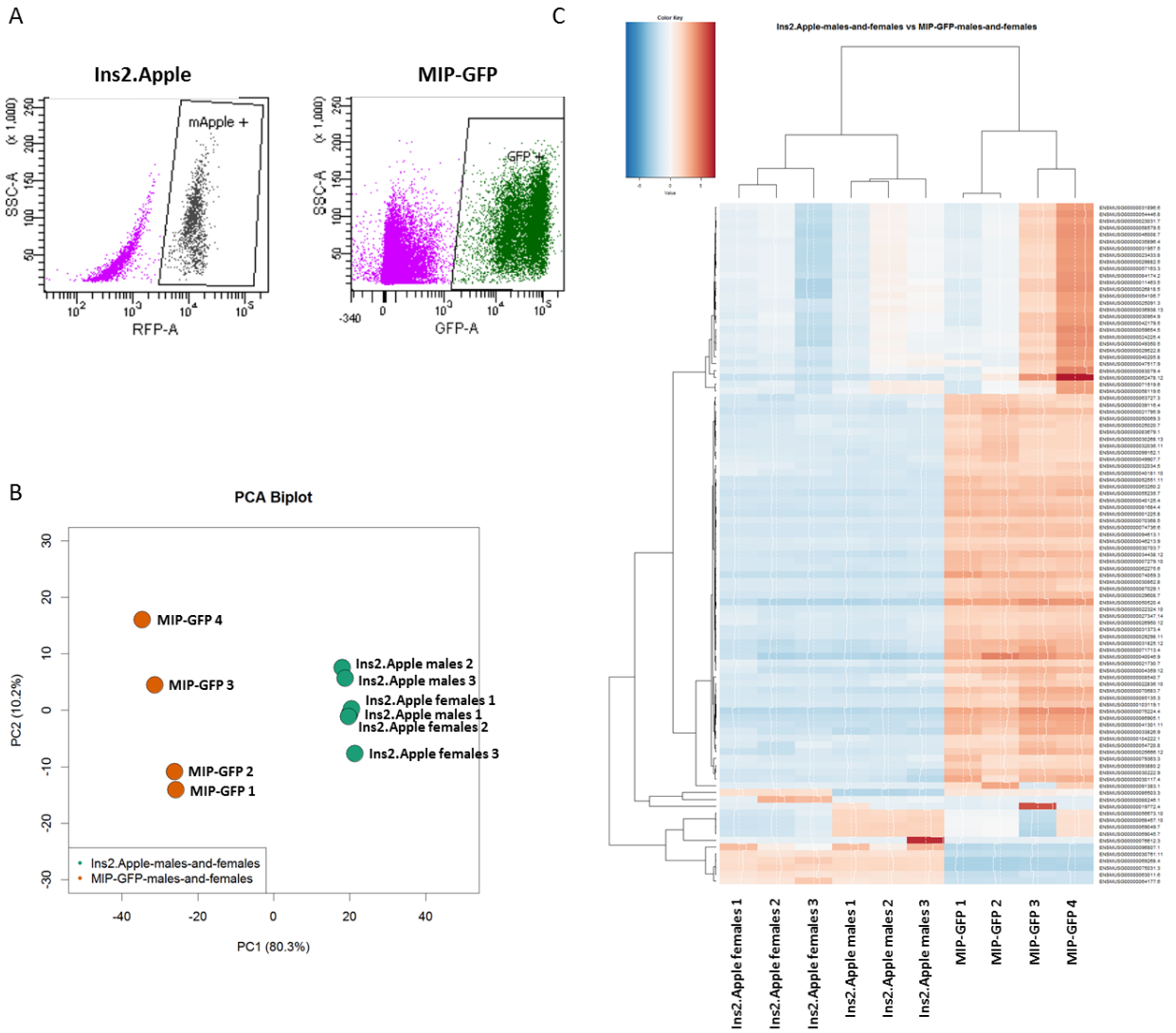

Figure 4.3. FACS purification of *Ins2*$^{Apple/+}$ and *MIP-GFP* β-cells for RNA-Seq. (A) FACS profiles of sorted β-cell populations from *Ins2*$^{Apple/+}$ and *MIP-GFP* mice. **(B)** Principal component analysis shows that the ten samples used for RNA-sequencing cluster by genotype, with some variation in the second principal component. **(C)** Heat map depicting gene clustering analysis using the top 500 differentially-expressed genes. J.P. Cartailler of Creative Data Solutions generated panels B and C.

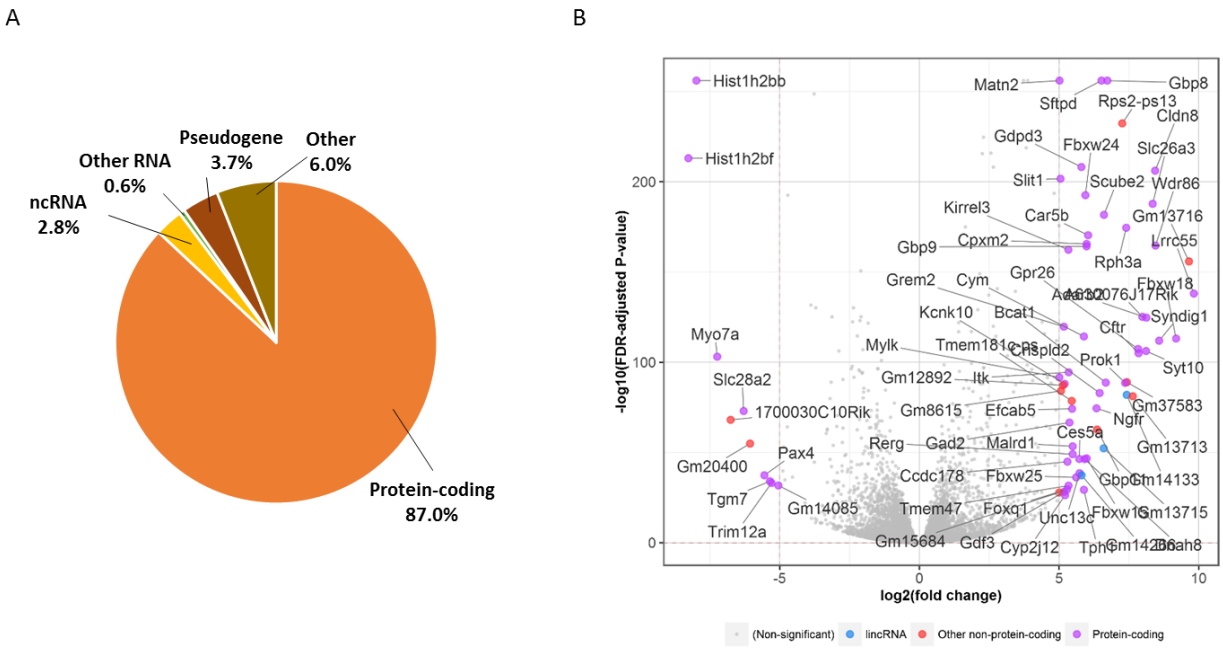

Figure 4.4. RNA-sequencing of *Ins2*$^{Apple/+}$ and *MIP-GFP* β-cells. With the assistance of J.P. Cartailler of Creative Data Solutions, we performed RNA-sequencing of FACS-purified β-cells from *Ins2*$^{Apple/+}$ and *MIP-GFP* animals at 8-9 weeks of age. **(A)** Pie chart showing the percentage of differentially-regulated genes that fall into biotype categories of protein-coding, non-coding RNA, other RNA, pseudogene, and other types of transcripts. **(B)** Volcano plot showing the most differentially-expressed genes in *MIP-GFP* β-cells based on the -$\log_{10}$ (FDR-adjusted P-value) and the $\log_2$ (fold change). Genes with a $\log_2$ (fold change) greater than 5 are labeled and grouped into categories based on biotype characterization.

To determine if the pregnancy-related genes known to upregulated in *MIP-GFP* β-cells are also upregulated in *Ins2*$^{Apple/+}$ β-cells, we compared their average expression levels in both alleles using raw count information from our RNA-seq dataset. We found that pregnancy-related genes are very highly expressed in *MIP-GFP* β-cells while expression levels are significantly lower in *Ins2*$^{Apple/+}$ β-cells (**Figure 4.2B**). These results suggest that, although the hGH minigene is present in the *Ins2*^{Apple} allele, it may not make a functional protein and does not induce a pregnancy-like phenotype in *Ins2*$^{Apple/+}$ mice.

Pathway Analysis and Upstream Regulator Prediction

Expression profiling of *MIP-GFP* β-cells revealed that approximately 9,000 genes are dysregulated compared to *Ins2*$^{Apple/+}$ β-cells. To correlate the functional abnormalities associated with β-cells from mice ectopically expressing hGH with the gene expression changes in *MIP-GFP* β-cells, we examined the expression of genes known to be involved in maintaining β-cell function. As previously-reported, *Slc2a2*, encoding GLUT2, is significantly downregulated in *MIP-GFP* β-cells (129). But we also observed that other critical genes, including *Ins1*, *Pdx1*, *Gck*, *Abcc8*, and *Hnf1a* are also significantly downregulated (**Figure 4.5A**).

To further explore the potential defects in *MIP-GFP* β-cells in an unsupervised way, we used DAVID v6.8 beta to search for enriched biological pathways among the top 3,000 up- or downregulated genes. Among the most upregulated pathways are those involved in protein processing (Protein processing in the ER, Protein export, and Ribosome) and oxidative phosphorylation (**Figure 4.5B**). The specific stress-related genes that are upregulated in *MIP-GFP* β-cells are shown in **Figure 4.5A**. Among the most downregulated pathways are those critical for

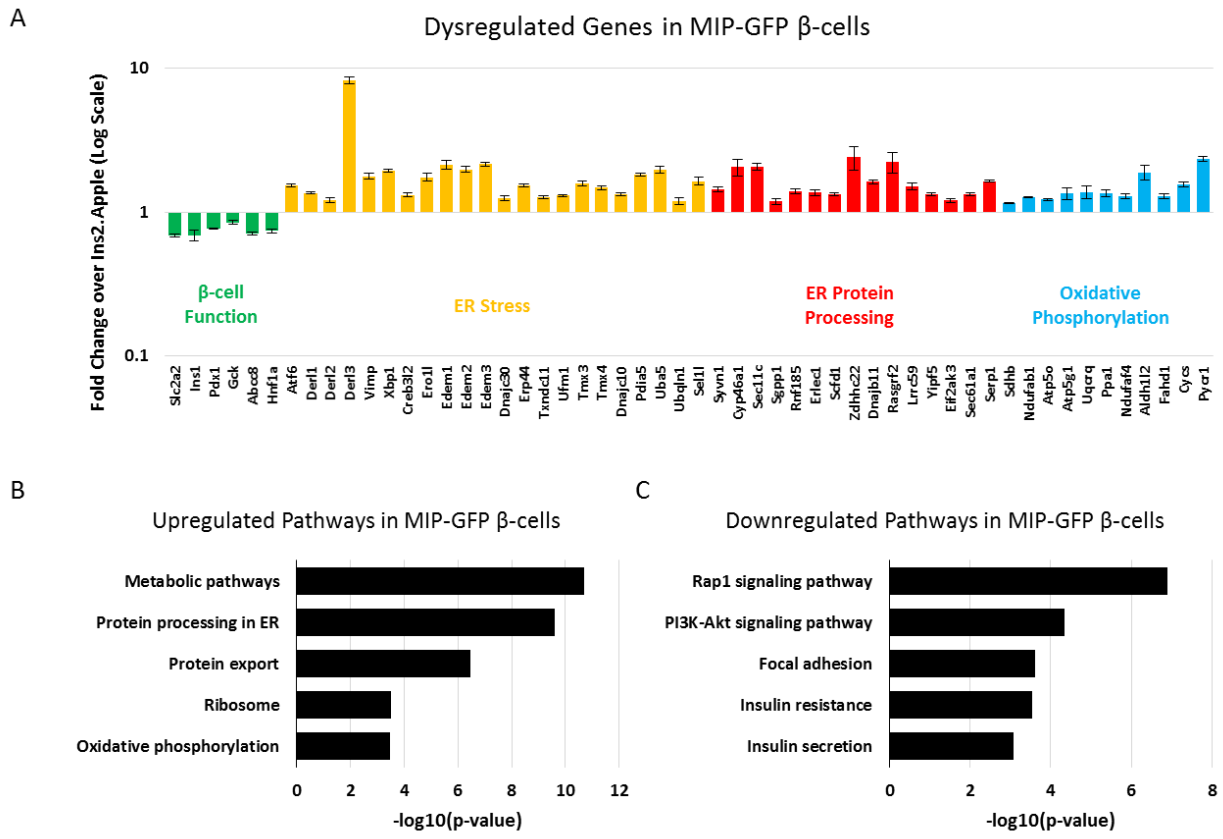

Figure 4.5. Dysregulated genes in *MIP-GFP* cells. (A) Selected differentially-expressed genes in *MIP-GFP* β-cells. *MIP-GFP* β-cells exhibit a decrease in expression of genes associated with β-cell function, and an increase in expression of genes associated with ER stress, ER protein processing, and oxidative phosphorylation, as indicated by the fold change in selected genes from our RNA-seq dataset. Genes involved in β-cell function were manually selected, whereas the remaining genes were identified by DAVID. All genes shown have FDR-adjusted p-values < 0.05. **(B, C)** We used the DAVID Bioinformatics Resource (version 6.8 Beta) to analyze enriched KEGG Pathway categories for genes that were significantly up- (B) or down-regulated (C) in *MIP-GFP* β-cells.

maintaining β-cell function (PI3K-Akt signaling pathway and insulin secretion) (**Figure 4.5C**). These results suggest that *MIP-GFP* β-cells downregulate genes and pathways critical for maintaining β-cell function and upregulate protein processing to the point of being subjected to ER stress.

Finally, to better understand the mechanisms by which these gene expression changes occur, we used iRegulon to predict common upstream regulators of the top 500 most upregulated genes in *MIP-GFP* β-cells. The top four predicted regulators are STAT5B, WISP2, IRF1, and ALX4 (**Figure 4.6**). The fact that many of the upregulated genes are predicted to have binding sites for STAT5B, a regulator previously implicated in mediating the effects of ectopic hGH expression (129), supports the idea that hGH is an important driver of gene expression observed in *MIP-GFP* β-cells. However, many of the upregulated genes are not predicted to be regulated by STAT5 signaling, suggesting that ectopic hGH is not the only contributor to the abnormalities in the *MIP-GFP* β-cells.

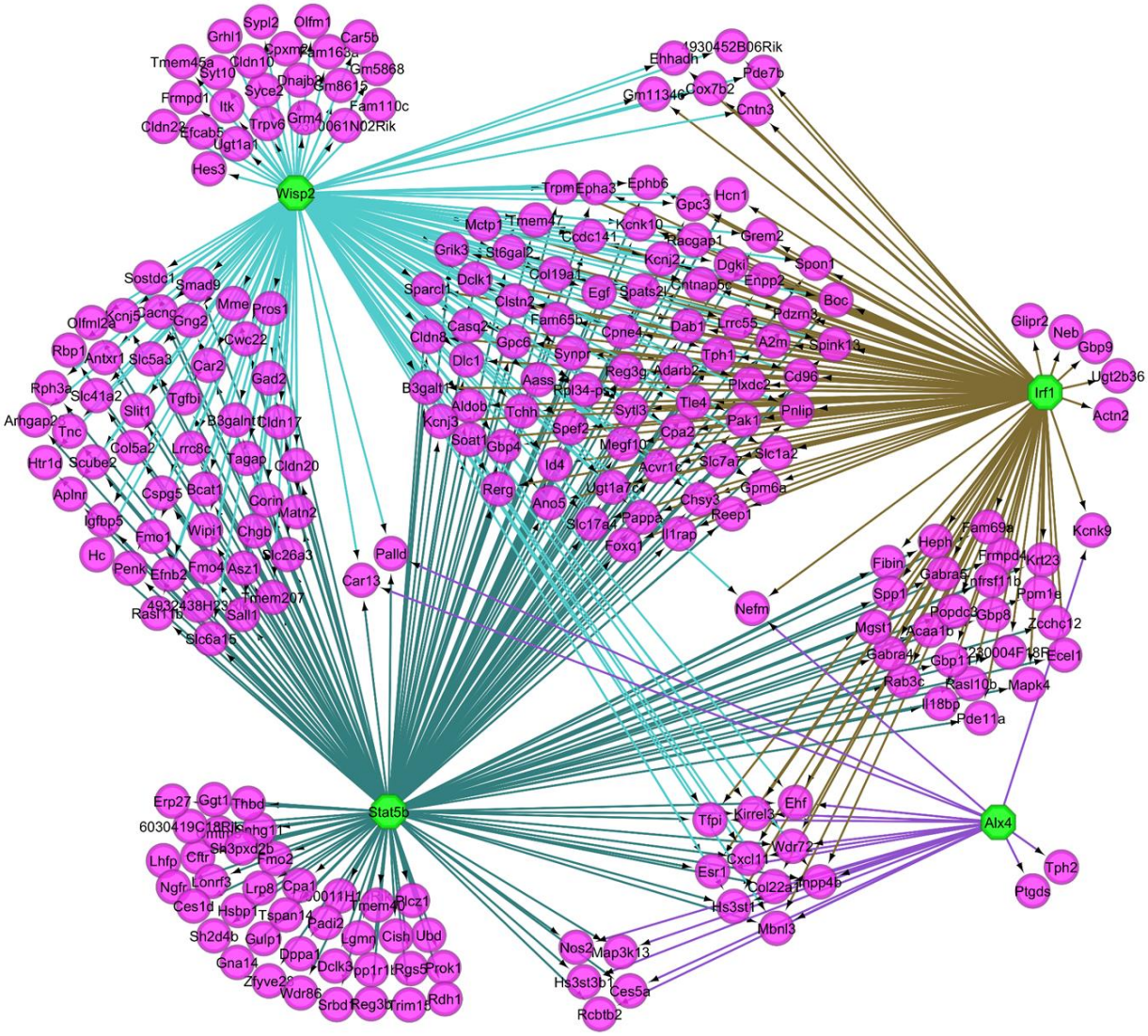

Figure 4.6. iRegulon-predicted network of regulators of the top 500 upregulated genes in *MIP-GFP* β-cells. Map depicting the top 4 predicted regulators (green octagons) and their predicted target genes (magenta circles).

Discussion

Using mice expressing a novel *Ins2.Apple* allele, which appears to escape the negative effects of the hGH minigene, we found that the widely-used *MIP-GFP* mice have severe defects in β-cell gene expression, some of which may be independent of hGH-driven STAT5 signaling.

MIP-GFP β-cells have decreased expression of critical functional genes

Our RNA-sequencing analysis using β-cells from *Ins2*$^{Apple/+}$ and *MIP-GFP* mice revealed the dysregulation of over 9,000 genes, due to the presence of the *MIP-GFP* transgene. It has previously been shown that β-cells from transgenic mice expressing the hGH minigene have impaired function, including decreased glucose tolerance (129; 152; 153). However, little is known about the underlying gene expression changes and molecular mechanisms responsible for this abnormality. Here, we demonstrate that, in addition to decreased expression of GLUT2, as previously described (129), several other critical β-cell function genes are downregulated in *MIP-GFP* β-cells. In particular, the downregulation of genes critical to the canonical GSIS pathway (*Gck*, encoding glucokinase, and *Abcc8*, encoding a component of the K_{ATP}-channel) provide a plausible explanation for the impairment in glucose tolerance observed in other mouse models expressing hGH.

MIP-GFP mice, however, despite having ectopic expression of hGH, do not have impaired glucose tolerance (113; 129), suggesting that the downregulation in these critical genes is not sufficient, at least within the timeframe of those studies, to cause glucose intolerance. An important caveat to this conclusion, however, is that background strain can hugely impact the severity of metabolic phenotypes (154). The transgenic mouse line (*Pdx1-Cre*) originally found to have

ectopic hGH expression and impaired glucose tolerance was maintained on a congenic C57BL/6 background (129), while the *MIP-GFP* mice cited as having normal glucose tolerance were maintained on a CD-1 background. Mice used here for RNA-sequencing were maintained on a mixed background of C57BL/6 and CD-1. Since the CD-1 background is an outbred strain, animals are more genetically diverse than inbred C57BL/6 animals, making it possible that mild metabolic abnormalities could be masked. Assessment of the *MIP-GFP* animals on an inbred C57BL/6 background is necessary to make sound conclusions about the effects of the transgene on β-cell function.

MIP-GFP β-cells exhibit gene expression changes associated with ER stress

In addition to having decreased expression of key functional genes, *MIP-GFP* β-cells have increased expression of genes involved in ER protein processing, ER stress, and oxidative phosphorylation. ER stress is thought to be a major cause of β-cell failure in the pathogenesis of T2D, caused by increased demand for insulin biosynthesis in the setting of insulin resistance (38; 39). More studies are needed to determine if *MIP-GFP* β-cells are, in fact, experiencing ER stress, rather than simply upregulating genes involved in protein processing pathways. The cause of the potential ER stress in these animals also remains to be determined. Since hGH appears to be expressed at a much higher level in *MIP-GFP* β-cells than in $Ins2^{Apple/+}$ β-cells, elevated STAT5 signaling may induce ER stress in an undetermined manner. It is also possible that differences in copy number of the alleles place varying levels of strain on the ER folding capacity of the β-cells from the two lines. H2B-Apple was strictly limited to one copy, since only heterozygous mice were used, but GFP could have been present in either one or two copies, since both heterozygous and hemizygous mice were used, potentially doubling the demand for GFP folding.

A network of dysregulated genes in *MIP-GFP* β-cells

We have previously postulated that STAT5 signaling is responsible for the pregnancy-like changes in gene expression observed in β-cells with ectopic hGH expression (129). However, we also observed phenotypic changes, such as impaired glucose tolerance, that were not explained by elevated STAT5 signaling. In support of this, our upstream regulator prediction analysis revealed at least three factors, other than STAT5, that could contribute to the observed gene expression changes. Among the predicted regulators are WISP2, IRF1, and ALX4. Interestingly, WISP2 has been shown to increase β-cell proliferation through AKT signaling (155), potentially contributing to increased β-cell mass in mouse models ectopically expressing hGH. Additionally, ALX4 is part of a locus associated with increased T2D risk in humans (156). While more work is needed to determine if these putative regulators control gene expression in *MIP-GFP* β-cells, our results suggest that a network of regulators, rather than a single factor, contribute to the abnormalities induced by the presence of the transgene.

An important caveat to these findings, however, is that we do not know which of the observed gene expression changes in the *MIP-GFP* β-cells are due to ectopic hGH expression or to confounding factors introduced by the experimental design. For example, some changes may be attributed to the difference in genetic background between the two moues strains used: *MIP-GFP* mice were a mixed background of C57BL/6 and CD-1 while $Ins2^{Apple/+}$ mice were pure C57BL/6. Additionally, allele design drastically differs between the two strains: the *MIP-GFP* allele is a transgene while the $Ins2^{Apple}$ allele is a knock-in allele. In order to definitively determine which gene expression changes are due to ectopic hGH expression, identical alleles, with one containing the hGH sequence and the other lacking it, need to be designed and studied further using whole transcriptome analysis.

CHAPTER V

TOWARDS A GENE CORRELATION NETWORK DESCRIBING β-CELL FAILURE

Introduction

In Type 2 diabetes mellitus (T2D) pancreatic β-cells fail in response to genetic susceptibility and metabolic stress due to mounting insulin resistance brought on by advancing age and obesity (37-40; 45). Insulin resistance occurs when target tissues no longer respond properly to insulin signaling, causing increased demand for insulin secretion, since glucose is not efficiently cleared from the blood (39). When insulin demand exceeds insulin secretory capacity, medical and dietary interventions become necessary to prevent further increases in plasma glucose concentration due to an increasing loss of β-cell function (37; 38; 40; 41; 157).

One factor that is widely accepted to increase risk for developing insulin resistance and T2D is obesity. In humans, weight gain of 5% is associated with a 20% increase in the risk for developing insulin resistance (158). Since obesity and insulin resistance are so tightly correlated, a common method to induce insulin resistance in rodent models is to administer a high-fat diet (HFD) (159). Insulin resistance induced by HFD is known to stimulate several responses in the β-cell, including increased insulin production, increased insulin secretion, and increased β-cell mass (159; 160). While the genes and gene networks that regulate the β-cell response to insulin resistance, or how these networks contribute to development of T2D, are not fully understood, metabolic stress, brought on by insulin resistance and other factors, is thought to disrupt the gene regulatory network (GRN) that maintains pancreatic β-cell function and identity.

Network biology can be used to catalog, integrate, and quantify genome-scale molecular interactions, from which key features relevant to regulation, disease, or other dysfunction can be identified and validated. Gene correlation networks (GCNs) provide an unbiased means for exploring the intrinsic organization of a transcriptome by extrapolating gene-to-gene relationships and organizing them into modules of coherently expressed genes (126; 161). In turn, these modules provide a framework for describing changes in gene expression across multiple conditions (162). GCNs can also be used as the basis to infer GRNs, which focus specifically on interactions between regulators and their putative targets in closely related conditions (162; 163). Since GCNs can integrate multiple RNA-Seq datasets, and become more informative as more datasets are incorporated, they can reveal patterns of gene co-expression that may not be identifiable in routine, pairwise comparisons (164). Such patterns reveal networks and subnetworks of genes that have critical cellular functions.

WGCNA is a software program that classifies genes into coherently expressed modules via hierarchical clustering (125). Due to the statistical power of approaches like WGCNA, modules of similarly regulated genes can be informative even when the differences between individual genes are small. WGCNA has been especially useful for identifying genes with high connectivity (centrality), often referred to simply as "hub" genes, that are of special interest because they have been shown to be resilient to large genetic background variations and therefore are vital for core biological functions. In this chapter, I will describe our collection of 17 RNA-seq datasets from FACS-purified β-cell populations under the conditions of chronically elevated $[Ca^{2+}]_i$, HFD-induced obesity, ectopic hGH expression, and sex differences, as well as our efforts towards using WGCNA to create a network to uncover hub genes regulating the β-cell response to various stressors.

Results

RNA expression profiling of β-cells from HFD-fed and chow-fed mice

Before collecting β-cell populations under the condition of obesity, we needed to first determine the time course over which HFD feeding disrupts glucose homeostasis. To this end, we measured weight gain, glucose tolerance, and insulin tolerance in male C57BL/6 mice given HFD versus a control diet for up to six weeks. After only one week of HFD, male mice had gained a significant amount of weight (3.7g) compared to male mice fed a control diet (0.7g) (**Figure 5.1A)**. After six weeks, mice fed HFD had gained 16g while mice fed a control diet had only gained 5.1g. HFD-fed male mice became glucose intolerant after only two weeks, and became more glucose intolerant with continuation of the HFD (**Figure 5.1B, C**). Furthermore, HFD-fed mice became insulin resistant after two weeks (**Figure 5.1D**).

To determine how HFD affects β-cell gene expression, we performed RNA-sequencing using FACS-purified β-cells from male *Ins2*$^{Apple/+}$ mice fed either a standard chow diet or a high-fat diet for 30 days (**Figure 5.2A**). A similar population of Apple-expressing cells was isolated from both chow-fed and HFD-fed mice (**Figure 5.2B**). Principal component analysis (PCA) and gene clustering analysis indicate that the samples and the top 500 differentially-expressed genes cluster largely by diet, with some variation (**Figure 5.2C, D**). Differential expression analysis of the six samples revealed 1,596 genes whose expression in HFD-fed β-cells differed from that of the chow-fed β-cells (based on a p-value < 0.05). Approximately 96% of the differentially-expressed genes encode proteins, 1.4% are non-coding RNAs, 0.6% are pseudogenes, and 2% are

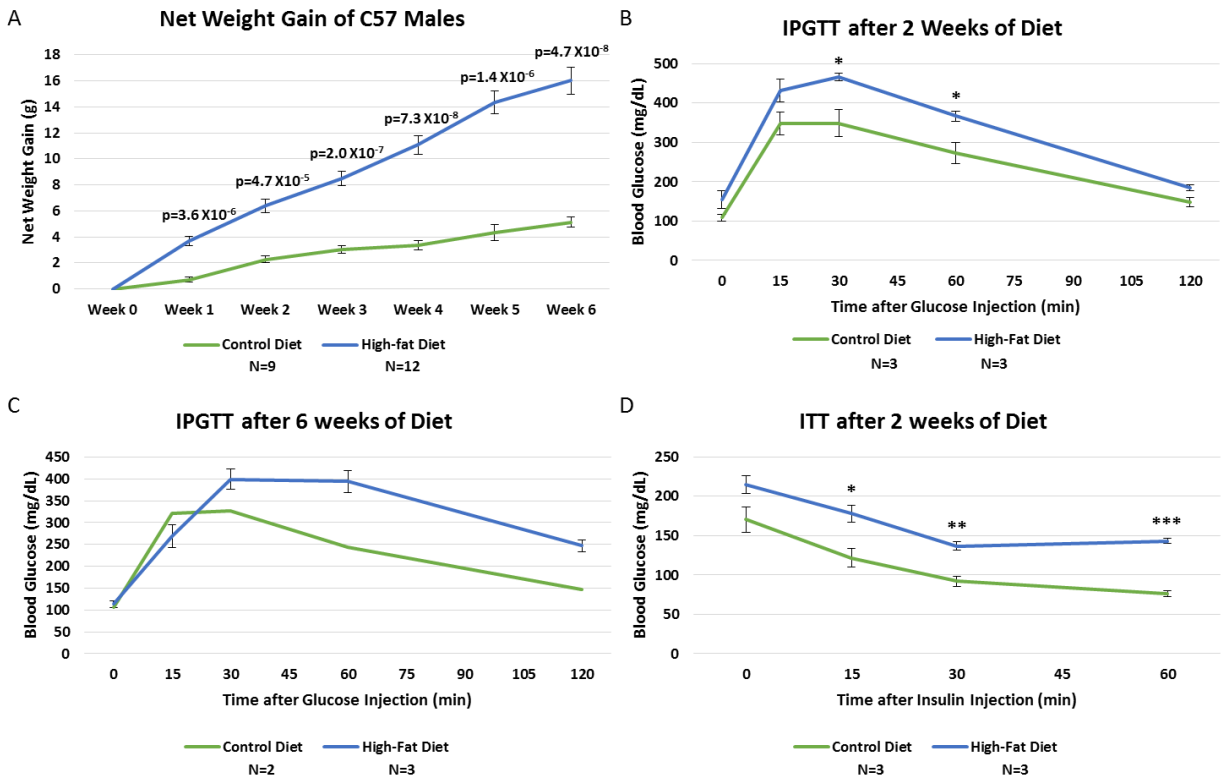

Figure 5.1 Glucose homeostasis in HFD-fed C57BL/6 animals. Male C57BL/6 mice were given either a 10% fat diet (control) or a 60% fat diet (high-fat) for up to 6 weeks. **(A)** Net weight gain in control-fed and HFD-fed males over a 6-week period. **(B, C)** Glucose tolerance tests of control-fed and HFD-fed males after 2 weeks (B) or 6 weeks (C) of experimental diets. **(D)** Insulin tolerance test in control-fed and HFD-fed males after 2 weeks of experimental diets. Error bars represent standard error. *p<0.05, **p<0.01, ***p<0.001.

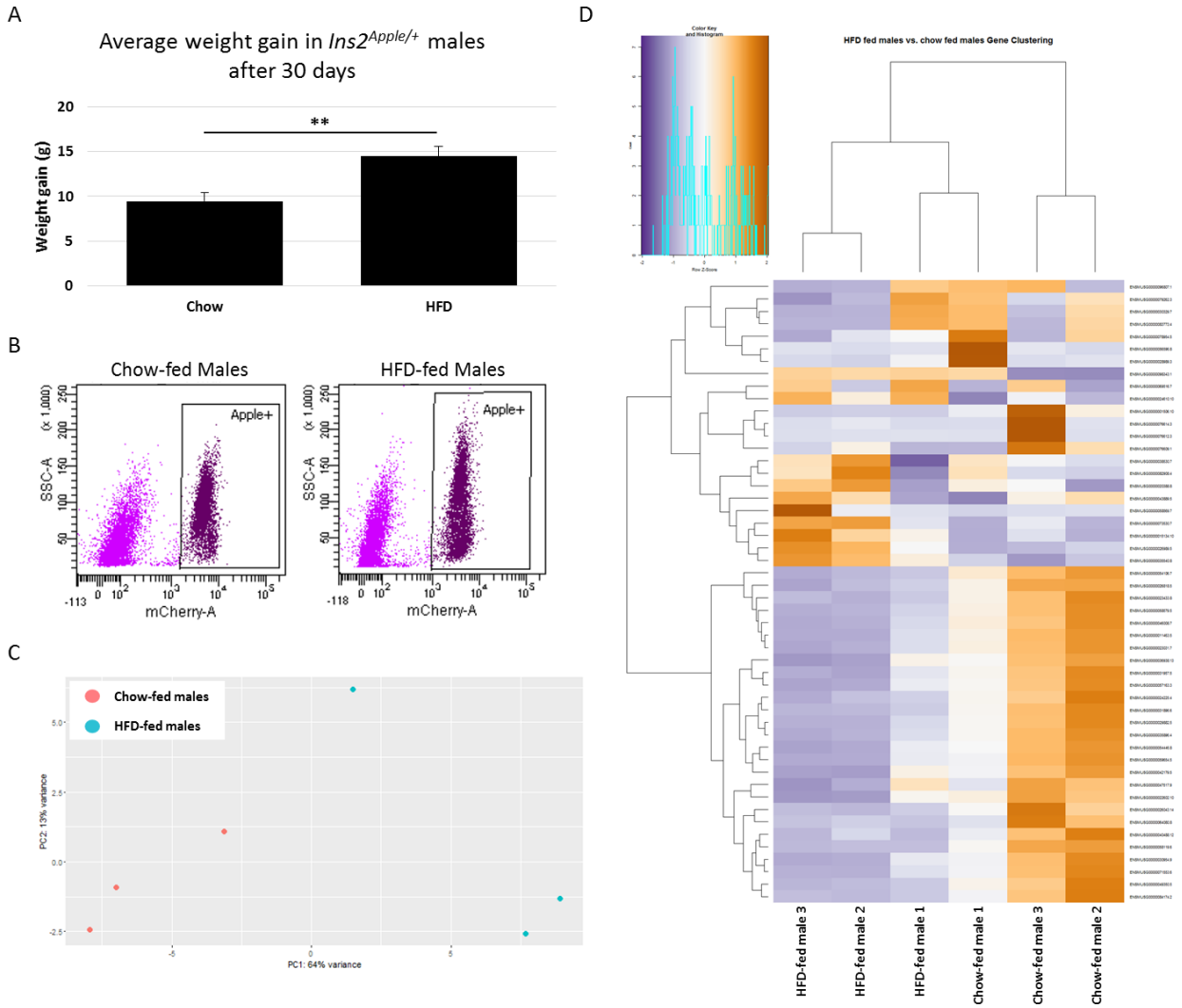

Figure 5.2 RNA-sequencing of *Ins*$^{Apple/+}$ β-cells from HFD- or chow-fed animals. We performed RNA-sequencing of FACS-purified β-cells from Ins2$^{Apple/+}$ animals fed either a high-fat diet or a chow diet. **(A)** Average weight gain in chow-fed and HFD-fed *Ins2*$^{Apple/+}$ males used for FACS and RNA-sequencing. **p<0.01. **(B)** FACS profiles of sorted populations from *Ins2*$^{Apple/+}$ mice indicating that β-cells from both groups can be purified similarly. **(C)** Principal component analysis shows that the six samples used for RNA-sequencing cluster by diet. **(D)** Heat map depicting gene clustering analysis. J.P. Cartailler of Creative Data Solutions generated panels C and D.

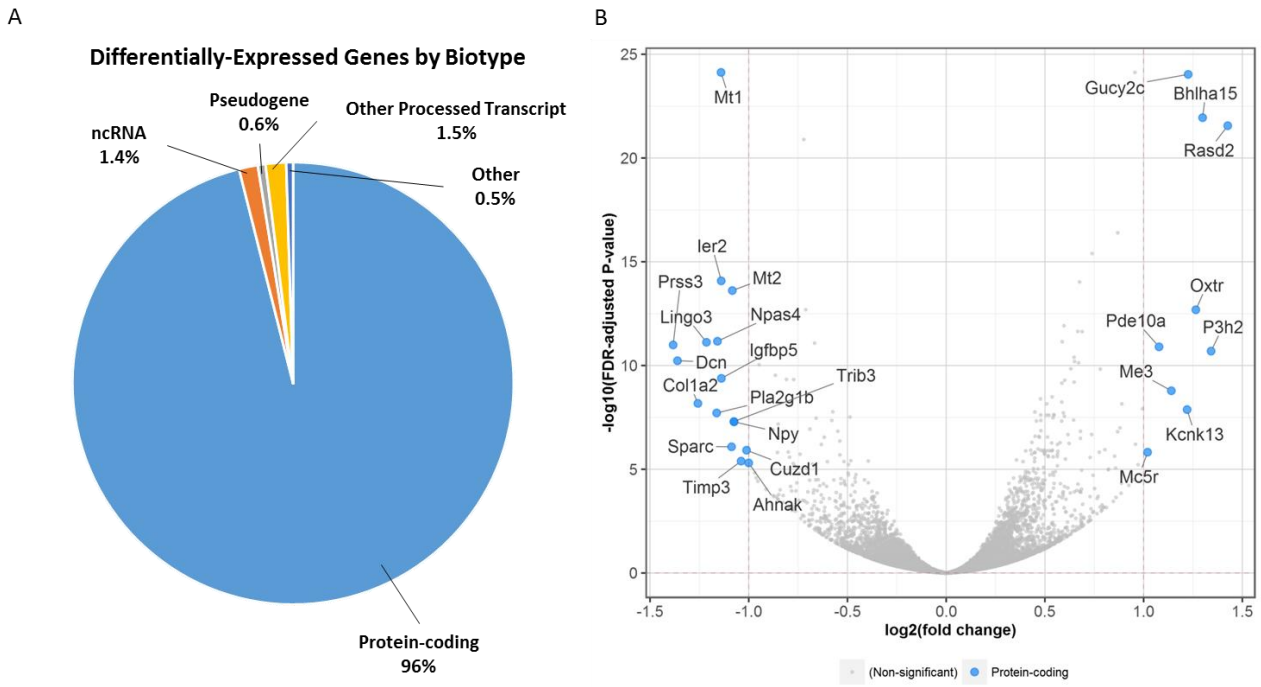

Figure 5.3 Differential expression analysis of *Ins*$^{Apple/+}$ β-cells from HFD- or chow-fed animals. With the assistance of J.P. Cartailler of Creative Data Solutions, we performed RNA-sequencing of FACS-purified β-cells from *Ins2*$^{Apple/+}$ mice fed either a chow or high-fat diet **(A)** Pie chart showing the percentage of differentially-regulated genes that fall into biotype categories of protein-coding, non-coding RNA, pseudogene, other processed transcripts, and other. **(B)** Volcano plot showing the most differentially expressed genes in HFD-fed *Ins2*$^{Apple/+}$ β-cells based on the -$\log_{10}$ (FDR-adjusted P-value) and the $\log_2$ (fold change). Genes with a $\log_2$ (fold change) greater than 3 are labeled and grouped into categories based on biotype characterization.

other types of transcripts (**Figure 5.3A**). Among the top upregulated genes in β-cells from HFD-fed *Ins2*$^{Apple/+}$ mice are *Gucy2*, encoding a guanylate cyclase, *Bhlha15*, a transcription factor called Mist-1, *Rasd2*, a monomeric G-protein called Rhes, *Oxtr*, the oxytocin receptor, and *Kcnk13*, a potassium channel (**Figure 5.3B**). Among the top down-regulated genes are *Mt1* and *Mt2*, cysteine-rich metal binding proteins called metallothionein 1 and 2, *Ier2*, an immediate early gene called Pip92, *Npas4*, an immediate early gene induced by ER stress, and *Igfbp5*, encoding an insulin-like growth factor binding protein (**Figure 5.3B**).

High-fat diet induces both β-cell proliferation and ER stress

To determine which functional categories are enriched in our RNA-seq dataset, we used the DAVID Bioinformatics Resource v6.8 beta to perform functional annotation clustering and KEGG pathway analysis. High-fat diet is known to stimulate an increase in β-cell mass (159; 160). In accordance with this observation, categories of cell division (enrichment score = 4.5) and kinetochore (enrichment score = 2.8) were both among the top upregulated categories in β-cells of HFD-fed mice (**Figure 5.4A**). Specific genes involved in cell division that are significantly upregulated in β-cells of HFD-fed mice are shown in **Figure 5.4F**.

In addition to promoting β-cell compensation through elevated proliferation, HFD is also known to cause ER stress, contributing to β-cell failure in T2D (51). Indeed, among the top upregulated categories of genes in β-cells of HFD-fed mice are protein transport (enrichment score = 13.0) and the unfolded protein response (enrichment score = 8.3) (**Figure 5.4A**), and among the top upregulated pathways in β-cells of HFD-fed mice are ER protein processing (p-value = 1.26 x

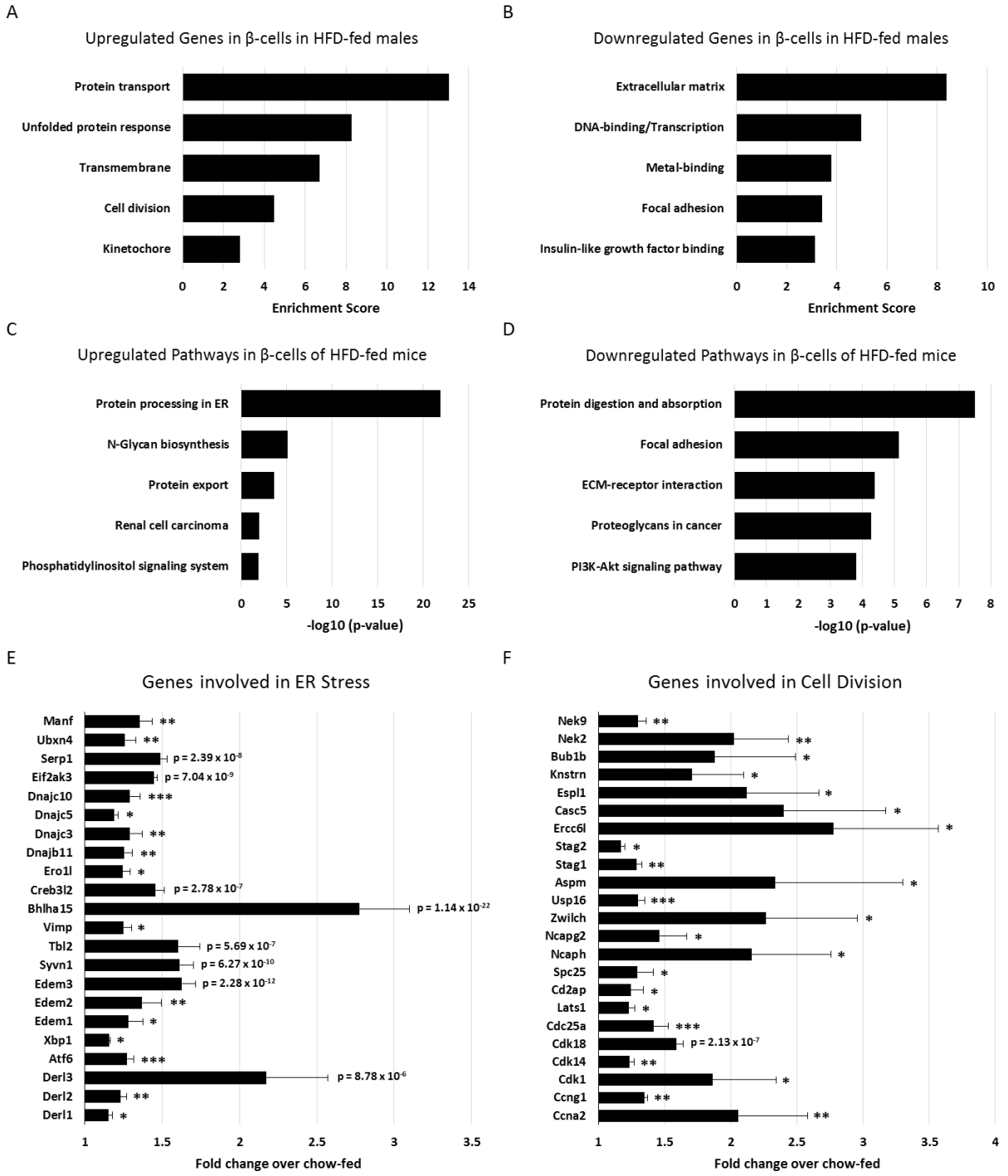

Figure 5.4 Functional annotation clustering and pathway analysis. We used the DAVID Bioinformatics Resource (version 6.8 Beta) to analyze enriched gene ontology and KEGG Pathway categories that were significantly up- or down-regulated in HFD-fed *Ins2*$^{Apple/+}$ β-cells. **(A)** The top up-regulated gene categories, **(B)** the top down-regulated gene categories, **(C)** the top up-regulated pathways, and **(D)** the top down-regulated pathways in HFD-fed *Ins2*$^{Apple/+}$ β-cells. Selected genes involved in **(E)** ER stress and **(F)** cell division that are upregulated in HFD-fed *Ins2*$^{Apple/+}$ β-cells. *p<0.05, **p<0.01, ***p<0.001.

10^{-22}) and protein export (p-value = 2.5 x 10^{-4}) (**Figure 5.4C**). Specific genes involved in ER Stress that are significantly upregulated in β-cells of HFD-fed mice are shown in **Figure 5.4E**.

Seventeen RNA-seq datasets from adult β-cells

To better understand the physiological and pathological changes that occur in pancreatic β-cells in response to metabolically- and genetically-induced stress, we have collected, processed, and analyzed 17 RNA-seq datasets from FACS-purified mouse β-cells at p60, as shown in **Table 5.1**. These 17 datasets originated from five different groups of mice that enabled us to perform four different pairwise comparisons using DESeq2 (123; 165) and to obtain the volcano plots shown in **Figure 5.5**. The collection and analysis of Groups A and B is described in Chapter III, and of Groups D and E, in Chapter IV. Comparison of Group A vs. B enabled us to assess the impact of chronically elevated $[Ca^{2+}]_i$ (excitotoxicity) on gene expression (**Figure 5.5A**). Comparison of C vs. D provided insight into the effects of obesity and a high fat diet (HFD) (**Figure 5.5B**). Comparison of A vs. both D and E (combined as six replicates) revealed the differences between β-cells of *MIP-GFP* and *Ins2*^{Apple} mice (**Figure 5.5C**). Finally, by comparing D vs. E, we were able determine the effect of sex in the setting of a standard diet (**Figure 5.5D**). The experimental paradigm, and number of genes affected by each perturbation, is summarized in **Table 5.2**.

Table 5.1: Genotype, fluorescent reporter, diet, and sex of experimental mice.

Group	**Genotype**	**Reporter**	**Diet**	**Sex**	**N**
A	Wildtype	*MIP-GFP*	Chow	Mixed	4
B	*Abcc8*$^{-/-}$	*MIP-GFP*	Chow	Mixed	4
C	Wildtype	*Ins2*$^{Apple/+}$	High Fat (60%)	Male	3
D	Wildtype	*Ins2*$^{Apple/+}$	Chow	Male	3
E	Wildtype	*Ins2*$^{Apple/+}$	Chow	Female	3

Table 5.2: Pairwise comparisons performed to assess the impact of four different variables on β-cell gene expression.

Comparison	**Variable**	**Genes affected ($p < 0.05$)**
A vs. B	Chronically elevated $[Ca^{2+}]_i$	4,208
C vs. D	Obesity/HFD	1,596
A vs. [D + E]	MIP-GFP transgene	9,128
D vs. E	Sex	657

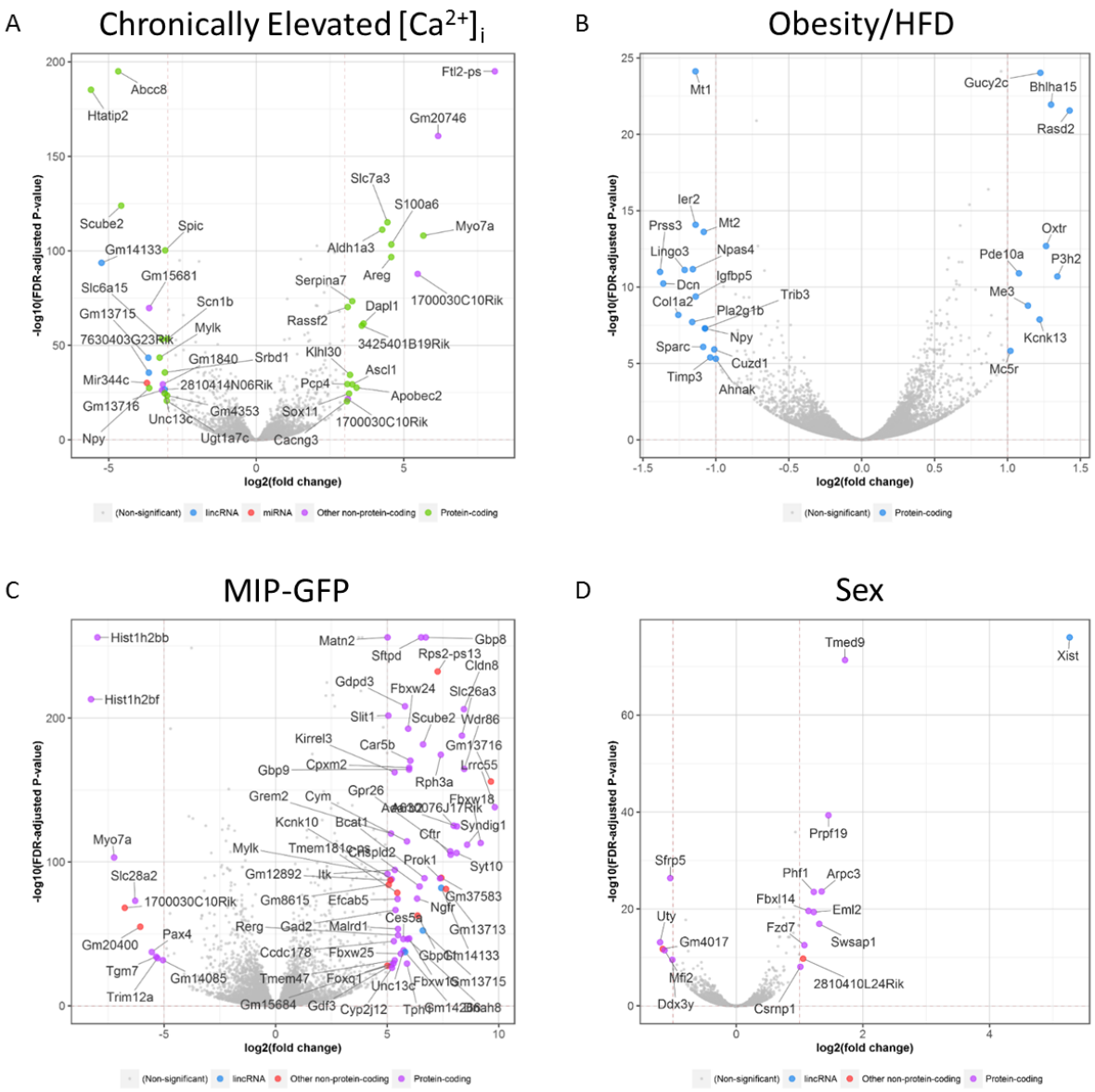

Figure 5.5. Volcano plots of genes that are differentially regulated in β-cells. The results of our four pairwise comparisons performed using DESeq and our 17 RNA-Seq datasets. Genes are indicated in different colors that reflect biotype.

Weighted gene correlation network analysis

We constructed a preliminary gene correlation network of the 17 datasets listed in **Table 5.1** using standard WGCNA. After filtering out genomic features with missing values and settling on a soft thresholding power of 0.8 (based on scale-free topology fit index), we used WGCNA to construct a gene correlation network, whose dendrogram is shown in **Figure 5.6**, consisting of fifteen modules (**Table 5.3**). Multiple modules contain hub genes with strong connectivity, two examples of which are shown in **Figures 5.7** and **5.8**. To better understand what these modules mean biologically, we analyzed the correlations between each module and specific traits. Traits used in this analysis were "*Abcc8* genotype," "Diet," "Sex," "Fluorescent Reporter," and "Genetic Background" (**Figure 5.9**). We found that several modules were significantly correlated with specific traits. For example, the green-yellow module (**Figure 5.7**) is positively correlated (0.83, $p = 4x10^{-5}$) with the "Diet" trait. Additionally, the yellow module (**Figure 5.8**) is negatively correlated (-0.8, $p = 1x10^{-4}$) with the "*Abcc8* Genotype" trait.

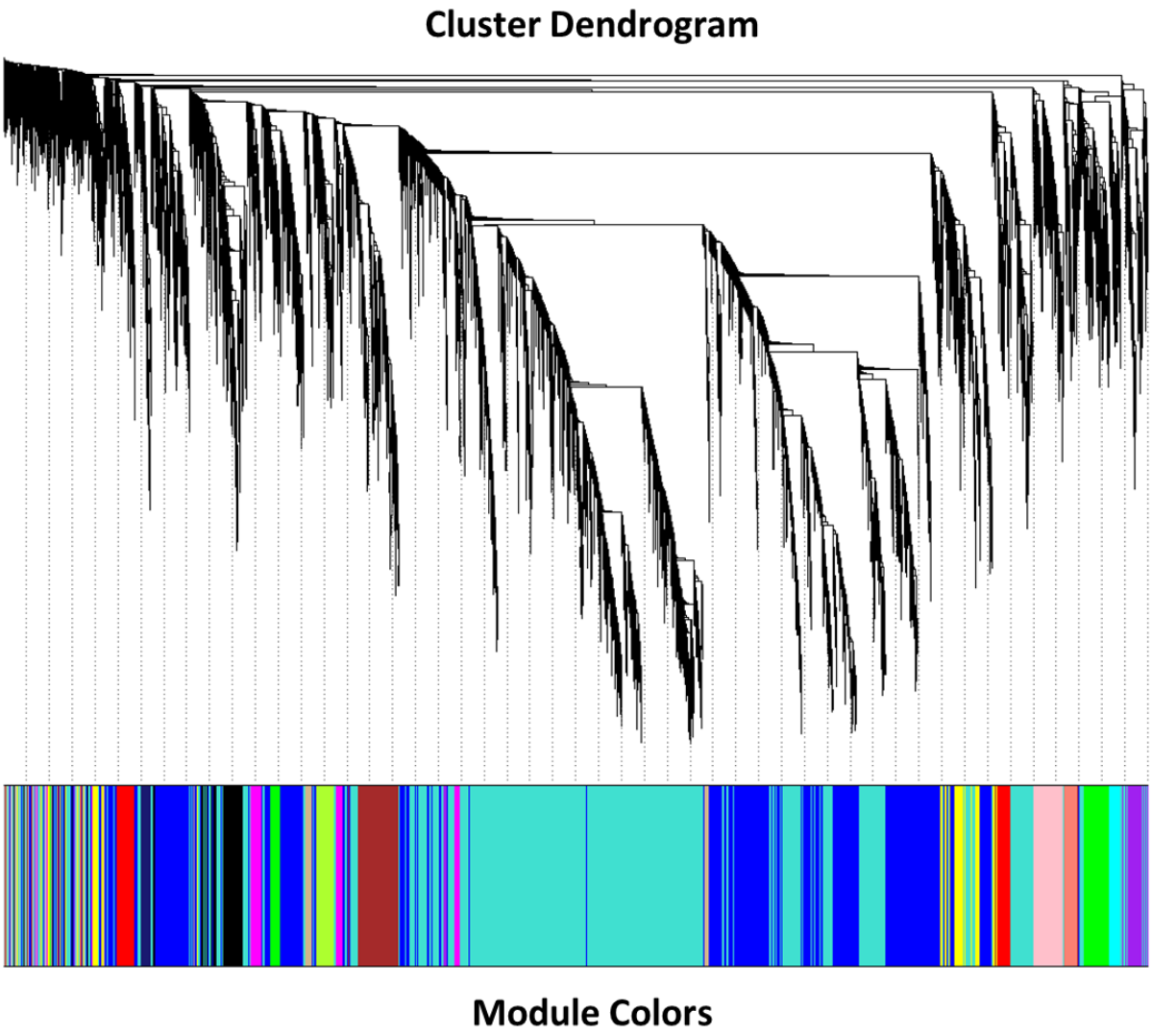

Figure 5.6. **Cluster Dendrogram of GCN**. Output obtained using WGCNA to process 17 RNA-Seq datasets from five different experimental conditions. Over 19,000 genes were organized into 15 modules.

Table 5.3: Preliminary WGCNA Results.

Module Name	**# of Genes**
Turquoise	7876
Blue	5316
Brown	769
Yellow	712
Green	655
Red	586
Black	536
Pink	529
Magenta	444
Purple	426
Greenyellow	302
Tan	247
Salmon	246
Cyan	198
Midnightblue	190

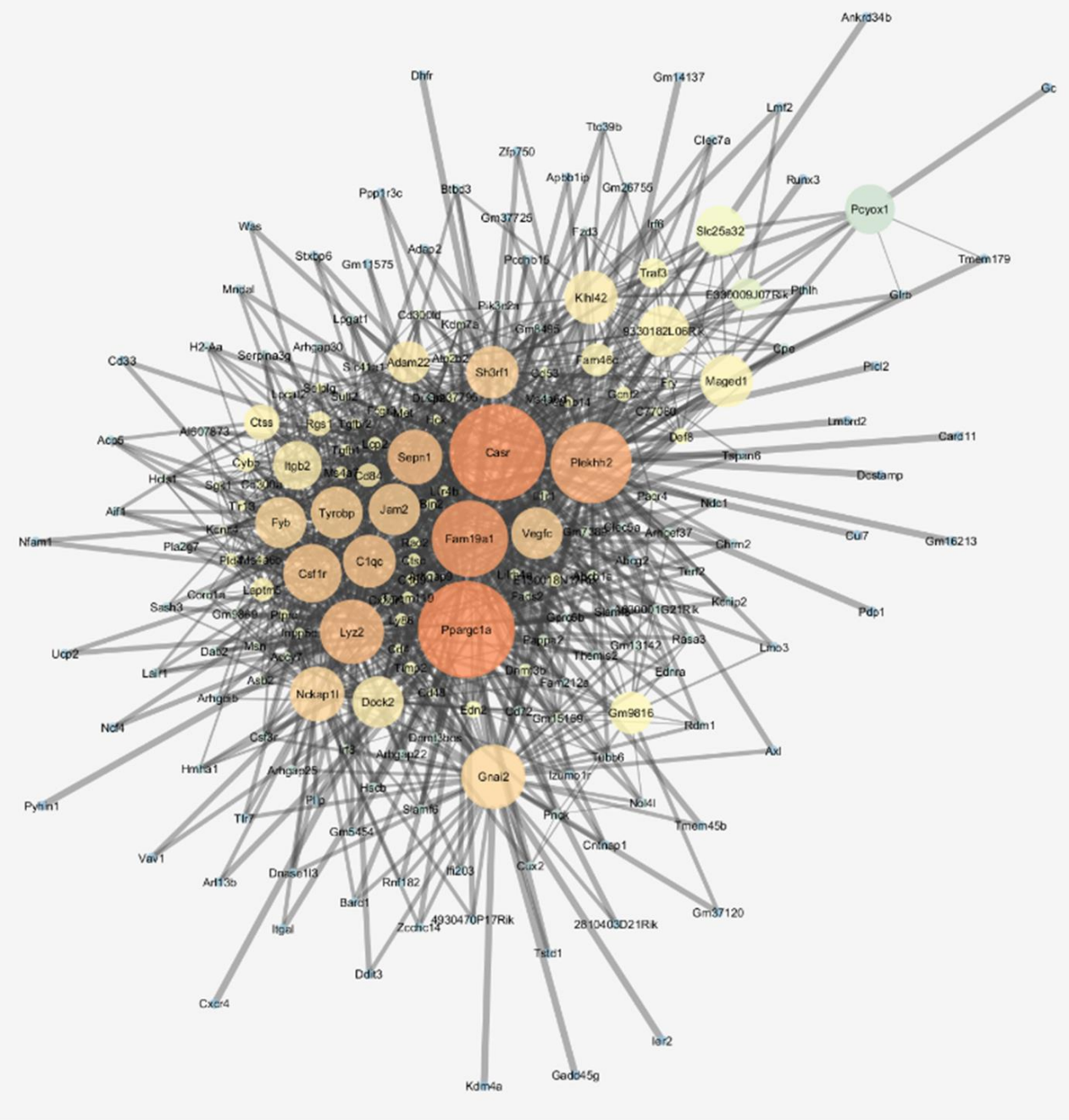

Green-Yellow Module

Figure 5.7. **WGCNA-derived Green-Yellow gene module.** Green-yellow module from standard WGCNA using 17 FACS-purified β-cell RNA-seq datasets. Circles, or nodes, contain the names of individual genes, and lines, or edges, form connections between nodes.

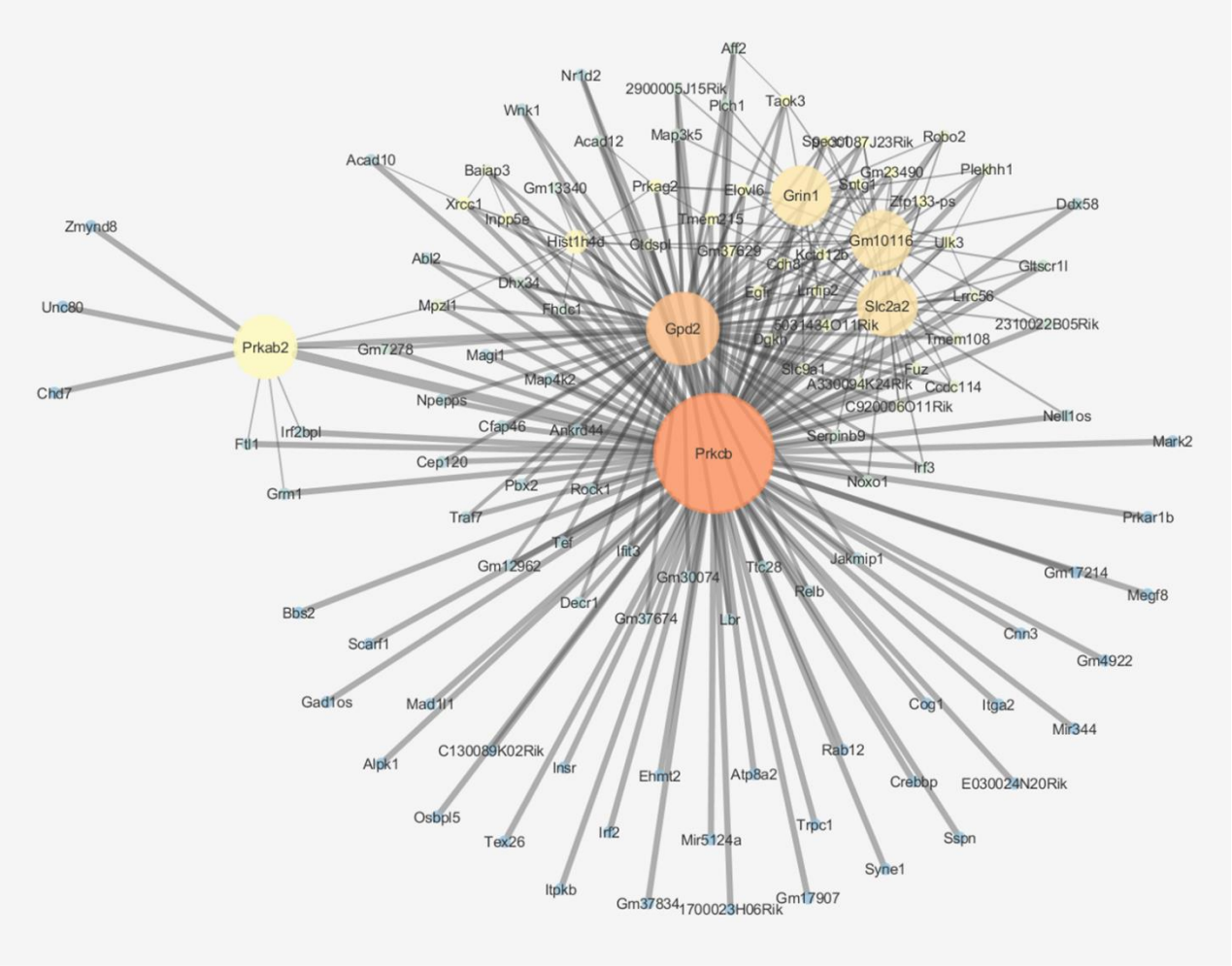

Yellow Module

Figure 5.8. **WGCNA-derived Yellow gene module.** Yellow module from standard WGCNA using 17 FACS-purified β-cell RNA-seq datasets. Circles, or nodes, contain the names of individual genes, and lines, or edges, form connections between nodes.

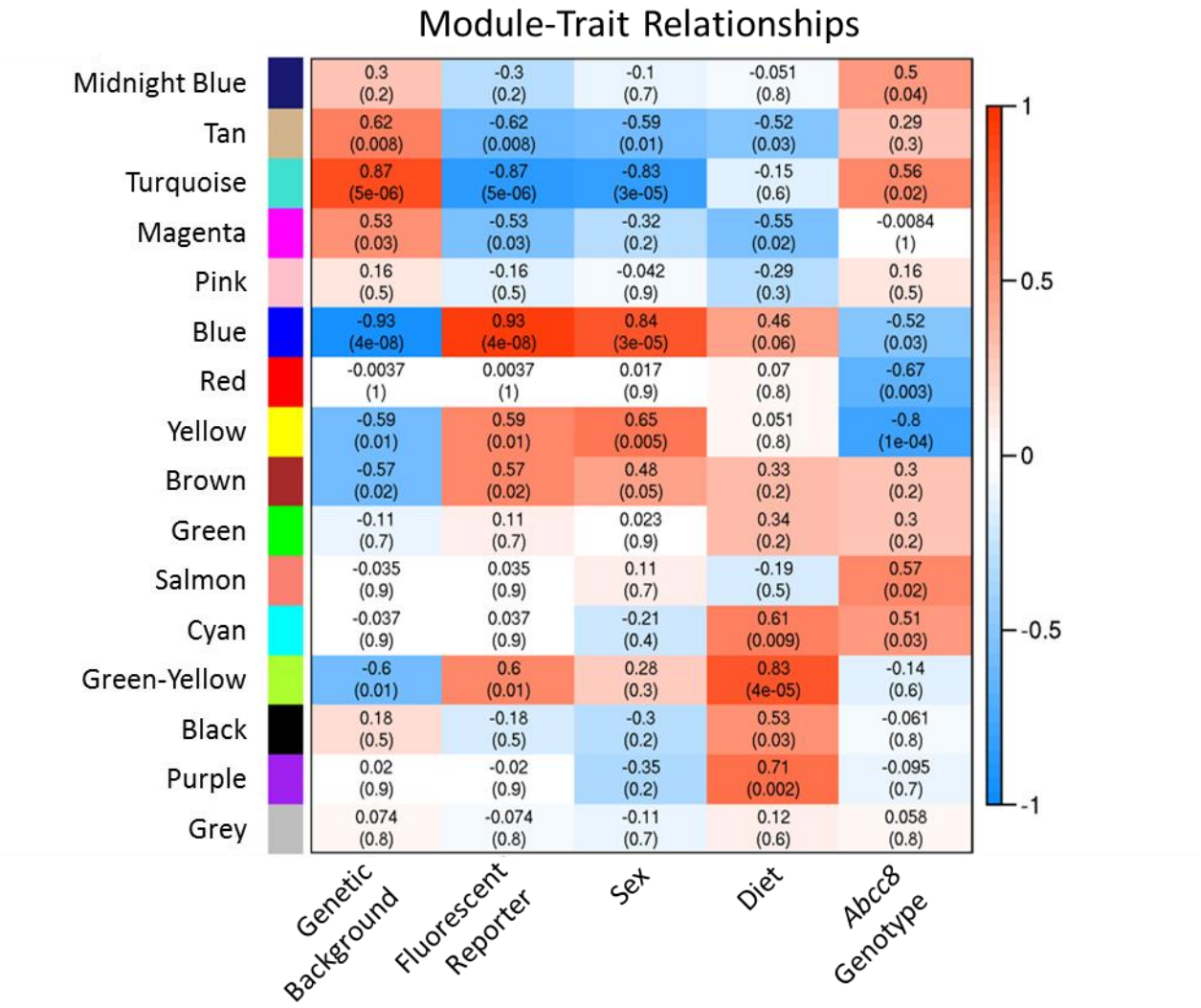

Figure 5.9. Module-trait relationships. For each gene, we plotted the strength of module membership against gene significance for a specific trait. This analysis yielded a correlation value of each module with each trait as well as a p-value (shown in parentheses above). A positive correlation value indicates a positive correlation while a negative correlation value indicates a negative correlation. Correlation values range from an absolute value of 1, indicating perfect correlation, to a value of 0, indicating no correlation. For example, the green-yellow module is positively correlated (0.83, $p = 4x10^{-5}$) with the "Diet" trait, and the yellow module is negatively correlated (-0.8, $p = 1x10^{-4}$) with the "*Abcc8* Genotype" trait. Red indicates strength of positive correlation. Blue indicates strength of negative correlation.

Discussion

Dysregulated genes in β-cells from obese mice

RNA-expression profiling of FACS-purified β-cells from HFD- or chow-fed *Ins2*$^{Apple/+}$ males at p60 revealed the dysregulation of 1,596 genes in response to obesity (**Figure 5.3**). Among the most upregulated genes is *Oxtr* (3-fold upregulated, $p = 2.05 \times 10^{-13}$), which encodes the oxytocin receptor. Oxytocin, a neuropeptide produced by hypothalamic neurons, has a stimulatory effect on insulin secretion in β-cells (166-168), and has anti-diabetic effects in both mice and humans (169). Upregulation of the oxytocin receptor in β-cells of HFD-fed mice could reflect an adaptive mechanism to allow for increased insulin secretion in the setting of obesity and insulin resistance.

Another highly upregulated gene is *Rasd2* (3.2-fold upregulated, $p = 2.77 \times 10^{-22}$), encoding a monomeric G-protein called Rhes. Interestingly, *Rasd2* expression is regulated in β-cells in a membrane depolarization- and calcium-dependent manner (170; 171). It has also been shown to bind and activate mTOR (172), a protein which stimulates β-cell proliferation (173-176). These previous studies suggest that Rhes may be a link between metabolic stimulation and compensatory β-cell proliferation, and, its upregulation in β-cells of HFD-fed mice supports this hypothesis.

Among the most highly downregulated genes in β-cells from HFD-fed mice is *Npas4* (2.7-fold downregulated, 6.76×10^{-12}), an immediate early gene that is induced by ER stress. Immediate early genes are activated as a first line of defense in cells undergoing stress. In β-cells, *Npas4* expression increases in response to membrane depolarization as well as ER stress-inducers, and has been shown to protect the β-cell from thapsigargen- and palmitate-induced dysfunction and

death (177). It has also been shown to protect β-cells from toxicity induced by the calcineurin inhibitor tacrolimus (178), though the mechanism has not been elucidated. Its downregulation suggests that β-cells in HFD-fed mice may be experiencing the late stages of ER stress, meaning that they have lost a key cytoprotective protein and may soon undergo cell death. This hypothesis is supported by functional annotation clustering as well as pathway analysis, which reveal significant upregulation of genes involved in the unfolded protein response and protein processing in the ER.

Exploration of preliminary modules

By performing WGCNA using 17 different RNA-seq datasets from populations of FACS-purified β-cells, we were able to classify over 19,000 genes into 15 preliminary modules. Several of these modules significantly correlate with specific traits represented by the different datasets. For instance, the yellow module, which correlates best with the *Abcc8* null allele, contains five hub genes. Among these, *Prkcb* shows the highest connectivity. This is both a plausible and informative finding since *Prkcb* belongs to a family of serine- and threonine protein kinases that are activated by calcium and diacylglycerol. The negative correlation of genes in this module with the *Abcc8* null genotype may reflect a negative feedback loop present in the β-cell which downregulates Ca^{2+}-responsive proteins/kinases to protect the cell from overactivation of downstream pathways in the case of chronically elevated $[Ca^{2+}]_i$. Similarly, there are multiple, densely connected hub genes in the green-yellow module, which correlates with HFD and obesity. Interestingly, *Ppargc1a*, a transcriptional coactivator whose expression has been associated with impaired glucose tolerance and reduced insulin secretion (179; 180), exhibits the highest

connectivity in this module. While much more work must be performed in order to fully understand what is represented by these modules, this initial analysis provides strong evidence that our method will yield informative information about how various stimuli affect the β-cell gene expression network.

Limitations of the current datasets

Although the 17 datasets we used to perform our preliminary WGCNA are of high quality and have yielded informative results, there are several confounding factors that exist. First, sex was not controlled in each of the datasets collected. The *MIP-GFP* and *Abcc8$^{-/-}$; MIP-GFP* datasets are from mice of mixed sexes, while the remaining datasets were collected in a sex-segregated manner. Second, not all datasets were collected using the same fluorescent reporter allele. Most datasets used the *Ins2.Apple* allele recently generated by our lab, but the *Abcc8$^{-/-}$* dataset contained the *MIP-GFP* allele. Third, genetic background of the mice was not consistent across all samples and is a confounding variable when considering the effects of the *MIP-GFP* allele compared to the *Ins2.Apple* allele. Finally, we neglected to collect datasets from HFD-fed *Ins2$^{Apple/+}$* females, preventing us from uncovering any sex-specific effects of obesity.

To eliminate these confounding factors, replacement datasets need to be collected that completely control for the factors of sex, fluorescent reporter allele, and genetic background. **Table 5.4** summarizes the total datasets that will be used in a future WGCNA, including the 15 replacement datasets that are yet to be obtained. To accomplish this task, *Abcc8$^{-/-}$* mice will be bred with *Ins2$^{Apple/+}$* mice and will be separated into sex-specific datasets to eliminate the confounding factors of fluorescent reporter allele, genetic background, and sex. Additionally, the

MIP-GFP allele will be obtained in a congenic C57BL/6 background, to eliminate the confounding effects of mixed background. Finally, *Ins2*$^{Apple/+}$ female mice will be subjected to the HFD paradigm. In total, this plan will generate 24 FACS-purified RNA-seq datasets for use in WGCNA. It is also important to note that combination of the male and female datasets will allow for analysis of six replicates for each perturbation, if sex-separation is not a critical consideration.

Table 5.4: Summary of replacement datasets to be obtained

Group	**Genotype**	**Background**	**Reporter**	**Diet**	**Sex**	**N**
A	Wildtype	C57BL/6	*MIP-GFP*	Chow	Male	3
B	Wildtype	C57BL/6	*MIP-GFP*	Chow	Female	3
C	*Abcc8*$^{-/-}$	C57BL/6	*Ins2*$^{Apple/+}$	Chow	Male	3
D	*Abcc8*$^{-/-}$	C57BL/6	*Ins2*$^{Apple/+}$	Chow	Female	3
E	Wildtype	C57BL/6	*Ins2*$^{Apple/+}$	High Fat	Male	3
F	Wildtype	C57BL/6	*Ins2*$^{Apple/+}$	High Fat	Female	3
G	Wildtype	C57BL/6	*Ins2*$^{Apple/+}$	Chow	Male	3
H	Wildtype	C57BL/6	*Ins2*$^{Apple/+}$	Chow	Female	3

CHAPTER VI

SIGNIFICANCE AND FUTURE DIRECTIONS

Significance

Throughout this thesis, I have described the collection of RNA-seq data from highly-pure mouse β-cell populations. The analysis of this large amount of high-throughput data has lead me to make two broad conclusions about the manner in which β-cells fail in response to increased metabolic load during the progression of T2D: (1) β-cells may fail in a heterogeneous manner, and (2) some responses to environmental stress are adaptive while others are maladaptive, resulting in a bi-phasic response.

Heterogeneity in β-cell failure

Although the pancreatic islets consist of a heterogeneous population of cell types (endocrine cells, neuronal cells, and supporting vasculature), the β-cells have historically been considered to be a homogenous population, with uniform gene expression profiles as well as equal capacity to proliferate and respond to insulin secretagogues. Recently, however, several reports have challenged this view and have identified distinct subpopulations of β-cells with unique gene expression profiles and properties.

Dorrell and colleagues utilized antibody-labeling coupled with flow cytometry of human islet cells to describe four antigenically-distinct β-cell subtypes which can be identified by differential expression of two markers: ST8SIA1 and CD9 (109). Importantly, these subtypes have

differences in expression of several key transcription factors (*SIX3*, *RFX6*, *MAFB*, and *NEUROD1*) as well as genes involved in insulin secretion (*GLUT2*, *PPP1R1A*, and *ABCC9*) and have differences in basal and glucose-stimulated insulin secretion, despite uniform expression of insulin mRNA and protein. Bader and colleagues identified a factor in mouse β-cells, called *Fltp*, which distinguishes proliferation-competent from mature populations (110). *Fltp* is a Wnt/planar-cell polarity factor that appears to be expressed when precursor cells differentiate into mature β-cells. These sub-populations exhibit different responses to metabolic stress, with the $Fltp^-$ population compensating for increased metabolic demand through proliferation in response to pregnancy. Johnston and colleagues took a functional rather than a genetics approach to identify "hub" β-cells whose electrical firing activity precedes the rest of the population (108). Importantly, these hub cells are vital for coordinating electrical response to glucose stimulation and may be necessary for insulin secretion. Segerstolpe and colleagues performed single-cell RNA-sequencing on human islet cells and discovered at least five subpopulations of β-cells based on differential expression of *RBP4, FFAR4, ID1, ID2,* and *ID3* (112). Finally, our studies describing the β-cell response to chronically-elevated $[Ca^{2+}]_i$ identified at least four subpopulations of β-cells based on heterogeneous protein expression of ALDH1A3 and S100A6 (**Figure 3.9**). However, the functional significance of these subgroups is yet to be determined.

Taken together, the results of these studies, although different, suggest that distinct β-cell subpopulations exist and that the responses to stimuli or stress may not be uniform within the entire β-cell population. In support of this, Dorrell and colleagues discovered that the distribution of β-cell subtypes was altered in patients with T2D (109), but it is unknown if the abnormal distribution precedes or follows the development of the disease. β-cell heterogeneity is an area that greatly merits further study since many questions are left unanswered: How many β-cell subpopulations

exist and how can we define them? Are different subpopulations more susceptible to environmental stress than others? Does the distribution of subpopulations predispose an individual to the development of T2D? How stable are these subpopulations and does their distribution change over time? Additional studies using single-cell transcriptome analysis are necessary to answer these questions and to fully understand heterogeneity in β-cell failure.

Adaptive vs. maladaptive responses

After thorough examination of RNA-sequencing datasets representing β-cell responses to different types of stress, we observed gene expression changes that likely represent adaptive responses, meaning that they are beneficial to the β-cell, as well as changes that likely represent maladaptive responses and are deleterious to the β-cell. In the β-cells exposed to chronically-elevated $[Ca^{2+}]_{i,}$ we observed an increase in the expression of several Ca^{2+}-binding proteins, including members of the *S100* gene family as well as *Pcp4*, a Ca^{2+}/calmodulin-binding protein that protects neurons from Ca^{2+}-induced excitotoxicity (130). Though further experimentation is necessary to test this hypothesis, we think it likely that these changes are adaptive, allowing for binding and sequestering of excess Ca^{2+} to prevent overactivation of downstream pathways. We also observed decrease in β-cell function and identity, with an increase in genes associated with dedifferentiation, such as *Aldh1a3*, and a decrease in genes associated with β-cell function, such as *Ins1, Slc2a2,* and *Gck*. These likely reflect maladaptive changes, since the dysregulation of these genes is deleterious to β-cell function.

Another example comes from our analysis of dysregulated genes in β-cells from HFD-fed animals. We observed an increase in expression of cell cycle regulators, including *Cdk1* and

Ccna2, which likely reflects an adaptive mechanism, allowing expansion of β-cell mass to compensate for increased metabolic demand. Additionally, genes related to ER stress were significantly upregulated, suggesting a maladaptive response to HFD.

These observations of both adaptive and maladaptive responses to various stimuli prompted me to propose a bi-phasic model for β-cell stress (**Figure 6.1**). During the adaptive phase of environmental stress, gene expression changes occur that allow the β-cells to compensate and maintain their function. However, during the maladaptive phase, the β-cells are no longer able to compensate for the environmental stress, and gene expression changes occur that lead to β-cell dysfunction and/or death. While we have only explored the gene expression changes that occur in response to a few stimuli, we think it likely that this model is applicable to a variety of metabolic stresses.

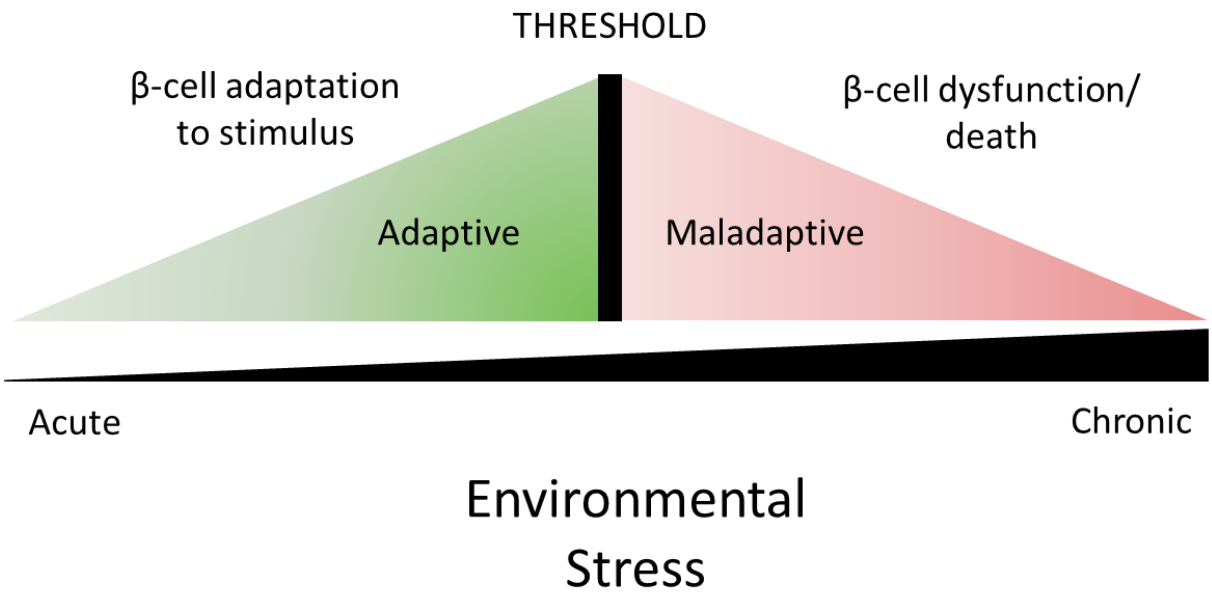

Figure 6.1. Bi-phasic model of the β-cell response to stress. Collectively, our results have lead us to propose a general model describing two phases in the β-cell response to environmental stress: the adaptive phase and the maladaptive phase. The adaptive phase likely occurs under acute exposure to a stimulus. During this phase, gene expression changes occur that allow the β-cell to adapt and compensate for increased metabolic demand. However, after a theoretical threshold is passed, perhaps under chronic exposure to the stimulus, the β-cell can no longer compensate, and maladaptive changes lead to dysfunction and/or death.

Future Directions

ASCL1 as a regulator of Ca^{2+}-dependent β-cell gene expression

In Chapter III, I described a putative network of Ca^{2+}-regulated genes in β-cells, at which ASCL1 was the center. We found that *Ascl1* is significantly upregulated in β-cells with chronically elevated $[Ca^{2+}]_i$, *Ascl1* expression is tightly controlled by Ca^{2+}-influx, and ASCL1 binding sites have been established in many of the genes upregulated in β-cells with chronically elevated $[Ca^{2+}]_i$. To our knowledge, this is the first time *Ascl1* expression or activity has been linked to Ca^{2+}-signaling. ASCL1 is known to play an important role in promoting neuronal differentiation (133-135; 143; 181), but a role for ASCL1 has not been established in β-cells.

Although all of my experiments were performed using mice or primary mouse islets, these approaches are limited by the difficulty of obtaining a sufficient number of cells for subsequent analyses, such as whole transcriptome sequencing or chromatin immunoprecipitation. To overcome this limitation, future studies may need to incorporate established, immortalized β-cell lines to better understand the role of ASCL1 at the molecular level.

While our preliminary data strongly suggests that ASCL1 plays a role in regulating Ca^{2+}-dependent gene expression in β-cells, we have no direct evidence that this is the case, or any idea of what genes are being regulated. To determine which genes are regulated by ASCL1, siRNA-mediated knockdown of *Ascl1* in β-cell lines would need to be performed. RNA-sequencing both with and without *Ascl1* knockdown, followed by differential expression analysis would identify genes whose expression is influenced by ASCL1 in β-cells. However, RNA-seq does not provide information about a direct binding relationship of transcription factors to DNA. In order to more

deeply understand how ASCL1 influences these genes, chromatin immunoprecipitation followed by next generation sequencing (ChIP-Seq) using an antibody against ASCL1 is necessary. The combination of RNA-seq and ChIP-seq data would provide a more complete picture of the role of ASCL1 in regulating gene expression in β-cells than either approach alone.

While the experiments described above, which would likely make use of immortalized β-cell lines, might provide insight into the genes that are regulated by ASCL1 and the genes to which ASCL1 directly binds, they are limited by the fact that immortalized β-cells differ from native β-cells in important ways, including deviations in glucose stimulated insulin secretion and misexpression of hexokinase (182). Thus, an alternative method to elucidating ASCL1 target genes in β-cells is to utilize a mouse model in which *Ascl1* has been deleted. Constitutive, whole-body knockout models of *Ascl1* have been generated (183-185), but null animals die shortly after birth due to defects in breathing and feeding (183). Therefore, a conditional *Ascl1* knockout model must be used in order to study gene expression in adult β-cells.

Guillemot and colleagues have generated an $Ascl1^{flox}$ allele that, when bred to homozygosity and in combination with a β-cell specific *Cre*-expressing allele, could be used to create a β-cell specific knockout of *Ascl1* (186). However, although the $Ascl1^{flox}$ allele contains a green fluorescent reporter, Venus, the protein is not expressed at a detectable level (186), eliminating the ability to genetically mark cells in which *Ascl1* has been removed. To overcome this limitation, it may be necessary to include a *Cre*-inducible fluorescent reporter allele to label *Ascl1*-deficent cells. After β-cell specific deletion of *Ascl1*, transcriptome analysis using FACS-purified β-cells would reveal which genes are directly regulated by ASCL1. Incorporation of this gene expression data with the ChIP-seq data generated above would yield a model describing the role of ASCL1 in regulating Ca^{2+}-dependent gene expression in β-cells.

Iterative weighted gene correlation network analysis

In Chapter V, I described the collection of seventeen different RNA-seq datasets and the WGCNA performed to identify modules of genes whose expression varies in response to metabolic stress. By identifying highly robust co-regulated gene modules and the hub genes they contain, and validating the function of these genes in cell culture systems and mice, a deeper understanding of the gene regulatory network that controls the adaptive and maladaptive responses of the β-cell to metabolic stress can be obtained.

The Magnuson lab has collaborated with Dr. Chris Stoeckert (University of Pennsylvania) to develop and document an extension of WGCNA called Iterative WGCNA (125; 187). The development of this tool was motivated by limitations in the hierarchical clustering algorithm used by WGCNA, which restricts gene cluster resolution. Iterative WGCNA extends the WGCNA method to determine the signed eigengene connectivity measure (k_{ME}) (125) of each gene and to assess the goodness of fit to an assigned module. This optimization strategy has been shown to be a highly robust means of evaluating goodness of fit (188).

While our preliminary results are already state-of-the-art in many ways, and point to many genes and pathways that are likely to be involved in the response of the β-cell to stress, additional bioinformatics analysis and molecular investigation is needed to more fully validate and understand the acquired data. Since several of the fifteen modules obtained from the standard WGCNA contain hub genes that are plausibly involved in the response of the β-cell to specific types of stress, iterative WGCNA would yield exceedingly more robust modules that may reveal groups of genes that are not yet evident using standard WGCNA.

To take full advantage of rich content of our adult mouse (p60) RNA-Seq datasets, as well as the very substantial effort that went into developing iterative WGCNA, the datasets described in **Table 5.4** should be re-processed using this newly available iterative WGCNA script. By improving the statistical associations within each module, this analysis would be more robust, enhancing the identification of new hub genes, the identification of upstream regulators, and the ability to correlate changes observed in mice with datasets derived from human cells and islets.

Network Validation

After modules have been generated, hub genes and putative upstream regulators associated with each specific metabolic stress and biological response can be more easily identified. For instance, the model I described in Chapter III highlights the potential importance of ASCL1, CEBPG, and RARG in the response of β-cells to chronically elevated $[Ca^{2+}]_i$. To perturb this predicted GCN, putative regulators such as these could be knocked down in β-cell lines using siRNA, similarly to the method I described above for ASCL1. If the GCN is altered in a predictable way, one could confidently say that the predicted regulators are valid. This experimental paradigm could be expanded to include additional predicted regulators after the derivation of additional modules by WGCNA. Moreover, by formally applying gene set enrichment analyses (189) and using pathway information from KEGG (190) and Reactome (191), pathways that correlate with each of the sixteen or more individual modules could be identified.

Collection of additional RNA-seq datasets

Since the 24 RNA-Seq datasets (**Table 5.4**) available for iterative WGCNA are only slightly above the minimum number recommended, and since the perturbations that I described in previous chapters have only scratched the surface of what is possible using WGCNA, it is vital to expand the number of datasets. By adding additional, highly controlled datasets, new modules of coordinately-regulated genes are likely to become evident, further increasing the scientific impact of the network. To achieve this goal, β-cell function needs to be perturbed in additional ways to not only obtain an expanded GCN, but also to be able to meaningfully interpret the new modules.

Rictor/mTORC2 signaling in β-cells. Signaling through the phosphotidylinositol-3-kinase (PI3K)/AKT/mTORC1 pathway has long been known to be essential for regulating β-cell mass (173-175). Signaling through Rictor/mTORC2/AKT-S473 is important for maintaining normal β-cell mass, and the phosphorylation of AKT-S473, by negatively regulating AKT-T308 phosphorylation, is necessary for maintaining a balance between β-cell proliferation and cell size (176). The role of Rictor/mTORC2 signaling through FOXO proteins has taken on greater significance in light of a recent report that failing β-cells in diabetic mice exhibit both a decrease in mitochondrial function and compensatory activation of signaling through Rictor/mTORC2 (94). The compensatory activation of Rictor/mTORC2 (176) is critical for inhibiting FOXO, which suppresses β-cell proliferation (192-195). Given this new evidence of a link between β-cell dedifferentiation and Rictor/mTORC2 signaling, investigating this signaling pathway in more depth would be prudent.

The Magnuson lab previously compared the mRNA transcriptional profiles of 43 genes in pancreatic islets from β-cell specific *Rictor* knockout (β*RicKO*) mice (176) and observed changes

in genes regulating cell proliferation and insulin secretion. While some of the transcriptional changes observed were easily explained, others were not. For example, an increase in expression of both *Ngn3* and *MafB*, genes normally only expressed in developing or immature β-cells, was observed in the β*Ric*KO mice. Given the recent findings of β-cell dedifferentiation, defined by expression of developmental markers (94), signaling via Rictor/mTORC2/AKT may contribute to the loss of β-cell identity in metabolically-stressed β-cells. Addition of RNA-sequencing datasets generated from FACS-purified β-cells from *Ins1*$^{Cre/+}$*; Rictor*$^{fl/fl}$*; Ins2*$^{Apple/+}$ mice to the iterative WGCNA pipeline would identify specific gene modules and allow for exploration of possible upstream regulators (**Table 6.1**).

Table 6.1: Summary of mice that could be used to explore the effects of Rictor/mTORC2 signaling on β-cell gene expression

Group	**Genotype**	**Reporter**	**Diet**	**Sex**	**N**
A	*Ins1*$^{Cre/+}$*; Rictor*$^{fl/fl}$	*Ins2*$^{Apple/+}$	Chow	Male	3
B	*Ins1*$^{Cre/+}$*; Rictor*$^{fl/fl}$	*Ins2*$^{Apple/+}$	Chow	Female	3

Excess metabolic flux in β-cells. The Magnuson lab has also previously collaborated with Dr. Yuval Dor to derive mice that contain a Cre-inducible, Rosa26 lox-stop-lox allele that expresses *Gck*^{Y214C}, an activated form of glucokinase identified in a pedigree with hyperinsulinemia, as well as a GFP reporter to genetically tag cells in which *Gck*^{Y214C} is expressed (46). When interbred with *Pdx1*^{CreER}, treatment with tamoxifen results in the pancreatic β-cell

specific expression of *Gck*^{Y214C}, causing an increase in metabolic flux, a transient increase in insulin secretion, and a reduction in the blood glucose concentration (46). The most interesting observation in this study was that hypoglycemia in these animals was short-lived, reaching a trough at 4 days past induction of the mutant *Gck*, after which the mice became hyperglycemic due to a fall in insulin secretion. This finding closely mimics the pattern observed in patients treated with glucokinase-activating (GKA) drugs: they experience a short period of improved blood glucose concentrations, but this effect disappears within a couple of months (196; 197). These studies further suggest that the loss of β-cell function after inducing expression of *Gck*^{Y214C} is due to β-cell apoptosis resulting from oxidative damage and DNA double-strand breaks (46). Based on these results, further assessment of the impact of increased glycolytic flux on β-cell gene expression is needed. *Gck*$^{Y214C/+}$ mice would be predicted to have increased metabolic flux, increased Ca^{2+}-flux and signaling, and, because of their higher than normal insulin secretion, increased Rictor/mTORC2/AKT-S473 signaling.

In addition, the prior study also revealed that β-cell membrane depolarization was both necessary and sufficient to trigger DNA damage, and that cellular damage was reduced by tacrolimus, a calcineurin inhibitor (46). This latter finding is consistent with the idea that aberrant Ca^{2+}-signaling (excitotoxicity) contributes to the failure of β-cells in T2D, a conclusion consistent with our findings that a chronic elevation in $[Ca^{2+}]_i$ impairs β-cell function and identity (Chapter III above).

In order to understand the gene expression changes that occur in the β-cell in both the hypoglycemic and glucotoxic phases of GCK activation, sex-segregated datasets at 4 days post tamoxifen injection (at the height of the hypoglycemic phase) and at 22 days post tamoxifen injection (at the height of the hyperglycemic phase) should be collected (**Table 6.2**). The collection

of these datasets will greatly increase our understanding of the binary phases of β-cell glucotoxicity.

Table 6.2: Summary of mice that could be used to explore the effects of excess metabolic flux on β-cell gene expression

Group	Genotype	Reporter	Days	Sex	N
A	*R26*$^{LSL.GckY214C/+}$*; Ins1*$^{CreER/+}$	GFP	4	Male	3
B	*R26*$^{LSL.GckY214C/+}$*; Ins1*$^{CreER/+}$	GFP	4	Female	3
C	*R26*$^{LSL.GckY214C/+}$*; Ins1*$^{CreER/+}$	GFP	22	Male	3
D	*R26*$^{LSL.GckY214C/+}$*; Ins1*$^{CreER/+}$	GFP	22	Female	3

Glucagon-like peptide-1 (GLP-1) signaling in β-cells. Incretins, such as glucagon-like peptide-1 (GLP-1), are released from the gut in response to food intake and elicit a variety of responses from the islet. First, they are known to enhance insulin release from the β-cell while simultaneously inhibiting glucagon release from the α-cell (198). Second, they have been shown to positively regulate β-cell mass by enhancing proliferation as well as islet neogenesis (199). While GLP-1 receptor (GLP1R) agonists are widely used as a treatment for T2D, there is increasing evidence that they may have long-term negative effects on β-cell function (200; 201), and much remains to be learned about the specific gene expression changes that are induced in β-cells in response to these drugs. For this reason, assessment of the effects of both acute and chronic stimulation of GLP-1 signaling on β-cell gene expression is needed.

To understand both the beneficial and detrimental effects of GLP1R signaling, β-cell RNA-seq datasets need to be collected from mice treated with Liraglutide for either 7 days, to examine acute effects, or 200 days, to examine chronic effects (**Table 6.3**). β-cell samples from 200-day old control mice also must be collected, since the 200-day treatment with Liraglutide goes well beyond p60. In addition, by collecting control datasets from mice that are approximately 260 days old (p260) one would be able to compare p60 and p260 datasets, thereby gaining new insights into how gene expression in β-cells changes with age.

Table 6.3: Summary of mice that could be used to explore the effects of excess GLP-1 signaling on β-cell gene expression

Group	**Treatment**	**Genotype**	**Days**	**Sex**	**N**
A	Liraglutide	*Ins2*$^{Apple/+}$	7	Male	3
B	Liraglutide	*Ins2*$^{Apple/+}$	7	Female	3
C	None	*Ins2*$^{Apple/+}$	200	Male	3
D	None	*Ins2*$^{Apple/+}$	200	Female	3
E	Liraglutide	*Ins2*$^{Apple/+}$	200	Male	3
F	Liraglutide	*Ins2*$^{Apple/+}$	200	Female	3

Closing remarks

The studies described herein have all utilized RNA-seq datasets from FACS-purified mouse β-cell populations under various genetic or metabolic stimuli. We examined the effects of chronically elevated $[Ca^{2+}]_i$ induced by constitutive loss of the K_{ATP}-channel, ectopic hGH expression driven by the *MIP-GFP* transgene, obesity induced by HFD feeding, and gender by separation of males and females. The overarching goal of these studies was to better understand the signaling pathways induced in β-cells in response to stress during the progression to T2D: specifically, how stress alters the gene regulatory network.

The key finding from the studies described in Chapter III was the discovery that chronically elevated $[Ca^{2+}]_i$, or excitotoxicity, has detrimental effects on the β-cell, including slight glucose intolerance, loss of β-cell identity, loss of islet morphology, and severe disruption in gene expression. We additionally identified two markers, S100A4 and S100A6, whose expression is directly controlled by Ca^{2+}-influx and which may serve as markers for excitotoxic stress. Finally, we identified a network of Ca^{2+}-regulated genes as well as a putative Ca^{2+}-dependent regulator, ASCL1, which we envision to be at the center of this network. This finding is particularly novel and interesting given that ASCL1 has never been studied in β-cells and has never before been shown to be regulated by Ca^{2+}-influx. We anticipate that further study of this transcription factor will be important for fully understanding how gene expression in the β-cell is regulated by chronically elevated $[Ca^{2+}]_i$.

In Chapter IV, I described the generation of a novel β-cell specific fluorescent reporter allele, *Ins2.Apple*, which we used to assess the effects of ectopic hGH on β-cell gene expression by comparing it to the *MIP-GFP* transgene. The key finding from these studies is that the *MIP-*

GFP transgene, which is widely used in the β-cell research community, induces enormous changes in β-cell gene expression, many of which indicate a decline in β-cell function as well as the induction of ER stress. These studies add to the pool of emerging evidence that alleles with ectopic hGH expression should be used with extreme caution.

Finally, in Chapter V, I detailed our efforts towards creating a gene-correlation network, which incorporates 17 RNA-seq datasets, to describe β-cell failure. While this analysis is not complete, it marks a major advance in the field toward understanding higher order comparisons between groups, rather than limiting studies to pairwise comparisons. We anticipate that the collection of additional datasets overtime will strengthen the correlations we have already identified and will increase our knowledge of the gene expression changes underlying β-cell failure in T2D.

Overall, these studies highlight the power of using whole transcriptome datasets from highly pure cell populations. By combining highly controlled and robust datasets from mouse cell populations with single-cell datasets from human patients, the field as a whole will be able to achieve a deep understanding of how β-cells fail in T2D.

APPENDICES

PERMISSIONS TO REPRODUCE COPYRIGHTED MATERIAL

APPENDIX A

Journal of Clinical Investigation:

Order detail ID:70325236
ISSN:1558-8238
Publication Type: e-Journal
Volume:
Issue:
Start page:
Publisher: AMERICAN SOCIETY FOR CLINICAL INVESTIGATION
Permission Status: **Granted**

Permission type: Republish or display content
Type of use: Republish in a thesis/dissertation

Order License Id: 4063810770279

Requestor type	Academic institution
Format	Print, Electronic
Portion	chart/graph/table/figure
Number of charts/graphs/tables/figures	1
Title or numeric reference of the portion(s)	Figure 2, Panels A and B
Title of the article or chapter the portion is from	ATP-sensitive potassium channelopathies: focus on insulin secretion
Editor of portion(s)	N/A
Author of portion(s)	Frances M. Ashcroft
Volume of serial or monograph	115
Issue, if republishing an article from a serial	8
Page range of portion	2049

Publication date of portion	August 1, 2005
Rights for	Main product
Duration of use	Life of current edition
Creation of copies for the disabled	no
With minor editing privileges	yes
For distribution to	United States
In the following language(s)	Original language of publication
With incidental promotional use	no
Lifetime unit quantity of new product	Up to 499
Made available in the following markets	Education
The requesting person/organization	Jennifer Stancill
Order reference number	
Author/Editor	Jennifer Stancill
The standard identifier of New Work	JSSThesis2017
Title of New Work	Dissecting Pancreatic β-cell Stress Using Whole Transcriptome Sequencing
Publisher of New Work	Vanderbilt University
Expected publication date	Mar 2017
Estimated size (pages)	160

APPENDIX B

Elsevier:

ELSEVIER LICENSE
TERMS AND CONDITIONS

Mar 07, 2017

This Agreement between Jennifer S Stancill ("You") and Elsevier ("Elsevier") consists of your license details and the terms and conditions provided by Elsevier and Copyright Clearance Center.

License Number	4063790152007
License date	Mar 07, 2017
Licensed Content Publisher	Elsevier
Licensed Content Publication	Cell Metabolism
Licensed Content Title	Impaired Islet Function in Commonly Used Transgenic Mouse Lines due to Human Growth Hormone Minigene Expression
Licensed Content Author	Bas Brouwers,Geoffroy de Faudeur,Anna B. Osipovich,Lotte Goyvaerts,Katleen Lemaire,Leen Boesmans,Elisa J.G. Cauwelier,Mikaela Granvik,Vincent P.E.G. Pruniau,Leentje Van Lommel,Jolien Van Schoors,Jennifer S. Stancill,Ilse Smolders,Vincent Goffin et al.
Licensed Content Date	2 December 2014
Licensed Content Volume	20
Licensed Content Issue	6
Licensed Content Pages	12
Start Page	979
End Page	990
Type of Use	reuse in a thesis/dissertation
Portion	figures/tables/illustrations
Number of figures/tables/illustrations	1
Format	both print and electronic

Are you the author of this Elsevier article?	Yes
Will you be translating?	No
Order reference number	
Original figure numbers	Figure 6
Title of your thesis/dissertation	Dissecting Pancreatic β-cell Stress Using Whole Transcriptome Sequencing
Expected completion date	Mar 2017
Estimated size (number of pages)	152
Elsevier VAT number	GB 494 6272 12
Requestor Location	Jennifer S Stancill 9465 MRBIV 2213 Garland Ave NASHVILLE, TN 37232 United States Attn: Jennifer S Stancill
Publisher Tax ID	98-0397604
Total	0.00 USD

Terms and Conditions

INTRODUCTION

1. The publisher for this copyrighted material is Elsevier. By clicking "accept" in connection with completing this licensing transaction, you agree that the following terms and conditions apply to this transaction (along with the Billing and Payment terms and conditions established by Copyright Clearance Center, Inc. ("CCC"), at the time that you opened your Rightslink account and that are available at any time at http://myaccount.copyright.com).

GENERAL TERMS

2. Elsevier hereby grants you permission to reproduce the aforementioned material subject to the terms and conditions indicated.

3. Acknowledgement: If any part of the material to be used (for example, figures) has appeared in our publication with credit or acknowledgement to another source, permission must also be sought from that source. If such permission is not obtained then that material may not be included in your publication/copies. Suitable acknowledgement to the source must be made, either as a footnote or in a reference list at the end of your publication, as follows:

"Reprinted from Publication title, Vol /edition number, Author(s), Title of article / title of chapter, Pages No., Copyright (Year), with permission from Elsevier [OR APPLICABLE SOCIETY COPYRIGHT OWNER]." Also Lancet special credit - "Reprinted from The Lancet, Vol. number, Author(s), Title of article, Pages No., Copyright (Year), with permission from Elsevier."

4. Reproduction of this material is confined to the purpose and/or media for which permission is hereby given.

5. Altering/Modifying Material: Not Permitted. However figures and illustrations may be altered/adapted minimally to serve your work. Any other abbreviations, additions, deletions and/or any other alterations shall be made only with prior written authorization of Elsevier Ltd. (Please contact Elsevier at permissions@elsevier.com). No modifications can be made to any Lancet figures/tables and they must be reproduced in full.
6. If the permission fee for the requested use of our material is waived in this instance, please be advised that your future requests for Elsevier materials may attract a fee.
7. Reservation of Rights: Publisher reserves all rights not specifically granted in the combination of (i) the license details provided by you and accepted in the course of this licensing transaction, (ii) these terms and conditions and (iii) CCC's Billing and Payment terms and conditions.
8. License Contingent Upon Payment: While you may exercise the rights licensed immediately upon issuance of the license at the end of the licensing process for the transaction, provided that you have disclosed complete and accurate details of your proposed use, no license is finally effective unless and until full payment is received from you (either by publisher or by CCC) as provided in CCC's Billing and Payment terms and conditions. If full payment is not received on a timely basis, then any license preliminarily granted shall be deemed automatically revoked and shall be void as if never granted. Further, in the event that you breach any of these terms and conditions or any of CCC's Billing and Payment terms and conditions, the license is automatically revoked and shall be void as if never granted. Use of materials as described in a revoked license, as well as any use of the materials beyond the scope of an unrevoked license, may constitute copyright infringement and publisher reserves the right to take any and all action to protect its copyright in the materials.
9. Warranties: Publisher makes no representations or warranties with respect to the licensed material.
10. Indemnity: You hereby indemnify and agree to hold harmless publisher and CCC, and their respective officers, directors, employees and agents, from and against any and all claims arising out of your use of the licensed material other than as specifically authorized pursuant to this license.
11. No Transfer of License: This license is personal to you and may not be sublicensed, assigned, or transferred by you to any other person without publisher's written permission.
12. No Amendment Except in Writing: This license may not be amended except in a writing signed by both parties (or, in the case of publisher, by CCC on publisher's behalf).
13. Objection to Contrary Terms: Publisher hereby objects to any terms contained in any purchase order, acknowledgment, check endorsement or other writing prepared by you, which terms are inconsistent with these terms and conditions or CCC's Billing and Payment terms and conditions. These terms and conditions, together with CCC's Billing and Payment terms and conditions (which are incorporated herein), comprise the entire agreement between you and publisher (and CCC) concerning this licensing transaction. In the event of any conflict between your obligations established by these terms and conditions and those established by CCC's Billing and Payment terms and conditions, these terms and conditions shall control.
14. Revocation: Elsevier or Copyright Clearance Center may deny the permissions described in this License at their sole discretion, for any reason or no reason, with a full refund payable to you. Notice of such denial will be made using the contact information provided by you. Failure to receive such notice will not alter or invalidate the denial. In no event will Elsevier or Copyright Clearance Center be responsible or liable for any costs, expenses or damage incurred by you as a result of a denial of your permission request, other than a refund of the amount(s) paid by you to Elsevier and/or Copyright Clearance Center for denied permissions.

REFERENCES

1. Ionescu-Tirgoviste C, Gagniuc PA, Gubceac E, Mardare L, Popescu I, Dima S, Militaru M: A 3D map of the islet routes throughout the healthy human pancreas. Sci Rep 2015;5:14634

2. Siddle K: Signalling by insulin and IGF receptors: supporting acts and new players. J Mol Endocrinol 2011;47:R1-10

3. Rask-Madsen C, Kahn CR: Tissue-specific insulin signaling, metabolic syndrome, and cardiovascular disease. Arterioscler Thromb Vasc Biol 2012;32:2052-2059

4. How Diabetes Works [article online], 22 June 2001. Available from http://health.howstuffworks.com/diseases-conditions/diabetes/diabetes.htm. Accessed 13 March 2017

5. Rowland AF, Fazakerley DJ, James DE: Mapping insulin/GLUT4 circuitry. Traffic 2011;12:672-681

6. Xu GG, Rothenberg PL: Insulin receptor signaling in the beta-cell influences insulin gene expression and insulin content: evidence for autocrine beta-cell regulation. Diabetes 1998;47:1243-1252

7. Leibiger IB, Leibiger B, Berggren PO: Insulin signaling in the pancreatic beta-cell. Annu Rev Nutr 2008;28:233-251

8. Rhodes CJ, White MF, Leahy JL, Kahn SE: Direct autocrine action of insulin on beta-cells: does it make physiological sense? Diabetes 2013;62:2157-2163

9. Campbell JE, Drucker DJ: Islet alpha cells and glucagon--critical regulators of energy homeostasis. Nat Rev Endocrinol 2015;11:329-338

10. Authier F, Desbuquois B: Glucagon receptors. Cell Mol Life Sci 2008;65:1880-1899

11. Hauge-Evans AC, King AJ, Carmignac D, Richardson CC, Robinson IC, Low MJ, Christie MR, Persaud SJ, Jones PM: Somatostatin secreted by islet delta-cells fulfills multiple roles as a paracrine regulator of islet function. Diabetes 2009;58:403-411

12. Batterham RL, Le Roux CW, Cohen MA, Park AJ, Ellis SM, Patterson M, Frost GS, Ghatei MA, Bloom SR: Pancreatic polypeptide reduces appetite and food intake in humans. J Clin Endocrinol Metab 2003;88:3989-3992

13. Lin S, Shi YC, Yulyaningsih E, Aljanova A, Zhang L, Macia L, Nguyen AD, Lin EJ, During MJ, Herzog H, Sainsbury A: Critical role of arcuate Y4 receptors and the melanocortin system in pancreatic polypeptide-induced reduction in food intake in mice. PloS one 2009;4:e8488

14. Asakawa A, Inui A, Yuzuriha H, Ueno N, Katsuura G, Fujimiya M, Fujino MA, Niijima A, Meguid MM, Kasuga M: Characterization of the effects of pancreatic polypeptide in the regulation of energy balance. Gastroenterology 2003;124:1325-1336

15. Prado CL, Pugh-Bernard AE, Elghazi L, Sosa-Pineda B, Sussel L: Ghrelin cells replace insulin-producing beta cells in two mouse models of pancreas development. Proc Natl Acad Sci U S A 2004;101:2924-2929

16. Arnes L, Hill JT, Gross S, Magnuson MA, Sussel L: Ghrelin expression in the mouse pancreas defines a unique multipotent progenitor population. PloS one 2012;7:e52026

17. Wierup N, Sundler F, Heller RS: The islet ghrelin cell. J Mol Endocrinol 2014;52:R35-49

18. Brissova M, Fowler MJ, Nicholson WE, Chu A, Hirshberg B, Harlan DM, Powers AC: Assessment of human pancreatic islet architecture and composition by laser scanning confocal microscopy. J Histochem Cytochem 2005;53:1087-1097

19. Prentki M, Matschinsky FM, Madiraju SR: Metabolic signaling in fuel-induced insulin secretion. Cell metabolism 2013;18:162-185

20. Henquin JC: The dual control of insulin secretion by glucose involves triggering and amplifying pathways in beta-cells. Diabetes Res Clin Pract 2011;93 Suppl 1:S27-31

21. Bruce Alberts AJ, Julian Lewis, Martin Raff, Keith Roberts, Peter Walter: *Molecular Biology of the Cell, Fourth Edition*. New York, Garland Science, 2002

22. Ashcroft FM: ATP-sensitive potassium channelopathies: focus on insulin secretion. The Journal of clinical investigation 2005;115:2047-2058

23. MacDonald PE, Wheeler MB: Voltage-dependent K(+) channels in pancreatic beta cells: role, regulation and potential as therapeutic targets. Diabetologia 2003;46:1046-1062

24. Vierra NC, Dadi PK, Jeong I, Dickerson M, Powell DR, Jacobson DA: Type 2 Diabetes-Associated K+ Channel TALK-1 Modulates beta-Cell Electrical Excitability, Second-Phase Insulin Secretion, and Glucose Homeostasis. Diabetes 2015;64:3818-3828

25. Shiota C, Larsson O, Shelton KD, Shiota M, Efanov AM, Hoy M, Lindner J, Kooptiwut S, Juntti-Berggren L, Gromada J, Berggren PO, Magnuson MA: Sulfonylurea receptor type 1 knock-out mice have intact feeding-stimulated insulin secretion despite marked impairment in their response to glucose. J Biol Chem 2002;277:37176-37183

26. Postic C, Shiota M, Niswender KD, Jetton TL, Chen Y, Moates JM, Shelton KD, Lindner J, Cherrington AD, Magnuson MA: Dual roles for glucokinase in glucose homeostasis as determined by liver and pancreatic beta cell-specific gene knock-outs using Cre recombinase. J Biol Chem 1999;274:305-315

27. Seghers V, Nakazaki M, DeMayo F, Aguilar-Bryan L, Bryan J: Sur1 knockout mice. A model for K(ATP) channel-independent regulation of insulin secretion. J Biol Chem 2000;275:9270-9277

28. Shiota M, Postic C, Fujimoto Y, Jetton TL, Dixon K, Pan D, Grimsby J, Grippo JF, Magnuson MA, Cherrington AD: Glucokinase gene locus transgenic mice are resistant to the development of obesity-induced type 2 diabetes. Diabetes 2001;50:622-629

29. Gloyn AL, Weedon MN, Owen KR, Turner MJ, Knight BA, Hitman G, Walker M, Levy JC, Sampson M, Halford S, McCarthy MI, Hattersley AT, Frayling TM: Large-scale association studies of variants in genes encoding the pancreatic beta-cell KATP channel subunits Kir6.2 (KCNJ11) and SUR1 (ABCC8) confirm that the KCNJ11 E23K variant is associated with type 2 diabetes. Diabetes 2003;52:568-572

30. Patch AM, Flanagan SE, Boustred C, Hattersley AT, Ellard S: Mutations in the ABCC8 gene encoding the SUR1 subunit of the KATP channel cause transient neonatal diabetes, permanent neonatal diabetes or permanent diabetes diagnosed outside the neonatal period. Diabetes Obes Metab 2007;9 Suppl 2:28-39

31. Slingerland AS, Hattersley AT: Mutations in the Kir6.2 subunit of the KATP channel and permanent neonatal diabetes: new insights and new treatment. Ann Med 2005;37:186-195

32. Stoffel M, Patel P, Lo YM, Hattersley AT, Lucassen AM, Page R, Bell JI, Bell GI, Turner RC, Wainscoat JS: Missense glucokinase mutation in maturity-onset diabetes of the young and mutation screening in late-onset diabetes. Nat Genet 1992;2:153-156

33. Gloyn AL, Siddiqui J, Ellard S: Mutations in the genes encoding the pancreatic beta-cell KATP channel subunits Kir6.2 (KCNJ11) and SUR1 (ABCC8) in diabetes mellitus and hyperinsulinism. Hum Mutat 2006;27:220-231

34. Miki T, Nagashima K, Tashiro F, Kotake K, Yoshitomi H, Tamamoto A, Gonoi T, Iwanaga T, Miyazaki J, Seino S: Defective insulin secretion and enhanced insulin action in KATP channel-deficient mice. Proc Natl Acad Sci U S A 1998;95:10402-10406

35. Miki T, Tashiro F, Iwanaga T, Nagashima K, Yoshitomi H, Aihara H, Nitta Y, Gonoi T, Inagaki N, Miyazaki J, Seino S: Abnormalities of pancreatic islets by targeted expression of a dominant-negative KATP channel. Proc Natl Acad Sci U S A 1997;94:11969-11973

36. National Diabetes Statistics Report: Estimates of Diabetes and Its Burden in the United States. Atlanta, GA, Centers for Disease Control and Prevention, 2014

37. Bensellam M, Laybutt DR, Jonas JC: The molecular mechanisms of pancreatic beta-cell glucotoxicity: recent findings and future research directions. Mol Cell Endocrinol 2012;364:1-27

38. Chang-Chen KJ, Mullur R, Bernal-Mizrachi E: Beta-cell failure as a complication of diabetes. Rev Endocr Metab Disord 2008;9:329-343

39. Muoio DM, Newgard CB: Mechanisms of disease:Molecular and metabolic mechanisms of insulin resistance and beta-cell failure in type 2 diabetes. Nat Rev Mol Cell Biol 2008;9:193-205

40. Poitout V, Robertson RP: Glucolipotoxicity: fuel excess and beta-cell dysfunction. Endocrine reviews 2008;29:351-366

41. Talchai C, Xuan S, Lin HV, Sussel L, Accili D: Pancreatic beta cell dedifferentiation as a mechanism of diabetic beta cell failure. Cell 2012;150:1223-1234

42. Frayling TM: Genome-wide association studies provide new insights into type 2 diabetes aetiology. Nat Rev Genet 2007;8:657-662

43. Prokopenko I, McCarthy MI, Lindgren CM: Type 2 diabetes: new genes, new understanding. Trends Genet 2008;24:613-621

44. Fuchsberger C, Flannick J, Teslovich TM, Mahajan A, Agarwala V, Gaulton KJ, Ma C, Fontanillas P, Moutsianas L, McCarthy DJ, Rivas MA, Perry JR, Sim X, Blackwell TW, Robertson NR, Rayner NW, Cingolani P, Locke AE, Fernandez Tajes J, Highland HM, Dupuis J, Chines PS, Lindgren CM, Hartl C, Jackson AU, Chen H, Huyghe JR, van de Bunt M, Pearson RD, Kumar A, Muller-Nurasyid M, Grarup N, Stringham HM, Gamazon ER, Lee J, Chen Y, Scott RA, Below JE, Chen P, Huang J, Go MJ, Stitzel ML, Pasko D, Parker SC, Varga TV, Green T, Beer NL, Day-Williams AG, Ferreira T, Fingerlin T, Horikoshi M, Hu C, Huh I, Ikram MK, Kim BJ, Kim Y, Kim YJ, Kwon MS, Lee J, Lee S, Lin KH, Maxwell TJ, Nagai Y, Wang X, Welch RP, Yoon J, Zhang W, Barzilai N, Voight BF, Han BG, Jenkinson CP, Kuulasmaa T, Kuusisto J, Manning A, Ng MC, Palmer ND, Balkau B, Stancakova A, Abboud HE, Boeing H, Giedraitis V, Prabhakaran D, Gottesman O, Scott J, Carey J, Kwan P, Grant G, Smith JD, Neale BM, Purcell S, Butterworth AS, Howson JM, Lee HM, Lu Y, Kwak SH, Zhao W, Danesh J, Lam VK, Park KS, Saleheen D, So WY, Tam CH, Afzal U, Aguilar D, Arya R, Aung T, Chan E, Navarro C, Cheng CY, Palli D, Correa A, Curran JE, Rybin D, Farook VS, Fowler SP, Freedman BI, Griswold M, Hale DE, Hicks PJ, Khor CC, Kumar S, Lehne B, Thuillier D, Lim WY, Liu J, van der Schouw YT, Loh M, Musani SK, Puppala S, Scott WR, Yengo L, Tan ST, Taylor HA, Jr., Thameem F, Wilson G, Sr., Wong TY, Njolstad PR, Levy JC, Mangino M, Bonnycastle LL, Schwarzmayr T, Fadista J, Surdulescu GL, Herder C, Groves CJ, Wieland T, Bork-Jensen J, Brandslund I, Christensen C, Koistinen HA, Doney AS, Kinnunen L, Esko T, Farmer AJ, Hakaste L, Hodgkiss D, Kravic J, Lyssenko V, Hollensted M, Jorgensen ME, Jorgensen T, Ladenvall C, Justesen JM, Karajamaki A, Kriebel J, Rathmann W, Lannfelt L, Lauritzen T, Narisu N, Linneberg A, Melander O, Milani L, Neville M, Orho-Melander M, Qi L, Qi Q, Roden M, Rolandsson O, Swift A, Rosengren AH, Stirrups K, Wood AR, Mihailov E, Blancher C, Carneiro MO, Maguire J, Poplin R, Shakir K, Fennell T, DePristo M, Hrabe de Angelis M, Deloukas P, Gjesing AP, Jun G, Nilsson P, Murphy J, Onofrio R, Thorand B, Hansen T, Meisinger C, Hu FB, Isomaa B, Karpe F, Liang L, Peters A, Huth C, O'Rahilly SP, Palmer CN, Pedersen O, Rauramaa R, Tuomilehto J, Salomaa V, Watanabe RM, Syvanen AC, Bergman RN, Bharadwaj D, Bottinger EP, Cho YS, Chandak GR, Chan JC, Chia KS, Daly MJ, Ebrahim SB, Langenberg C, Elliott P, Jablonski KA, Lehman DM, Jia W, Ma RC, Pollin TI, Sandhu M, Tandon N, Froguel P, Barroso I, Teo YY, Zeggini E, Loos RJ, Small KS, Ried JS, DeFronzo RA, Grallert H, Glaser B, Metspalu A, Wareham NJ, Walker M, Banks E, Gieger C, Ingelsson E, Im HK, Illig T, Franks PW, Buck G, Trakalo J, Buck D, Prokopenko I, Magi R, Lind L, Farjoun Y, Owen KR, Gloyn AL, Strauch K, Tuomi T, Kooner JS, Lee JY, Park

T, Donnelly P, Morris AD, Hattersley AT, Bowden DW, Collins FS, Atzmon G, Chambers JC, Spector TD, Laakso M, Strom TM, Bell GI, Blangero J, Duggirala R, Tai ES, McVean G, Hanis CL, Wilson JG, Seielstad M, Frayling TM, Meigs JB, Cox NJ, Sladek R, Lander ES, Gabriel S, Burtt NP, Mohlke KL, Meitinger T, Groop L, Abecasis G, Florez JC, Scott LJ, Morris AP, Kang HM, Boehnke M, Altshuler D, McCarthy MI: The genetic architecture of type 2 diabetes. Nature 2016;536:41-47

45. Robertson RP, Harmon J, Tran PO, Poitout V: Beta-cell glucose toxicity, lipotoxicity, and chronic oxidative stress in type 2 diabetes. Diabetes 2004;53 Suppl 1:S119-124

46. Tornovsky-Babeay S, Dadon D, Ziv O, Tzipilevich E, Kadosh T, Schyr-Ben Haroush R, Hija A, Stolovich-Rain M, Furth-Lavi J, Granot Z, Porat S, Philipson LH, Herold KC, Bhatti TR, Stanley C, Ashcroft FM, In't Veld P, Saada A, Magnuson MA, Glaser B, Dor Y: Type 2 diabetes and congenital hyperinsulinism cause DNA double-strand breaks and p53 activity in beta cells. Cell metabolism 2014;19:109-121

47. Halban PA, Polonsky KS, Bowden DW, Hawkins MA, Ling C, Mather KJ, Powers AC, Rhodes CJ, Sussel L, Weir GC: beta-cell failure in type 2 diabetes: postulated mechanisms and prospects for prevention and treatment. Diabetes Care 2014;37:1751-1758

48. Prentki M, Nolan CJ: Islet beta cell failure in type 2 diabetes. The Journal of clinical investigation 2006;116:1802-1812

49. Weir GC, Bonner-Weir S: Five stages of evolving beta-cell dysfunction during progression to diabetes. Diabetes 2004;53 Suppl 3:S16-21

50. Porat S, Weinberg-Corem N, Tornovsky-Babaey S, Schyr-Ben-Haroush R, Hija A, Stolovich-Rain M, Dadon D, Granot Z, Ben-Hur V, White P, Girard CA, Karni R, Kaestner KH, Ashcroft FM, Magnuson MA, Saada A, Grimsby J, Glaser B, Dor Y: Control of pancreatic beta cell regeneration by glucose metabolism. Cell metabolism 2011;13:440-449

51. Ozcan U, Cao Q, Yilmaz E, Lee AH, Iwakoshi NN, Ozdelen E, Tuncman G, Gorgun C, Glimcher LH, Hotamisligil GS: Endoplasmic reticulum stress links obesity, insulin action, and type 2 diabetes. Science 2004;306:457-461

52. Fonseca SG, Gromada J, Urano F: Endoplasmic reticulum stress and pancreatic beta-cell death. Trends Endocrinol Metab 2011;22:266-274

53. Lenzen S: Oxidative stress: the vulnerable beta-cell. Biochemical Society transactions 2008;36:343-347

54. Page KA, Reisman T: Interventions to preserve beta-cell function in the management and prevention of type 2 diabetes. Curr Diab Rep 2013;13:252-260

55. Del Guerra S, Lupi R, Marselli L, Masini M, Bugliani M, Sbrana S, Torri S, Pollera M, Boggi U, Mosca F, Del Prato S, Marchetti P: Functional and molecular defects of pancreatic islets in human type 2 diabetes. Diabetes 2005;54:727-735

56. Meda P: Protein-mediated interactions of pancreatic islet cells. Scientifica (Cairo) 2013;2013:621249

57. Brereton MF, Iberl M, Shimomura K, Zhang Q, Adriaenssens AE, Proks P, Spiliotis, II, Dace W, Mattis KK, Ramracheya R, Gribble FM, Reimann F, Clark A, Rorsman P, Ashcroft FM: Reversible changes in pancreatic islet structure and function produced by elevated blood glucose. Nature communications 2014;5:4639

58. Wang Z, York NW, Nichols CG, Remedi MS: Pancreatic beta cell dedifferentiation in diabetes and redifferentiation following insulin therapy. Cell metabolism 2014;19:872-882

59. Wang YJ, Schug J, Won KJ, Liu C, Naji A, Avrahami D, Golson ML, Kaestner KH: Single-Cell Transcriptomics of the Human Endocrine Pancreas. Diabetes 2016;65:3028-3038

60. Cinti F, Bouchi R, Kim-Muller JY, Ohmura Y, Sandoval PR, Masini M, Marselli L, Suleiman M, Ratner LE, Marchetti P, Accili D: Evidence of beta-Cell Dedifferentiation in Human Type 2 Diabetes. J Clin Endocrinol Metab 2016;101:1044-1054

61. Butler AE, Dhawan S, Hoang J, Cory M, Zeng K, Fritsch H, Meier JJ, Rizza RA, Butler PC: beta-Cell Deficit in Obese Type 2 Diabetes, a Minor Role of beta-Cell Dedifferentiation and Degranulation. J Clin Endocrinol Metab 2016;101:523-532

62. Lawlor N, George J, Bolisetty M, Kursawe R, Sun L, Sivakamasundari V, Kycia I, Robson P, Stitzel ML: Single-cell transcriptomes identify human islet cell signatures and reveal cell-type-specific expression changes in type 2 diabetes. Genome Res 2017;27:208-222

63. Weir GC, Aguayo-Mazzucato C, Bonner-Weir S: beta-cell dedifferentiation in diabetes is important, but what is it? Islets 2013;5:233-237

64. Clapham DE: Calcium signaling. Cell 2007;131:1047-1058

65. Mellstrom B, Savignac M, Gomez-Villafuertes R, Naranjo JR: Ca2+-operated transcriptional networks: molecular mechanisms and in vivo models. Physiol Rev 2008;88:421-449

66. Shivaswamy V, Boerner B, Larsen J: Post-Transplant Diabetes Mellitus: Causes, Treatment, and Impact on Outcomes. Endocrine reviews 2016;37:37-61

67. Soleimanpour SA, Crutchlow MF, Ferrari AM, Raum JC, Groff DN, Rankin MM, Liu C, De Leon DD, Naji A, Kushner JA, Stoffers DA: Calcineurin signaling regulates human islet {beta}-cell survival. J Biol Chem 2010;285:40050-40059

68. Heit JJ, Apelqvist AA, Gu X, Winslow MM, Neilson JR, Crabtree GR, Kim SK: Calcineurin/NFAT signalling regulates pancreatic beta-cell growth and function. Nature 2006;443:345-349

69. Goodyer WR, Gu X, Liu Y, Bottino R, Crabtree GR, Kim SK: Neonatal beta cell development in mice and humans is regulated by calcineurin/NFAT. Dev Cell 2012;23:21-34

70. Easom RA: CaM kinase II: a protein kinase with extraordinary talents germane to insulin exocytosis. Diabetes 1999;48:675-684

71. Wenham RM, Landt M, Easom RA: Glucose activates the multifunctional Ca2+/calmodulin-dependent protein kinase II in isolated rat pancreatic islets. J Biol Chem 1994;269:4947-4952

72. Dadi PK, Vierra NC, Ustione A, Piston DW, Colbran RJ, Jacobson DA: Inhibition of pancreatic beta-cell Ca2+/calmodulin-dependent protein kinase II reduces glucose-stimulated calcium influx and insulin secretion, impairing glucose tolerance. J Biol Chem 2014;289:12435-12445

73. Mayr B, Montminy M: Transcriptional regulation by the phosphorylation-dependent factor CREB. Nature reviews Molecular cell biology 2001;2:599-609

74. Jhala US, Canettieri G, Screaton RA, Kulkarni RN, Krajewski S, Reed J, Walker J, Lin X, White M, Montminy M: cAMP promotes pancreatic beta-cell survival via CREB-mediated induction of IRS2. Genes Dev 2003;17:1575-1580

75. Lin X, Taguchi A, Park S, Kushner JA, Li F, Li Y, White MF: Dysregulation of insulin receptor substrate 2 in beta cells and brain causes obesity and diabetes. The Journal of clinical investigation 2004;114:908-916

76. Kubota N, Terauchi Y, Tobe K, Yano W, Suzuki R, Ueki K, Takamoto I, Satoh H, Maki T, Kubota T, Moroi M, Okada-Iwabu M, Ezaki O, Nagai R, Ueta Y, Kadowaki T, Noda T: Insulin receptor substrate 2 plays a crucial role in beta cells and the hypothalamus. The Journal of clinical investigation 2004;114:917-927

77. Persaud SJ, Liu B, Sampaio HB, Jones PM, Muller DS: Calcium/calmodulin-dependent kinase IV controls glucose-induced Irs2 expression in mouse beta cells via activation of cAMP response element-binding protein. Diabetologia 2011;54:1109-1120

78. Liu B, Barbosa-Sampaio H, Jones PM, Persaud SJ, Muller DS: The CaMK4/CREB/IRS-2 cascade stimulates proliferation and inhibits apoptosis of beta-cells. PloS one 2012;7:e45711

79. Screaton RA, Conkright MD, Katoh Y, Best JL, Canettieri G, Jeffries S, Guzman E, Niessen S, Yates JR, 3rd, Takemori H, Okamoto M, Montminy M: The CREB coactivator TORC2 functions as a calcium- and cAMP-sensitive coincidence detector. Cell 2004;119:61-74

80. Koo SH, Flechner L, Qi L, Zhang X, Screaton RA, Jeffries S, Hedrick S, Xu W, Boussouar F, Brindle P, Takemori H, Montminy M: The CREB coactivator TORC2 is a key regulator of fasting glucose metabolism. Nature 2005;437:1109-1111

81. Blanchet E, Van de Velde S, Matsumura S, Hao E, LeLay J, Kaestner K, Montminy M: Feedback Inhibition of CREB Signaling Promotes Beta Cell Dysfunction in Insulin Resistance. Cell reports 2015;10:1149-1157

82. Epstein PN, Overbeek PA, Means AR: Calmodulin-induced early-onset diabetes in transgenic mice. Cell 1989;58:1067-1073

83. Bernal-Mizrachi E, Cras-Meneur C, Ye BR, Johnson JD, Permutt MA: Transgenic overexpression of active calcineurin in beta-cells results in decreased beta-cell mass and hyperglycemia. PloS one 2010;5:e11969

84. Sattler R, Tymianski M: Molecular mechanisms of calcium-dependent excitotoxicity. J Mol Med (Berl) 2000;78:3-13

85. Arundine M, Tymianski M: Molecular mechanisms of calcium-dependent neurodegeneration in excitotoxicity. Cell Calcium 2003;34:325-337

86. Xu G, Chen J, Jing G, Shalev A: Preventing beta-cell loss and diabetes with calcium channel blockers. Diabetes 2012;61:848-856

87. Winarto A, Miki T, Seino S, Iwanaga T: Morphological changes in pancreatic islets of KATP channel-deficient mice: the involvement of KATP channels in the survival of insulin cells and the maintenance of islet architecture. Archives of histology and cytology 2001;64:59-67

88. Collombat P, Xu X, Ravassard P, Sosa-Pineda B, Dussaud S, Billestrup N, Madsen OD, Serup P, Heimberg H, Mansouri A: The ectopic expression of Pax4 in the mouse pancreas converts progenitor cells into alpha and subsequently beta cells. Cell 2009;138:449-462

89. Collombat P, Hecksher-Sorensen J, Krull J, Berger J, Riedel D, Herrera PL, Serup P, Mansouri A: Embryonic endocrine pancreas and mature beta cells acquire alpha and PP cell phenotypes upon Arx misexpression. The Journal of clinical investigation 2007;117:961-970

90. Yang YP, Thorel F, Boyer DF, Herrera PL, Wright CV: Context-specific alpha- to-beta-cell reprogramming by forced Pdx1 expression. Genes Dev 2011;25:1680-1685

91. Dhawan S, Georgia S, Tschen SI, Fan GP, Bhushan A: Pancreatic beta Cell Identity Is Maintained by DNA Methylation-Mediated Repression of Arx. Dev Cell 2011;20:419-429

92. Papizan JB, Singer RA, Tschen SI, Dhawan S, Friel JM, Hipkens SB, Magnuson MA, Bhushan A, Sussel L: Nkx2.2 repressor complex regulates islet beta-cell specification and prevents beta-to-alpha-cell reprogramming. Genes Dev 2011;25:2291-2305

93. Thorel F, Nepote V, Avril I, Kohno K, Desgraz R, Chera S, Herrera PL: Conversion of adult pancreatic alpha-cells to beta-cells after extreme beta-cell loss. Nature 2010;464:1149-1154

94. Kim-Muller JY, Fan J, Kim YJ, Lee SA, Ishida E, Blaner WS, Accili D: Aldehyde dehydrogenase 1a3 defines a subset of failing pancreatic beta cells in diabetic mice. Nature communications 2016;7:12631

95. Dahan T, Ziv O, Horwitz E, Zemmour H, Lavi J, Swisa A, Leibowitz G, Ashcroft FM, Veld PI, Glaser B, Dor Y: Pancreatic Beta Cells Express the Fetal Islet Hormone Gastrin in Rodent and Human Diabetes. Diabetes 2016;

96. Mouse Genome Sequencing C, Waterston RH, Lindblad-Toh K, Birney E, Rogers J, Abril JF, Agarwal P, Agarwala R, Ainscough R, Alexandersson M, An P, Antonarakis SE, Attwood J,

Baertsch R, Bailey J, Barlow K, Beck S, Berry E, Birren B, Bloom T, Bork P, Botcherby M, Bray N, Brent MR, Brown DG, Brown SD, Bult C, Burton J, Butler J, Campbell RD, Carninci P, Cawley S, Chiaromonte F, Chinwalla AT, Church DM, Clamp M, Clee C, Collins FS, Cook LL, Copley RR, Coulson A, Couronne O, Cuff J, Curwen V, Cutts T, Daly M, David R, Davies J, Delehaunty KD, Deri J, Dermitzakis ET, Dewey C, Dickens NJ, Diekhans M, Dodge S, Dubchak I, Dunn DM, Eddy SR, Elnitski L, Emes RD, Eswara P, Eyras E, Felsenfeld A, Fewell GA, Flicek P, Foley K, Frankel WN, Fulton LA, Fulton RS, Furey TS, Gage D, Gibbs RA, Glusman G, Gnerre S, Goldman N, Goodstadt L, Grafham D, Graves TA, Green ED, Gregory S, Guigo R, Guyer M, Hardison RC, Haussler D, Hayashizaki Y, Hillier LW, Hinrichs A, Hlavina W, Holzer T, Hsu F, Hua A, Hubbard T, Hunt A, Jackson I, Jaffe DB, Johnson LS, Jones M, Jones TA, Joy A, Kamal M, Karlsson EK, Karolchik D, Kasprzyk A, Kawai J, Keibler E, Kells C, Kent WJ, Kirby A, Kolbe DL, Korf I, Kucherlapati RS, Kulbokas EJ, Kulp D, Landers T, Leger JP, Leonard S, Letunic I, Levine R, Li J, Li M, Lloyd C, Lucas S, Ma B, Maglott DR, Mardis ER, Matthews L, Mauceli E, Mayer JH, McCarthy M, McCombie WR, McLaren S, McLay K, McPherson JD, Meldrim J, Meredith B, Mesirov JP, Miller W, Miner TL, Mongin E, Montgomery KT, Morgan M, Mott R, Mullikin JC, Muzny DM, Nash WE, Nelson JO, Nhan MN, Nicol R, Ning Z, Nusbaum C, O'Connor MJ, Okazaki Y, Oliver K, Overton-Larty E, Pachter L, Parra G, Pepin KH, Peterson J, Pevzner P, Plumb R, Pohl CS, Poliakov A, Ponce TC, Ponting CP, Potter S, Quail M, Reymond A, Roe BA, Roskin KM, Rubin EM, Rust AG, Santos R, Sapojnikov V, Schultz B, Schultz J, Schwartz MS, Schwartz S, Scott C, Seaman S, Searle S, Sharpe T, Sheridan A, Shownkeen R, Sims S, Singer JB, Slater G, Smit A, Smith DR, Spencer B, Stabenau A, Stange-Thomann N, Sugnet C, Suyama M, Tesler G, Thompson J, Torrents D, Trevaskis E, Tromp J, Ucla C, Ureta-Vidal A, Vinson JP, Von Niederhausern AC, Wade CM, Wall M, Weber RJ, Weiss RB, Wendl MC, West AP, Wetterstrand K, Wheeler R, Whelan S, Wierzbowski J, Willey D, Williams S, Wilson RK, Winter E, Worley KC, Wyman D, Yang S, Yang SP, Zdobnov EM, Zody MC, Lander ES: Initial sequencing and comparative analysis of the mouse genome. Nature 2002;420:520-562

97. Yue F, Cheng Y, Breschi A, Vierstra J, Wu W, Ryba T, Sandstrom R, Ma Z, Davis C, Pope BD, Shen Y, Pervouchine DD, Djebali S, Thurman RE, Kaul R, Rynes E, Kirilusha A, Marinov GK, Williams BA, Trout D, Amrhein H, Fisher-Aylor K, Antoshechkin I, DeSalvo G, See L-H, Fastuca M, Drenkow J, Zaleski C, Dobin A, Prieto P, Lagarde J, Bussotti G, Tanzer A, Denas O, Li K, Bender MA, Zhang M, Byron R, Groudine MT, McCleary D, Pham L, Ye Z, Kuan S, Edsall L, Wu Y-C, Rasmussen MD, Bansal MS, Kellis M, Keller CA, Morrissey CS, Mishra T, Jain D, Dogan N, Harris RS, Cayting P, Kawli T, Boyle AP, Euskirchen G, Kundaje A, Lin S, Lin Y, Jansen C, Malladi VS, Cline MS, Erickson DT, Kirkup VM, Learned K, Sloan CA, Rosenbloom KR, Lacerda de Sousa B, Beal K, Pignatelli M, Flicek P, Lian J, Kahveci T, Lee D, James Kent W, Ramalho Santos M, Herrero J, Notredame C, Johnson A, Vong S, Lee K, Bates D, Neri F, Diegel M, Canfield T, Sabo PJ, Wilken MS, Reh TA, Giste E, Shafer A, Kutyavin T, Haugen E, Dunn D, Reynolds AP, Neph S, Humbert R, Scott Hansen R, De Bruijn M, Selleri L, Rudensky A, Josefowicz S, Samstein R, Eichler EE, Orkin SH, Levasseur D, Papayannopoulou T, Chang K-H, Skoultchi A, Gosh S, Disteche C, Treuting P, Wang Y, Weiss MJ, Blobel GA, Cao X, Zhong S, Wang T, Good PJ, Lowdon RF, Adams LB, Zhou X-Q, Pazin MJ, Feingold EA, Wold B, Taylor J, Mortazavi A, Weissman SM, Stamatoyannopoulos JA, Snyder MP, Guigo R, Gingeras TR, Gilbert DM, Hardison RC, Beer MA, Ren B, The Mouse EC: A comparative encyclopedia of DNA elements in the mouse genome. Nature 2014;515:355-364

98. Artner I, Hang Y, Mazur M, Yamamoto T, Guo M, Lindner J, Magnuson MA, Stein R: MafA and MafB regulate genes critical to beta-cells in a unique temporal manner. Diabetes 2010;59:2530-2539

99. Dai C, Brissova M, Hang Y, Thompson C, Poffenberger G, Shostak A, Chen Z, Stein R, Powers AC: Islet-enriched gene expression and glucose-induced insulin secretion in human and mouse islets. Diabetologia 2012;55:707-718

100. Magnuson MA, Osipovich AB: Pancreas-specific Cre driver lines and considerations for their prudent use. Cell metabolism 2013;18:9-20

101. Dorrell C, Abraham SL, Lanxon-Cookson KM, Canaday PS, Streeter PR, Grompe M: Isolation of major pancreatic cell types and long-term culture-initiating cells using novel human surface markers. Stem Cell Res 2008;1:183-194

102. Dorrell C, Schug J, Lin CF, Canaday PS, Fox AJ, Smirnova O, Bonnah R, Streeter PR, Stoeckert CJ, Jr., Kaestner KH, Grompe M: Transcriptomes of the major human pancreatic cell types. Diabetologia 2011;54:2832-2844

103. Ackermann AM, Wang Z, Schug J, Naji A, Kaestner KH: Integration of ATAC-seq and RNA-seq identifies human alpha cell and beta cell signature genes. Mol Metab 2016;5:233-244

104. Benner C, van der Meulen T, Caceres E, Tigyi K, Donaldson CJ, Huising MO: The transcriptional landscape of mouse beta cells compared to human beta cells reveals notable species differences in long non-coding RNA and protein-coding gene expression. BMC Genomics 2014;15:620

105. Blodgett DM, Nowosielska A, Afik S, Pechhold S, Cura AJ, Kennedy NJ, Kim S, Kucukural A, Davis RJ, Kent SC, Greiner DL, Garber MG, Harlan DM, diIorio P: Novel Observations From Next-Generation RNA Sequencing of Highly Purified Human Adult and Fetal Islet Cell Subsets. Diabetes 2015;64:3172-3181

106. Bramswig NC, Everett LJ, Schug J, Dorrell C, Liu C, Luo Y, Streeter PR, Naji A, Grompe M, Kaestner KH: Epigenomic plasticity enables human pancreatic alpha to beta cell reprogramming. The Journal of clinical investigation 2013;123:1275-1284

107. Nica AC, Ongen H, Irminger JC, Bosco D, Berney T, Antonarakis SE, Halban PA, Dermitzakis ET: Cell-type, allelic, and genetic signatures in the human pancreatic beta cell transcriptome. Genome Res 2013;23:1554-1562

108. Johnston NR, Mitchell RK, Haythorne E, Pessoa MP, Semplici F, Ferrer J, Piemonti L, Marchetti P, Bugliani M, Bosco D, Berishvili E, Duncanson P, Watkinson M, Broichhagen J, Trauner D, Rutter GA, Hodson DJ: Beta Cell Hubs Dictate Pancreatic Islet Responses to Glucose. Cell metabolism 2016;24:389-401

109. Dorrell C, Schug J, Canaday PS, Russ HA, Tarlow BD, Grompe MT, Horton T, Hebrok M, Streeter PR, Kaestner KH, Grompe M: Human islets contain four distinct subtypes of beta cells. Nature communications 2016;7:11756

110. Bader E, Migliorini A, Gegg M, Moruzzi N, Gerdes J, Roscioni SS, Bakhti M, Brandl E, Irmler M, Beckers J, Aichler M, Feuchtinger A, Leitzinger C, Zischka H, Wang-Sattler R, Jastroch M, Tschop M, Machicao F, Staiger H, Haring HU, Chmelova H, Chouinard JA, Oskolkov N, Korsgren O, Speier S, Lickert H: Identification of proliferative and mature beta-cells in the islets of Langerhans. Nature 2016;535:430-434

111. Xin Y, Kim J, Okamoto H, Ni M, Wei Y, Adler C, Murphy AJ, Yancopoulos GD, Lin C, Gromada J: RNA Sequencing of Single Human Islet Cells Reveals Type 2 Diabetes Genes. Cell metabolism 2016;24:608-615

112. Segerstolpe A, Palasantza A, Eliasson P, Andersson EM, Andreasson AC, Sun X, Picelli S, Sabirsh A, Clausen M, Bjursell MK, Smith DM, Kasper M, Ammala C, Sandberg R: Single-Cell Transcriptome Profiling of Human Pancreatic Islets in Health and Type 2 Diabetes. Cell metabolism 2016;24:593-607

113. Hara M, Wang X, Kawamura T, Bindokas VP, Dizon RF, Alcoser SY, Magnuson MA, Bell GI: Transgenic mice with green fluorescent protein-labeled pancreatic beta -cells. Am J Physiol Endocrinol Metab 2003;284:E177-183

114. Srinivas S, Watanabe T, Lin CS, William CM, Tanabe Y, Jessell TM, Costantini F: Cre reporter strains produced by targeted insertion of EYFP and ECFP into the ROSA26 locus. BMC Dev Biol 2001;1:4

115. Araki K, Araki M, Yamamura K: Site-directed integration of the cre gene mediated by Cre recombinase using a combination of mutant lox sites. Nucleic Acids Res 2002;30:e103

116. Wakae-Takada N, Xuan S, Watanabe K, Meda P, Leibel RL: Molecular basis for the regulation of islet beta cell mass in mice: the role of E-cadherin. Diabetologia 2013;56:856-866

117. Chen SX, Osipovich AB, Ustione A, Potter LA, Hipkens S, Gangula R, Yuan W, Piston DW, Magnuson MA: Quantification of factors influencing fluorescent protein expression using RMCE to generate an allelic series in the ROSA26 locus in mice. Dis Model Mech 2011;4:537-547

118. Rodriguez CI, Buchholz F, Galloway J, Sequerra R, Kasper J, Ayala R, Stewart AF, Dymecki SM: High-efficiency deleter mice show that FLPe is an alternative to Cre-loxP. Nat Genet 2000;25:139-140

119. Burlison JS, Long Q, Fujitani Y, Wright CV, Magnuson MA: Pdx-1 and Ptf1a concurrently determine fate specification of pancreatic multipotent progenitor cells. Developmental biology 2008;316:74-86

120. Dadi PK, Vierra NC, Jacobson DA: Pancreatic beta-cell-specific ablation of TASK-1 channels augments glucose-stimulated calcium entry and insulin secretion, improving glucose tolerance. Endocrinology 2014;155:3757-3768

121. Dobin A, Davis CA, Schlesinger F, Drenkow J, Zaleski C, Jha S, Batut P, Chaisson M, Gingeras TR: STAR: ultrafast universal RNA-seq aligner. Bioinformatics 2013;29:15-21

122. Anders S, Pyl PT, Huber W: HTSeq--a Python framework to work with high-throughput sequencing data. Bioinformatics 2015;31:166-169

123. Love MI, Huber W, Anders S: Moderated estimation of fold change and dispersion for RNA-seq data with DESeq2. Genome Biol 2014;15:550

124. Janky R, Verfaillie A, Imrichova H, Van de Sande B, Standaert L, Christiaens V, Hulselmans G, Herten K, Naval Sanchez M, Potier D, Svetlichnyy D, Kalender Atak Z, Fiers M, Marine JC, Aerts S: iRegulon: from a gene list to a gene regulatory network using large motif and track collections. PLoS Comput Biol 2014;10:e1003731

125. Langfelder P, Horvath S: WGCNA: an R package for weighted correlation network analysis. BMC Bioinformatics 2008;9:559

126. Zhang B, Horvath S: A general framework for weighted gene co-expression network analysis. Stat Appl Genet Mol Biol 2005;4:Article17

127. Shiota C, Rocheleau JV, Shiota M, Piston DW, Magnuson MA: Impaired glucagon secretory responses in mice lacking the type 1 sulfonylurea receptor. Am J Physiol Endocrinol Metab 2005;289:E570-577

128. De Leon DD, Li C, Delson MI, Matschinsky FM, Stanley CA, Stoffers DA: Exendin-(9-39) corrects fasting hypoglycemia in SUR-1-/- mice by lowering cAMP in pancreatic beta-cells and inhibiting insulin secretion. J Biol Chem 2008;283:25786-25793

129. Brouwers B, de Faudeur G, Osipovich AB, Goyvaerts L, Lemaire K, Boesmans L, Cauwelier EJ, Granvik M, Pruniau VP, Van Lommel L, Van Schoors J, Stancill JS, Smolders I, Goffin V, Binart N, in't Veld P, Declercq J, Magnuson MA, Creemers JW, Schuit F, Schraenen A: Impaired islet function in commonly used transgenic mouse lines due to human growth hormone minigene expression. Cell metabolism 2014;20:979-990

130. Kanazawa Y, Makino M, Morishima Y, Yamada K, Nabeshima T, Shirasaki Y: Degradation of PEP-19, a calmodulin-binding protein, by calpain is implicated in neuronal cell death induced by intracellular Ca2+ overload. Neuroscience 2008;154:473-481

131. Okazaki K, Niki I, Iino S, Kobayashi S, Hidaka H: A role of calcyclin, a Ca(2+)-binding protein, on the Ca(2+)-dependent insulin release from the pancreatic beta cell. J Biol Chem 1994;269:6149-6152

132. Fadista J, Vikman P, Laakso EO, Mollet IG, Esguerra JL, Taneera J, Storm P, Osmark P, Ladenvall C, Prasad RB, Hansson KB, Finotello F, Uvebrant K, Ofori JK, Di Camillo B, Krus U, Cilio CM, Hansson O, Eliasson L, Rosengren AH, Renstrom E, Wollheim CB, Groop L: Global genomic and transcriptomic analysis of human pancreatic islets reveals novel genes influencing glucose metabolism. Proc Natl Acad Sci U S A 2014;111:13924-13929

133. Castro DS, Martynoga B, Parras C, Ramesh V, Pacary E, Johnston C, Drechsel D, Lebel-Potter M, Garcia LG, Hunt C, Dolle D, Bithell A, Ettwiller L, Buckley N, Guillemot F: A novel

function of the proneural factor Ascl1 in progenitor proliferation identified by genome-wide characterization of its targets. Genes Dev 2011;25:930-945

134. Webb AE, Pollina EA, Vierbuchen T, Urban N, Ucar D, Leeman DS, Martynoga B, Sewak M, Rando TA, Guillemot F, Wernig M, Brunet A: FOXO3 shares common targets with ASCL1 genome-wide and inhibits ASCL1-dependent neurogenesis. Cell reports 2013;4:477-491

135. Raposo AA, Vasconcelos FF, Drechsel D, Marie C, Johnston C, Dolle D, Bithell A, Gillotin S, van den Berg DL, Ettwiller L, Flicek P, Crawford GE, Parras CM, Berninger B, Buckley NJ, Guillemot F, Castro DS: Ascl1 Coordinately Regulates Gene Expression and the Chromatin Landscape during Neurogenesis. Cell reports 2015;

136. Dufer M, Haspel D, Krippeit-Drews P, Aguilar-Bryan L, Bryan J, Drews G: Oscillations of membrane potential and cytosolic Ca(2+) concentration in SUR1(-/-) beta cells. Diabetologia 2004;47:488-498

137. Nenquin M, Szollosi A, Aguilar-Bryan L, Bryan J, Henquin JC: Both triggering and amplifying pathways contribute to fuel-induced insulin secretion in the absence of sulfonylurea receptor-1 in pancreatic beta-cells. J Biol Chem 2004;279:32316-32324

138. Mourad NI, Nenquin M, Henquin JC: Metabolic amplification of insulin secretion by glucose is independent of beta-cell microtubules. Am J Physiol Cell Physiol 2011;300:C697-706

139. Wright A, Burden AC, Paisey RB, Cull CA, Holman RR, Group UKPDS: Sulfonylurea inadequacy: efficacy of addition of insulin over 6 years in patients with type 2 diabetes in the U.K. Prospective Diabetes Study (UKPDS 57). Diabetes Care 2002;25:330-336

140. Kligman D, Hilt DC: The S100 protein family. Trends in biochemical sciences 1988;13:437-443

141. Udovichenko IP, Gibbs D, Williams DS: Actin-based motor properties of native myosin VIIa. J Cell Sci 2002;115:445-450

142. Giannone G, Ronde P, Gaire M, Beaudouin J, Haiech J, Ellenberg J, Takeda K: Calcium rises locally trigger focal adhesion disassembly and enhance residency of focal adhesion kinase at focal adhesions. J Biol Chem 2004;279:28715-28723

143. Pang ZP, Yang N, Vierbuchen T, Ostermeier A, Fuentes DR, Yang TQ, Citri A, Sebastiano V, Marro S, Sudhof TC, Wernig M: Induction of human neuronal cells by defined transcription factors. Nature 2011;476:220-223

144. Brun PJ, Grijalva A, Rausch R, Watson E, Yuen JJ, Das BC, Shudo K, Kagechika H, Leibel RL, Blaner WS: Retinoic acid receptor signaling is required to maintain glucose-stimulated insulin secretion and beta-cell mass. FASEB J 2015;29:671-683

145. Lu M, Seufert J, Habener JF: Pancreatic beta-cell-specific repression of insulin gene transcription by CCAAT/enhancer-binding protein beta. Inhibitory interactions with basic helix-loop-helix transcription factor E47. J Biol Chem 1997;272:28349-28359

146. Matsuda T, Kido Y, Asahara S, Kaisho T, Tanaka T, Hashimoto N, Shigeyama Y, Takeda A, Inoue T, Shibutani Y, Koyanagi M, Hosooka T, Matsumoto M, Inoue H, Uchida T, Koike M, Uchiyama Y, Akira S, Kasuga M: Ablation of C/EBPbeta alleviates ER stress and pancreatic beta cell failure through the GRP78 chaperone in mice. The Journal of clinical investigation 2010;120:115-126

147. Moutier E, Ye T, Choukrallah MA, Urban S, Osz J, Chatagnon A, Delacroix L, Langer D, Rochel N, Moras D, Benoit G, Davidson I: Retinoic acid receptors recognize the mouse genome through binding elements with diverse spacing and topology. J Biol Chem 2012;287:26328-26341

148. Thompson M, Andrade VA, Andrade SJ, Pusl T, Ortega JM, Goes AM, Leite MF: Inhibition of the TEF/TEAD transcription factor activity by nuclear calcium and distinct kinase pathways. Biochem Biophys Res Commun 2003;301:267-274

149. Pontoglio M, Sreenan S, Roe M, Pugh W, Ostrega D, Doyen A, Pick AJ, Baldwin A, Velho G, Froguel P, Levisetti M, Bonner-Weir S, Bell GI, Yaniv M, Polonsky KS: Defective insulin secretion in hepatocyte nuclear factor 1alpha-deficient mice. The Journal of clinical investigation 1998;101:2215-2222

150. Brinster RL, Allen JM, Behringer RR, Gelinas RE, Palmiter RD: Introns increase transcriptional efficiency in transgenic mice. Proc Natl Acad Sci U S A 1988;85:836-840

151. Orban PC, Chui D, Marth JD: Tissue- and site-specific DNA recombination in transgenic mice. Proc Natl Acad Sci U S A 1992;89:6861-6865

152. Baan M, Kibbe CR, Bushkofsky JR, Harris TW, Sherman DS, Davis DB: Transgenic expression of the human growth hormone minigene promotes pancreatic beta-cell proliferation. Am J Physiol Regul Integr Comp Physiol 2015;309:R788-794

153. Oropeza D, Jouvet N, Budry L, Campbell JE, Bouyakdan K, Lacombe J, Perron G, Bergeron V, Neuman JC, Brar HK, Fenske RJ, Meunier C, Sczelecki S, Kimple ME, Drucker DJ, Screaton RA, Poitout V, Ferron M, Alquier T, Estall JL: Phenotypic Characterization of MIP-CreERT1Lphi Mice With Transgene-Driven Islet Expression of Human Growth Hormone. Diabetes 2015;64:3798-3807

154. Berglund ED, Li CY, Poffenberger G, Ayala JE, Fueger PT, Willis SE, Jewell MM, Powers AC, Wasserman DH: Glucose metabolism in vivo in four commonly used inbred mouse strains. Diabetes 2008;57:1790-1799

155. Chowdhury S, Wang X, Srikant CB, Li Q, Fu M, Gong YJ, Ning G, Liu JL: IGF-I stimulates CCN5/WISP2 gene expression in pancreatic beta-cells, which promotes cell proliferation and survival against streptozotocin. Endocrinology 2014;155:1629-1642

156. Sladek R, Rocheleau G, Rung J, Dina C, Shen L, Serre D, Boutin P, Vincent D, Belisle A, Hadjadj S, Balkau B, Heude B, Charpentier G, Hudson TJ, Montpetit A, Pshezhetsky AV, Prentki M, Posner BI, Balding DJ, Meyre D, Polychronakos C, Froguel P: A genome-wide association study identifies novel risk loci for type 2 diabetes. Nature 2007;445:881-885

157. Muoio DM, Newgard CB: Mechanisms of disease: molecular and metabolic mechanisms of insulin resistance and beta-cell failure in type 2 diabetes. Nature reviews Molecular cell biology 2008;9:193-205

158. Everson SA, Goldberg DE, Helmrich SP, Lakka TA, Lynch JW, Kaplan GA, Salonen JT: Weight gain and the risk of developing insulin resistance syndrome. Diabetes Care 1998;21:1637-1643

159. Golson ML, Misfeldt AA, Kopsombut UG, Petersen CP, Gannon M: High Fat Diet Regulation of beta-Cell Proliferation and beta-Cell Mass. Open Endocrinol J 2010;4

160. Sachdeva MM, Stoffers DA: Minireview: Meeting the demand for insulin: molecular mechanisms of adaptive postnatal beta-cell mass expansion. Mol Endocrinol 2009;23:747-758

161. Oldham MC, Konopka G, Iwamoto K, Langfelder P, Kato T, Horvath S, Geschwind DH: Functional organization of the transcriptome in human brain. Nature neuroscience 2008;11:1271-1282

162. Feltus FA, Ficklin SP, Gibson SM, Smith MC: Maximizing capture of gene co-expression relationships through pre-clustering of input expression samples: an Arabidopsis case study. BMC systems biology 2013;7:44

163. Ivliev AE, t Hoen PA, Sergeeva MG: Coexpression network analysis identifies transcriptional modules related to proastrocytic differentiation and sprouty signaling in glioma. Cancer research 2010;70:10060-10070

164. Gaiteri C, Ding Y, French B, Tseng GC, Sibille E: Beyond modules and hubs: the potential of gene coexpression networks for investigating molecular mechanisms of complex brain disorders. Genes Brain Behav 2014;13:13-24

165. Varet H, Brillet-Gueguen L, Coppee JY, Dillies MA: SARTools: A DESeq2- and EdgeR-Based R Pipeline for Comprehensive Differential Analysis of RNA-Seq Data. PLoS One 2016;11:e0157022

166. Gao ZY, Drews G, Henquin JC: Mechanisms of the stimulation of insulin release by oxytocin in normal mouse islets. Biochem J 1991;276 (Pt 1):169-174

167. Gao ZY, Henquin JC: Arginine vasopressin and oxytocin effects in mouse pancreatic beta-cells. Receptors involved in stimulation of insulin release. Diabetes 1993;42:914-921

168. Bobbioni-Harsch E, Frutiger S, Hughes G, Panico M, Etienne A, Zappacosta F, Morris HR, Jeanrenaud B: Physiological concentrations of oxytocin powerfully stimulate insulin secretionin vitro. Endocrine 1995;3:55-59

169. Zhang H, Wu C, Chen Q, Chen X, Xu Z, Wu J, Cai D: Treatment of obesity and diabetes using oxytocin or analogs in patients and mouse models. PloS one 2013;8:e61477

170. Chan SL, Monks LK, Gao H, Deaville P, Morgan NG: Identification of the monomeric G-protein, Rhes, as an efaroxan-regulated protein in the pancreatic beta-cell. Br J Pharmacol 2002;136:31-36

171. Taylor JP, Jackson DA, Morgan NG, Chan SL: Rhes expression in pancreatic beta-cells is regulated by efaroxan in a calcium-dependent process. Biochem Biophys Res Commun 2006;349:809-815

172. Subramaniam S, Napolitano F, Mealer RG, Kim S, Errico F, Barrow R, Shahani N, Tyagi R, Snyder SH, Usiello A: Rhes, a striatal-enriched small G protein, mediates mTOR signaling and L-DOPA-induced dyskinesia. Nat Neurosci 2011;15:191-193

173. Dickson LM, Rhodes CJ: Pancreatic beta-cell growth and survival in the onset of type 2 diabetes: a role for protein kinase B in the Akt? Am J Physiol Endocrinol Metab 2004;287:E192-198

174. Terauchi Y, Takamoto I, Kubota N, Matsui J, Suzuki R, Komeda K, Hara A, Toyoda Y, Miwa I, Aizawa S, Tsutsumi S, Tsubamoto Y, Hashimoto S, Eto K, Nakamura A, Noda M, Tobe K, Aburatani H, Nagai R, Kadowaki T: Glucokinase and IRS-2 are required for compensatory beta cell hyperplasia in response to high-fat diet-induced insulin resistance. The Journal of clinical investigation 2007;117:246-257

175. Heit JJ, Karnik SK, Kim SK: Intrinsic regulators of pancreatic beta-cell proliferation. Annu Rev Cell Dev Biol 2006;22:311-338

176. Gu Y, Lindner J, Kumar A, Yuan W, Magnuson MA: Rictor/mTORC2 is essential for maintaining a balance between beta-cell proliferation and cell size. Diabetes 2011;60:827-837

177. Sabatini PV, Krentz NA, Zarrouki B, Westwell-Roper CY, Nian C, Uy RA, Shapiro AM, Poitout V, Lynn FC: Npas4 is a novel activity-regulated cytoprotective factor in pancreatic beta-cells. Diabetes 2013;62:2808-2820

178. Speckmann T, Sabatini PV, Nian C, Smith RG, Lynn FC: Npas4 Transcription Factor Expression Is Regulated by Calcium Signaling Pathways and Prevents Tacrolimus-induced Cytotoxicity in Pancreatic Beta Cells. J Biol Chem 2016;291:2682-2695

179. Besseiche A, Riveline JP, Gautier JF, Breant B, Blondeau B: Metabolic roles of PGC-1alpha and its implications for type 2 diabetes. Diabetes Metab 2015;41:347-357

180. Valtat B, Riveline JP, Zhang P, Singh-Estivalet A, Armanet M, Venteclef N, Besseiche A, Kelly DP, Tronche F, Ferre P, Gautier JF, Breant B, Blondeau B: Fetal PGC-1alpha overexpression programs adult pancreatic beta-cell dysfunction. Diabetes 2013;62:1206-1216

181. Vierbuchen T, Ostermeier A, Pang ZP, Kokubu Y, Sudhof TC, Wernig M: Direct conversion of fibroblasts to functional neurons by defined factors. Nature 2010;463:1035-1041

182. Skelin M, Rupnik M, Cencic A: Pancreatic beta cell lines and their applications in diabetes mellitus research. ALTEX 2010;27:105-113

183. Guillemot F, Lo LC, Johnson JE, Auerbach A, Anderson DJ, Joyner AL: Mammalian achaete-scute homolog 1 is required for the early development of olfactory and autonomic neurons. Cell 1993;75:463-476

184. Leung CT, Coulombe PA, Reed RR: Contribution of olfactory neural stem cells to tissue maintenance and regeneration. Nat Neurosci 2007;10:720-726

185. Kim EJ, Ables JL, Dickel LK, Eisch AJ, Johnson JE: Ascl1 (Mash1) defines cells with long-term neurogenic potential in subgranular and subventricular zones in adult mouse brain. PloS one 2011;6:e18472

186. Pacary E, Heng J, Azzarelli R, Riou P, Castro D, Lebel-Potter M, Parras C, Bell DM, Ridley AJ, Parsons M, Guillemot F: Proneural transcription factors regulate different steps of cortical neuron migration through Rnd-mediated inhibition of RhoA signaling. Neuron 2011;69:1069-1084

187. Langfelder P, Horvath S: Fast R Functions for Robust Correlations and Hierarchical Clustering. J Stat Softw 2012;46

188. Juhl K, Sarkar SA, Wong R, Jensen J, Hutton JC: Mouse pancreatic endocrine cell transcriptome defined in the embryonic Ngn3-null mouse. Diabetes 2008;57:2755-2761

189. Subramanian A, Tamayo P, Mootha VK, Mukherjee S, Ebert BL, Gillette MA, Paulovich A, Pomeroy SL, Golub TR, Lander ES, Mesirov JP: Gene set enrichment analysis: a knowledge-based approach for interpreting genome-wide expression profiles. Proc Natl Acad Sci U S A 2005;102:15545-15550

190. Kanehisa M, Goto S, Furumichi M, Tanabe M, Hirakawa M: KEGG for representation and analysis of molecular networks involving diseases and drugs. Nucleic Acids Res 2009;

191. Vastrik I, D'Eustachio P, Schmidt E, Gopinath G, Croft D, de Bono B, Gillespie M, Jassal B, Lewis S, Matthews L, Wu G, Birney E, Stein L: Reactome: a knowledge base of biologic pathways and processes. Genome Biol 2007;8:R39

192. Kitamura T, Nakae J, Kitamura Y, Kido Y, Biggs WH, 3rd, Wright CV, White MF, Arden KC, Accili D: The forkhead transcription factor Foxo1 links insulin signaling to Pdx1 regulation of pancreatic beta cell growth. The Journal of clinical investigation 2002;110:1839-1847

193. Elrick LJ, Docherty K: Phosphorylation-dependent nucleocytoplasmic shuttling of pancreatic duodenal homeobox-1. Diabetes 2001;50:2244-2252

194. Johnson JD, Bernal-Mizrachi E, Alejandro EU, Han Z, Kalynyak TB, Li H, Beith JL, Gross J, Warnock GL, Townsend RR, Permutt MA, Polonsky KS: Insulin protects islets from apoptosis via Pdx1 and specific changes in the human islet proteome. Proc Natl Acad Sci U S A 2006;103:19575-19580

195. Wu H, MacFarlane WM, Tadayyon M, Arch JR, James RF, Docherty K: Insulin stimulates pancreatic-duodenal homoeobox factor-1 (PDX1) DNA-binding activity and insulin promoter activity in pancreatic beta cells. Biochem J 1999;344 Pt 3:813-818

196. Matschinsky FM: GKAs for diabetes therapy: why no clinically useful drug after two decades of trying? Trends Pharmacol Sci 2013;34:90-99

197. Matschinsky FM, Zelent B, Doliba NM, Kaestner KH, Vanderkooi JM, Grimsby J, Berthel SJ, Sarabu R: Research and development of glucokinase activators for diabetes therapy: theoretical and practical aspects. Handb Exp Pharmacol 2011:357-401

198. Garber AJ: Incretin effects on beta-cell function, replication, and mass: the human perspective. Diabetes Care 2011;34 Suppl 2:S258-263

199. Xu G, Stoffers DA, Habener JF, Bonner-Weir S: Exendin-4 stimulates both beta-cell replication and neogenesis, resulting in increased beta-cell mass and improved glucose tolerance in diabetic rats. Diabetes 1999;48:2270-2276

200. van Raalte DH, Verchere CB: Glucagon-Like Peptide-1 Receptor Agonists: Beta-Cell Protection or Exhaustion? Trends in endocrinology and metabolism: TEM 2016;27:442-445

201. Abdulreda MH, Rodriguez-Diaz R, Caicedo A, Berggren PO: Liraglutide Compromises Pancreatic beta Cell Function in a Humanized Mouse Model. Cell Metab 2016;23:541-546